CRCLEME
Cooperative Research Centre for
Landscape Evolution & Mineral Exploration

CSIRO
EXPLORATION
AND MINING

AMIRA
Australian Mineral Industries Research Association Limited ACN 004 448 266

OPEN FILE
REPORT
SERIES

THE DISTRIBUTION OF GOLD AND OTHER ELEMENTS IN SOILS AT MULLINE, WESTERN AUSTRALIA

M.J. Lintern and C.R.M. Butt

CRC LEME OPEN FILE REPORT 47

November 1998

(CSIRO Division of Exploration Geoscience Report 159R, 1991.
Second impression 1998)

AMIRA
Australian Mineral Industries Research Association Limited ACN 004 448 266

CRCLEME
Cooperative Research Centre for
Landscape Evolution & Mineral Exploration

CSIRO
EXPLORATION
AND MINING

THE DISTRIBUTION OF GOLD AND OTHER ELEMENTS IN SOILS AT MULLINE, WESTERN AUSTRALIA

M.J. Lintern and C.R.M. Butt

CRC LEME OPEN FILE REPORT 47

November 1998

(CSIRO Division of Exploration Geoscience Report 159R, 1991.
Second impression 1998)

CRC LEME is an unincorporated joint venture between The Australian National University,
University of Canberra, Australian Geological Survey Organisation and CSIRO Exploration and Mining
Headquarters: CRC LEME c/o CSIRO Exploration and Mining, Private Bag, PO Wembley, Western Australia, 6014

RESEARCH ARISING FROM CSIRO/AMIRA REGOLITH GEOCHEMISTRY PROJECTS 1987-1993

In 1987, CSIRO commenced a series of multi-client research projects in regolith geology and geochemistry which were sponsored by companies in the Australian mining industry, through the Australian Mineral Industries Research Association Limited (AMIRA). The initial research program, "Exploration for concealed gold deposits, Yilgarn Block, Western Australia" (1987-1993) had the aim of developing improved geological, geochemical and geophysical methods for mineral exploration that would facilitate the location of blind, buried or deeply weathered gold deposits. The program included the following projects:

P240: Laterite geochemistry for detecting concealed mineral deposits (1987-1991). Leader: Dr R.E. Smith.
Its scope was development of methods for sampling and interpretation of multi-element laterite geochemistry data and application of multi-element techniques to gold and polymetallic mineral exploration in weathered terrain. The project emphasised viewing laterite geochemical dispersion patterns in their regolith-landform context at local and district scales. It was supported by 30 companies.

P241: Gold and associated elements in the regolith - dispersion processes and implications for exploration (1987-1991). Leader: Dr C.R.M. Butt.
The project investigated the distribution of ore and indicator elements in the regolith. It included studies of the mineralogical and geochemical characteristics of weathered ore deposits and wall rocks, and the chemical controls on element dispersion and concentration during regolith evolution. This was to increase the effectiveness of geochemical exploration in weathered terrain through improved understanding of weathering processes. It was supported by 26 companies.

These projects represented "an opportunity for the mineral industry to participate in a multi-disciplinary program of geoscience research aimed at developing new geological, geochemical and geophysical methods for exploration in deeply weathered Archaean terrains". This initiative recognised the unique opportunities, created by exploration and open-cut mining, to conduct detailed studies of the weathered zone, with particular emphasis on the near-surface expression of gold mineralisation. The skills of existing and specially recruited research staff from the Floreat Park and North Ryde laboratories (of the then Divisions of Minerals and Geochemistry, and Mineral Physics and Mineralogy, subsequently Exploration Geoscience and later Exploration and Mining) were integrated to form a task force with expertise in geology, mineralogy, geochemistry and geophysics. Several staff participated in more than one project. Following completion of the original projects, two continuation projects were developed.

P240A: Geochemical exploration in complex lateritic environments of the Yilgarn Craton, Western Australia (1991-1993). Leaders: Drs R.E. Smith and R.R. Anand.
The approach of viewing geochemical dispersion within a well-controlled and well-understood regolith-landform and bedrock framework at detailed and district scales continued. In this extension, focus was particularly on areas of transported cover and on more complex lateritic environments typified by the Kalgoorlie regional study. This was supported by 17 companies.

P241A: Gold and associated elements in the regolith - dispersion processes and implications for exploration. Leader: Dr. C.R.M. Butt.
The significance of gold mobilisation under present-day conditions, particularly the important relationship with pedogenic carbonate, was investigated further. In addition, attention was focussed on the recognition of primary lithologies from their weathered equivalents. This project was supported by 14 companies.

Although the confidentiality periods of the research reports have expired, the last in December 1994, they have not been made public until now. Publishing the reports through the CRC LEME Report Series is seen as an appropriate means of doing this. By making available the results of the research and the authors' interpretations, it is hoped that the reports will provide source data for future research and be useful for teaching. CRC LEME acknowledges the Australian Mineral Industries Research Association and CSIRO Division of Exploration and Mining for authorisation to publish these reports. It is intended that publication of the reports will be a substantial additional factor in transferring technology to aid the Australian Mineral Industry.

This report (CRC LEME Open File Report 47) is a Second impression (second printing) of CSIRO, Division of Explorationn Geoscience Restricted Report 159R, first issued in 1991, which formed part of the CSIRO/AMIRA Project P241.

Copies of this publication can be obtained from:
The Publication Officer, c/- CRC LEME, CSIRO Exploration and Mining, PMB, Wembley, WA 6014, Australia. Information on other publications in this series may be obtained from the above or from http://leme.anu.edu.au/

Cataloguing-in-Publication:
Lintern, M.J.
The distribution of gold and other elements in soils at Mulline, Western Australia
ISBN 0 642 28211 0
1. Soils survey - Western Australia 2. Gold ores - Western Australia 3. Geochemistry.
I. Butt, C.R.M. II. Title
CRC LEME Open File Report 47.
ISSN 1329-4768

PREFACE

The CSIRO-AMIRA project "Exploration for Concealed Gold Deposits, Yilgarn Block, Western Australia" has as its overall aim the development of improved geological, geochemical and geophysical methods for mineral exploration that will facilitate the location of blind, concealed or deeply weathered gold deposits. This Report presents results of research conducted as part of Module 2 of this project (AMIRA Project 241): "Gold and Associated Elements in the Regolith - Dispersion Processes and Implications for Exploration".

The objectives of this module are, *inter alia*, to suggest improvements in techniques of sampling and data interpretation for gold exploration, and to increase knowledge of the properties and genesis of the regolith. This report describes the geochemistry and mineralogy of soils in the Mulline area west of Menzies. The results contribute strongly to the objectives of the module by (i) providing further evidence (already demonstrated at Mt. Hope and Panglo) of the association between Au and the alkaline earth metals, (ii) examining the distribution of other elements in the soil. The association between gold and carbonate is more complicated at Mulline because of the presence of considerable quantities of ferruginous material and massive carbonate structures. Gold was found to be associated with both ferruginous and calcareous material in the soil profiles, and its distribution is controlled by the presence or absence of these components. The results emphasize the importance of sampling the correct horizon and material when soil sampling for gold exploration.

C.R.M. Butt,
Project Leader.
February, 1991.

ABSTRACT

Soils, lateritic gravels, calcretes and saprolites were sampled at the Peach Tree and Lady Gladys gold prospects in the Mulline area, 50 km west of Menzies. Each of these sites has moderate reserves of gold as laterite-hosted deposits that are characterized by ferruginous gravels invaded by pedogenic carbonate.

Strong associations were found between gold and iron, and gold and the alkaline earth metals. In particular, gold distribution appears to be positively correlated with calcium and magnesium in the top 0.5m of the soil profile and with iron in various zones beneath this. The alkaline earth metals are present as calcite and dolomite and iron as goethite or hematite. The association with Fe oxides is probably related to the formation of the deep lateritic regolith during the Tertiary, whereas the association with the pedogenic carbonates is of more recent origin, related to weathering under recently imposed semi-arid climates. The study has demonstrated the importance of selecting the correct soil horizon when sampling for gold and support similar data from elsewhere in the Yilgarn Block, Western Australia.

CONTENTS

THE DISTRIBUTION OF GOLD AND OTHER ELEMENTS IN SOILS AT MULLINE, WESTERN AUSTRALIA

M.J. Lintern and C.R.M. Butt

1.0 INTRODUCTION

The principal objective of this study was to determine the validity of largely anecdotal evidence pertaining to the association of Au with carbonate that had been widely reported from the Western Australian goldfields (e.g., Geological Survey, 1969; K. Schulz, personal communication, 1985). The sites at Peach Tree and Lady Gladys were chosen, therefore, because of the presence of Au occurring within surficial material containing carbonate. Currently, the sites are being explored and evaluated by Pancontinental Mining Ltd.

The soils were collected in 1987 but work was temporarily halted when it became evident that the complexity of the soils was such that geochemical associations of Au were difficult to establish. Instead, studies at Mt. Hope and Panglo (Lintern, 1989; Lintern and Scott, 1990) were given greater emphasis by the research group because these demonstrated the Au-carbonate association more effectively. As a consequence, the situation at Peach Tree and Lady Gladys can be better explained with the benefit of the data obtained, and interpretation techniques used, at the other two sites.

The Peach Tree and Lady Gladys gold prospects are situated in the Mulline area, approximately 50 km west of Menzies (Figure 1). The name "Mulline" originated from a granite outcrop situated 8 km NNW of the township of the same name (named by Surveyor Brazier in 1894) after an aboriginal word (Ian Elliot, Department of Lands Administration, personal communication, 1991) The township (now abandoned) is located near to the Peach Tree prospect and is the close to the site of an underground gold deposit mined earlier in the century. This deposit was situated in basalt and hornblende-schist zones with mineralization controlled by quartz veining and shears. Alteration of the primary deposit included silicification and the formation of hydromica. Minerals associated with Au included pyrite, galena, sphalerite and chalcopyrite. Production figures reported were 4.2 tonnes of Au grading 25.3 g/t (Geological Survey, 1990).

The region is characterized by the local preservation of essentially complete lateritic regoliths, especially over mafic rocks. The lateritic gravels and duricrusts have become enriched in Au over primary mineralization and, at Peach Tree and Lady Gladys, these constitute small lateritic Au deposits. Mulline is situated close to the "Menzies Line", a narrow east-west transitional zone across which there are marked changes in soil types, vegetation associations and groundwater quality (Butt et al., 1977). The changes are probably a response to climatic factors, although the sharpness with which the changes occur is more abrupt than any climatic gradient.

South of the Menzies Line, soils are predominantly neutral to alkaline, orange to red loams, with extensive development of pedogenic calcrete. Non-calcareous earthy sand soils occupy high landscape positions, principally over granitic rocks. Groundwaters tend to be saline, neutral to acid. Average annual rainfall generally exceeds 225 mm, falling mainly in winter; annual evaporation is less than 2500 mm and annual mean temperature below 19^{o} C. Vegetation immediately south of the Line is typical of that within the Coolgardie Botanical District (Aplin, 1976; Diels, 1906), comprising woodlands of mixed eucalypts, especially salmon and gimlet

gums (*Eucalyptus salmonophloia* and *E. salubris*) and shrublands of mulga (*Acacia* spp.), *Grevillea* spp., mallee (*Eucalyptus* spp.) and sheoak (*Casuarina* spp.).

North of the Menzies Line, soils are predominantly neutral to acid, red, non-calcareous earths, sands and lithosols, with extensive development of red-brown siliceous hardpans. Groundwater (or valley) calcretes are common in major drainages. Groundwaters are less saline than in the south, and are neutral to alkaline. Annual rainfall is generally less than 225 mm, falling mainly in the summer, with annual evaporation exceeding 2500 mm and annual mean temperatures exceeding 19°C. The vegetation is typical of that found within the Austin Botanical District, comprising shrublands dominated by mulga, with eucalypts, such as the river red gum (*E. camaldulensis*) common only along water courses and some valley calcretes.

At Peach Tree and Lady Gladys, the soils are alkaline, with strong development of pedogenic carbonates invading the pre-existing lateritic gravels; the vegetation is an open eucalypt woodland (mainly *E. salmonophloia*) with a sparse understorey of *Acacia* spp. and *Melaleuca* spp. shrubs. The sites are thus fairly typical of conditions south of the Menzies Line. However, the soils and vegetation of the district are also responding closely to the geological setting; eucalypt woodlands are present mainly on the mafic rocks of the greenstone belts and pedogenic calcretes only appear to be abundant close to specific source units. Indeed, the Menzies Line here extends unusually far north (see map in Butt et al., 1977), following the Davyhurst-Mt. Ida greenstone belt to beyond Bottle Creek, 65 km north.

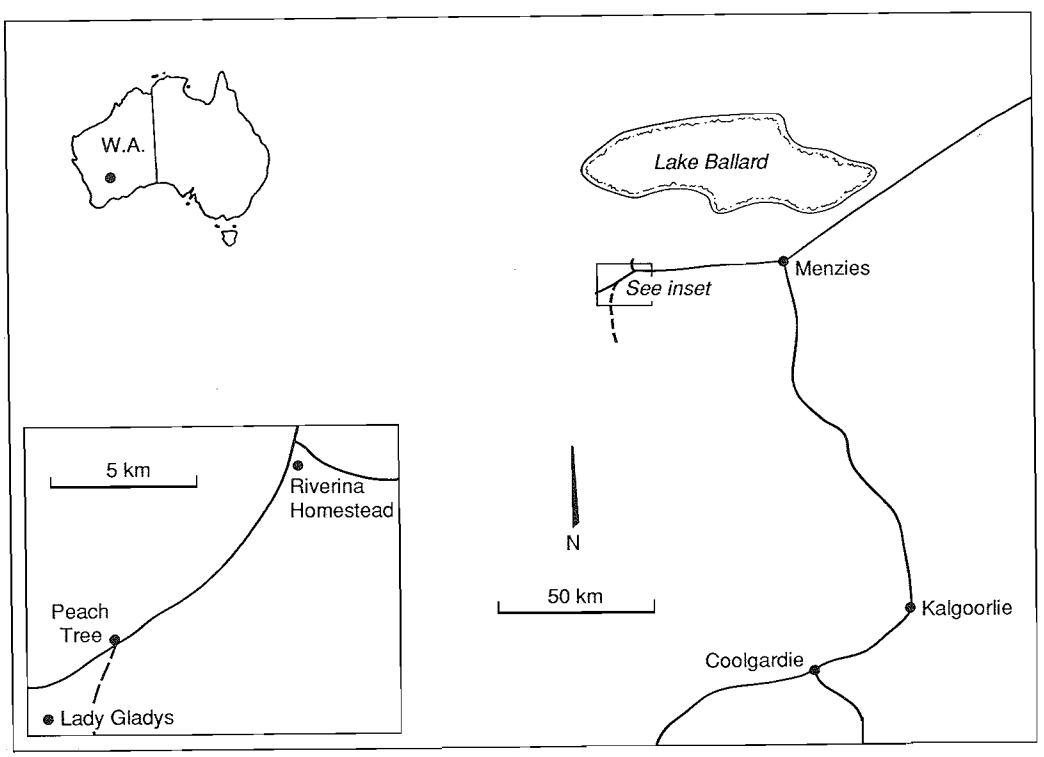

Figure 1: Map showing the locations of Peach Tree and Lady Gladys.

2.0 METHODS

Sampling sites were selected from data supplied by Pancontinental Mining Ltd. At both sites, trenches or shallow trial pits exposed the top 1 to 2m of the regolith and several profiles were sampled at each site. Profiles close to and away from (probable) primary mineralization were sampled by vertical channel sampling from the surface to the base of the pits. Deeper profiles were collected by sub-sampling reverse circulation (RC) drill cuttings.

At Peach Tree, in addition to soil profiles, drill cuttings were sampled from two grid lines on traverses that extended from mineralization to background zones low in Au. Adjacent traverses were selected (25m apart) to reduce differences due to sub- sample or spatial inhomogeneities. Samples were taken from bagged RC cuttings for depths of 0-1m and 3-4m. A number of additional samples were taken at both sites and the results are tabulated in Appendix 1.

Samples were analyzed by a variety of instrumental techniques. Mineralogy and geochemical contents were determined by XRD, XRF, ASV (for Au) and ICP using techniques previously described (Lintern *et al.*, 1988; Lintern, 1989). In addition, a few selected samples were analysed for Au by AAS after fire assay fusion.

3.0 RESULTS AND DISCUSSION

The results from each profile are described and plotted in turn. However, elements occurring close to or below detection limits have not been plotted but are tabulated with other data in Appendix 1.

3.1 Peach Tree

The location of the traverses, trench, profiles and sampling points are found in Figure 2. The soil anomaly/laterite gold resource at Peach Tree is hosted by lateritic gravels and duricrusts which contain pedogenic carbonates in the upper two metres of the profile. The gold enrichment (as shown by the isopachs in Figure 2) trends approximately E-W and has quite well-defined southern and western boundaries that parallel the occurrence of the lateritic materials. Thus, to the south, soils are developed directly from saprolite, with little or no lateritic gravel, and to the west there are outcrops of fresh rock. From the south in particular, the lateritic materials are seen to form a low mound with an east-west trend. The shallow N-S trench cut in the centre of the anomaly shows that carbonates are abundant in the near-surface horizons. A massive "bar" of strongly indurated carbonate cross-cuts the trench, striking approximately E-W along the axis of the gold anomaly. The amount of carbonate enrichment appears to decrease away from this bar and the lateritic gravels, exposed at the south end of the trench and nearby drill holes, are carbonate-free. It appears that the primary source of the gold has an east-west strike, parallel with lineaments interpreted from aerial photography. This source may be related to the carbonate bar exposed in the trench. Indeed, the bar may also reflect a Ca-rich rock (e.g. carbonate alteration) and hence represent the source unit for much of the pedogenic carbonate.

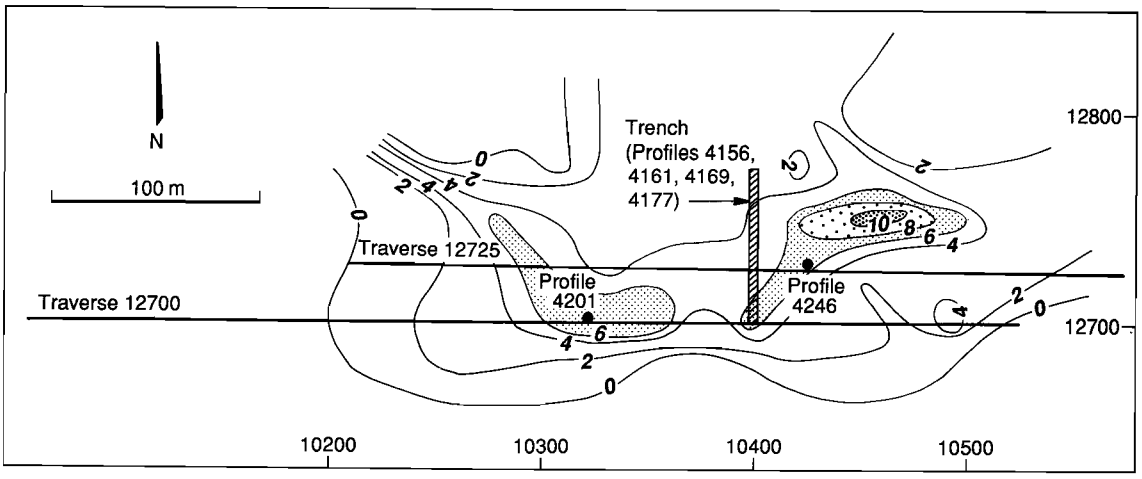

Figure 2a: Plan showing sample locations at Peach Tree. Isopachs (metres >0.5 g/t Au) indicate location of potentially economic gold resource (primarily laterite), as supplied by Pancontinental Mining Ltd.

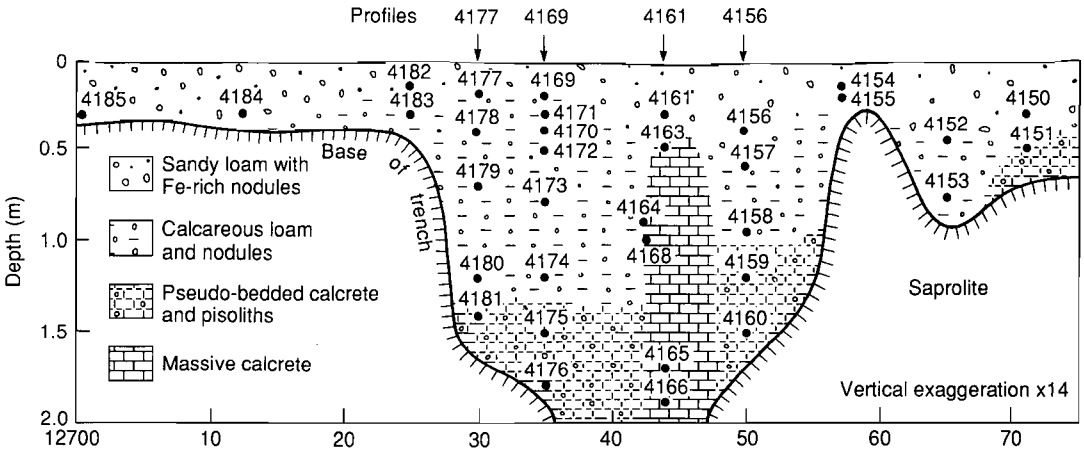

Figure 2b: Section of the trench at Peach Tree showing locations of samples.

3.1.1 Profile 4156 (10400E 12750N)

Depth (m)	Field description
0-0.4	Red calcareous clay-rich loam with Fe oxide and calcrete pisoliths and nodules
0.4-0.6	Orange loam with Fe oxide pisoliths and calcrete nodules. Some calcrete nodules enclose Fe oxide-rich pisoliths
0.6-0.95	Similar; Fe oxide-rich pisoliths more abundant
0.95-1.2	Pseudo-bedded calcretes enclosing Fe oxide-rich pisoliths
1.2-1.5	Fe oxide-rich pisoliths with some calcrete layers

The alkaline earth metals (Ca and Mg) dominate most soil horizons as calcite and dolomite. The greatest concentrations occur between 0.5 and 1.0m but are high throughout. Silicon, Al, Fe and Ti concentrations each show a distinct minimum where the alkaline earth elements are at a maximum. This strongly suggests that the introduction of carbonate has diluted the concentrations of these elements. Silicon concentrations are higher above the carbonate horizon, whereas Al concentrations are higher below; these distributions correspond to those of detrital quartz and kaolinite, respectively.

The Au distribution is strongly associated with the carbonate horizon. However, the Au maximum (0.92 ppm) is slightly below (0.25m) the maxima of the alkaline earth metals and coincident with the peak Fe concentration. The next highest Au value (0.86 ppm) is coincident with the highest Ca and Mg concentration and lowest Fe concentration.

The minor and trace elements fall into three groups showing similar distributions: (i) As, Co, Cr, Cu, Ga, Nb, Ni, Pb, Sc, V and Zr form negative associations with the alkaline earth metals and are probably associated with clay or Fe oxide minerals; (ii) Ba, S, and Sr are positively associated with the alkaline earth metals. Barium and S are probably present as secondary barite, similar to occurrences at Mt. Hope and Panglo (Lintern, 1989; Lintern and Scott, 1990); (iii) Ce, La, Mn, Nd, Rb, Y and Zn, which decrease in abundance with depth.

Figure 3: Distribution of elements in Profile 4156. (following pages)

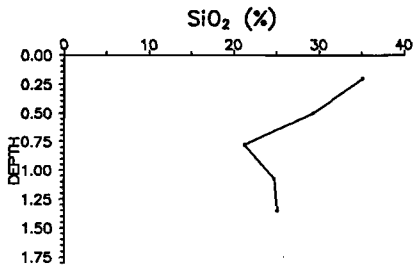
SiO2 (%)
0 10 20 30 40
DEPTH
0.00 0.25 0.50 0.75 1.00 1.25 1.50 1.75

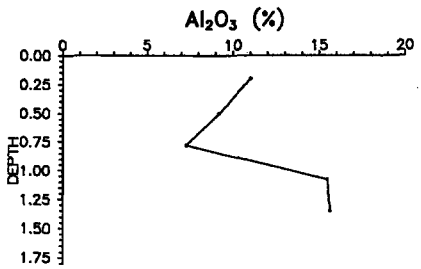
Al2O3 (%)
0 5 10 15 20
DEPTH
0.00 0.25 0.50 0.75 1.00 1.25 1.50 1.75

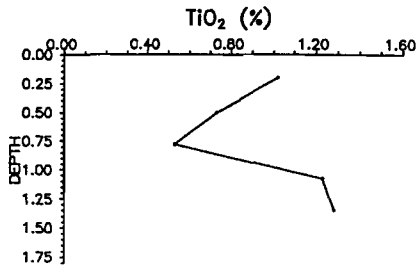
TiO2 (%)
0.00 0.40 0.80 1.20 1.60
DEPTH
0.00 0.25 0.50 0.75 1.00 1.25 1.50 1.75

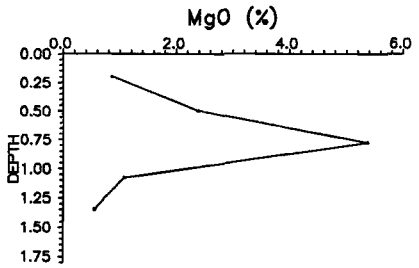
MgO (%)
0.0 2.0 4.0 6.0
DEPTH
0.00 0.25 0.50 0.75 1.00 1.25 1.50 1.75

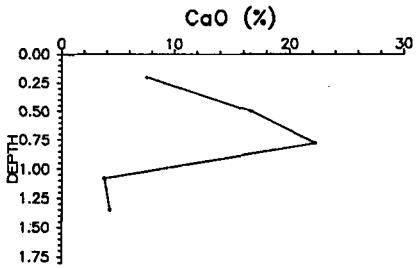
CaO (%)
0 10 20 30
DEPTH
0.00 0.25 0.50 0.75 1.00 1.25 1.50 1.75

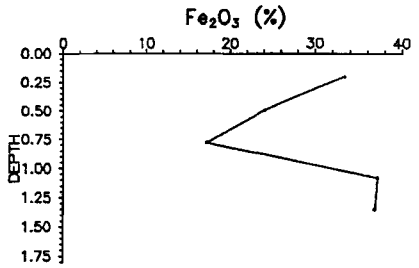
Fe2O3 (%)
0 10 20 30 40
DEPTH
0.00 0.25 0.50 0.75 1.00 1.25 1.50 1.75

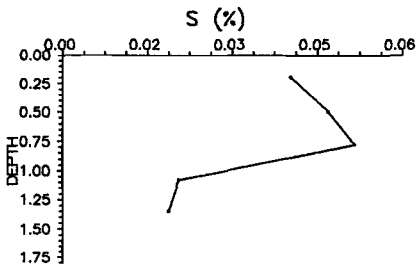
S (%)
0.00 0.02 0.03 0.05 0.06
DEPTH
0.00 0.25 0.50 0.75 1.00 1.25 1.50 1.75

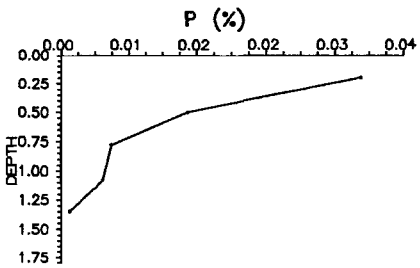
P (%)
0.00 0.01 0.02 0.02 0.03 0.04
DEPTH
0.00 0.25 0.50 0.75 1.00 1.25 1.50 1.75

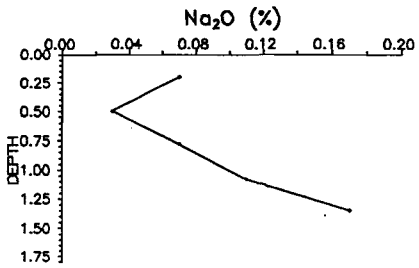
Na2O (%)
0.00 0.04 0.08 0.12 0.16 0.20
DEPTH
0.00 0.25 0.50 0.75 1.00 1.25 1.50 1.75

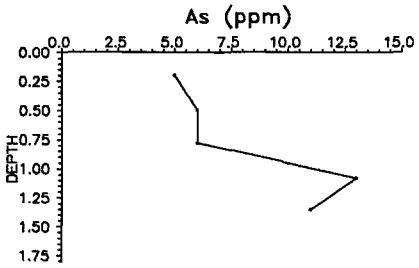
As (ppm)
0.0 2.5 5.0 7.5 10.0 12.5 15.0
DEPTH
0.00 0.25 0.50 0.75 1.00 1.25 1.50 1.75

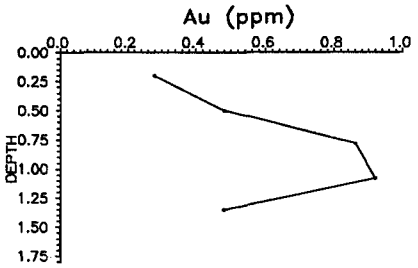
Au (ppm)
0.0 0.2 0.4 0.6 0.8 1.0
DEPTH
0.00 0.25 0.50 0.75 1.00 1.25 1.50 1.75

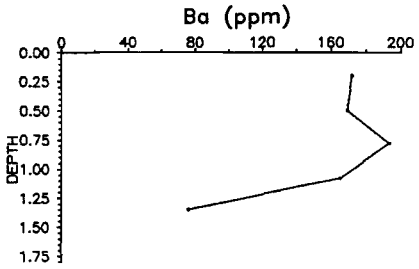
Ba (ppm)
0 40 80 120 160 200
DEPTH
0.00 0.25 0.50 0.75 1.00 1.25 1.50 1.75

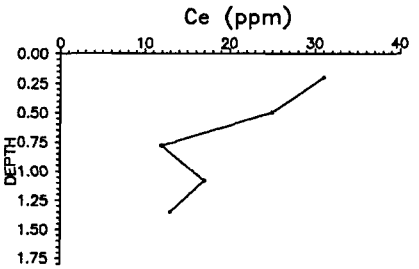
Ce (ppm)
0 10 20 30 40
DEPTH
0.00 0.25 0.50 0.75 1.00 1.25 1.50 1.75

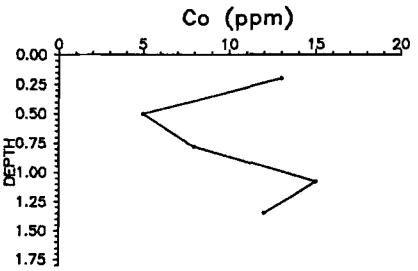
Co (ppm)
0 5 10 15 20
DEPTH
0.00 0.25 0.50 0.75 1.00 1.25 1.50 1.75

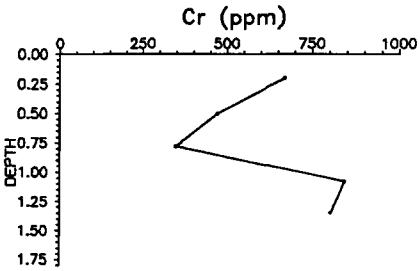
Cr (ppm)
0 250 500 750 1000
DEPTH
0.00 0.25 0.50 0.75 1.00 1.25 1.50 1.75

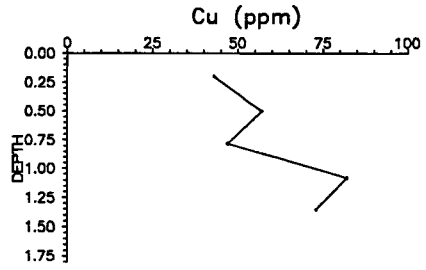
Cu (ppm)
0
25
50
75
100
DEPTH
0.00
0.25
0.50
0.75
1.00
1.25
1.50
1.75

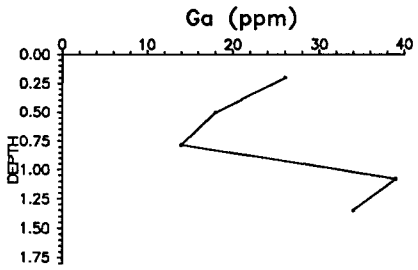
Ga (ppm)
0
10
20
30
40
DEPTH
0.00
0.25
0.50
0.75
1.00
1.25
1.50
1.75

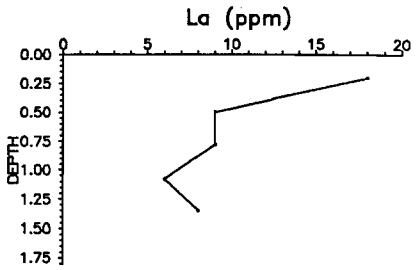
La (ppm)
0
5
10
15
20
DEPTH
0.00
0.25
0.50
0.75
1.00
1.25
1.50
1.75

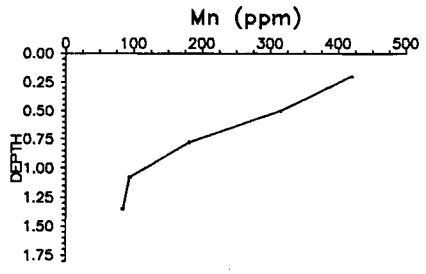
Mn (ppm)
0
100
200
300
400
500
DEPTH
0.00
0.25
0.50
0.75
1.00
1.25
1.50
1.75

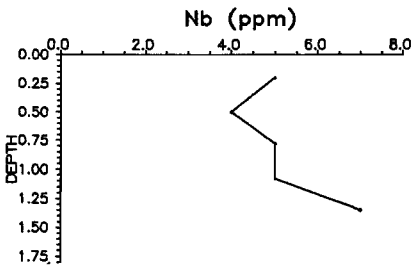
Nb (ppm)
0.0
2.0
4.0
6.0
8.0
DEPTH
0.00
0.25
0.50
0.75
1.00
1.25
1.50
1.75

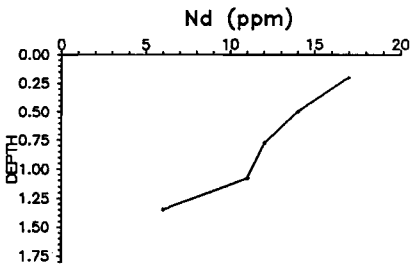
Nd (ppm)
0
5
10
15
20
DEPTH
0.00
0.25
0.50
0.75
1.00
1.25
1.50
1.75

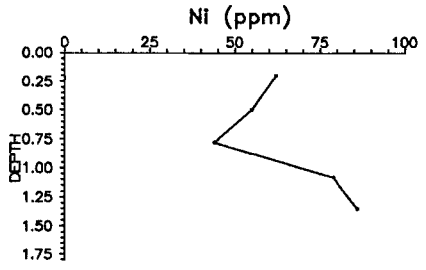
Ni (ppm)
0
25
50
75
100
DEPTH
0.00
0.25
0.50
0.75
1.00
1.25
1.50
1.75

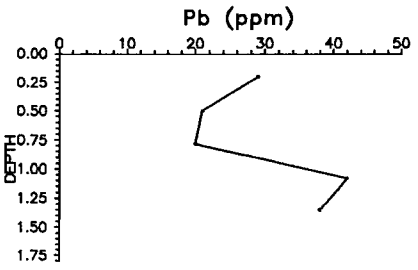
Pb (ppm)
0
10
20
30
40
50
DEPTH
0.00
0.25
0.50
0.75
1.00
1.25
1.50
1.75

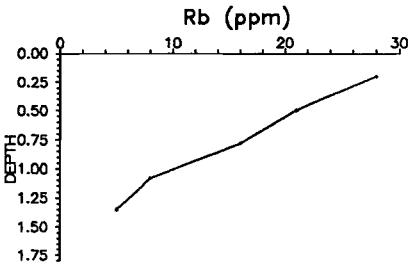
Rb (ppm)
0
10
20
30
DEPTH
0.00
0.25
0.50
0.75
1.00
1.25
1.50
1.75

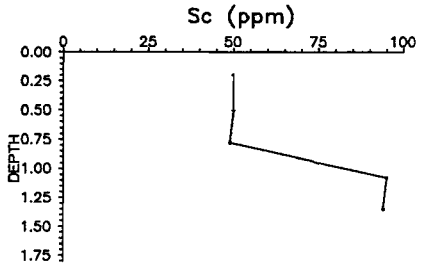
Sc (ppm)
0
25
50
75
100
DEPTH
0.00
0.25
0.50
0.75
1.00
1.25
1.50
1.75

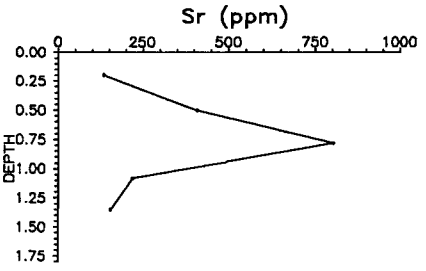
Sr (ppm)
0
250
500
750
1000
DEPTH
0.00
0.25
0.50
0.75
1.00
1.25
1.50
1.75

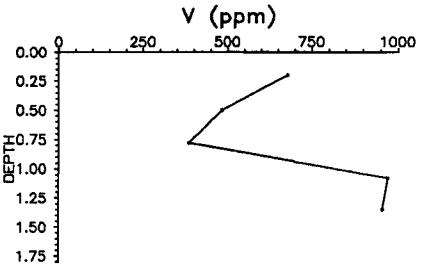
V (ppm)
0
250
500
750
1000
DEPTH
0.00
0.25
0.50
0.75
1.00
1.25
1.50
1.75

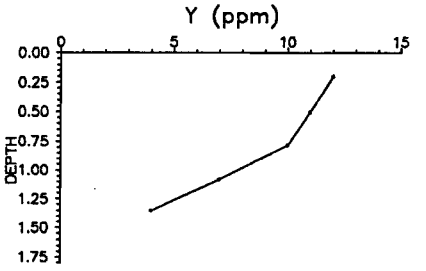
Y (ppm)
0
5
10
15
DEPTH
0.00
0.25
0.50
0.75
1.00
1.25
1.50
1.75

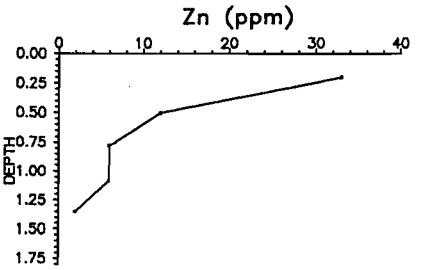
Zn (ppm)
0
10
20
30
40
DEPTH
0.00
0.25
0.50
0.75
1.00
1.25
1.50
1.75

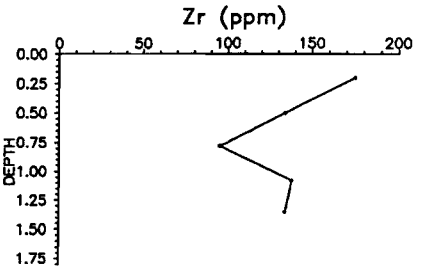
Zr (ppm)
0
50
100
150
200
DEPTH
0.00
0.25
0.50
0.75
1.00
1.25
1.50
1.75

3.1.2 Profile 4161 (10400E 12744N)

Depth (m)	Field description
0-0.3	Red calcareous clay loam
0.3-0.9	Coarse carbonate nodules, some enclosing ferruginous pisoliths, in calcareous clay matrix overlying massive calcrete
0.9-1.7	Massive calcrete enclosing ferruginous pisoliths
1.7-1.9	Fe oxide-rich pisoliths in carbonate

Samples from this profile are taken from the massive carbonate bar described in Section 3.1. They are dominated by carbonate, although significant amounts of ferruginous pisolitic material are found at the surface and cemented within massive carbonate exposed in the trench. The carbonate distribution, as reflected by the Ca values, is bi-modal with nodular carbonate (mostly calcite) occurring in the top half of the profile and massive calcrete (calcite and some dolomite) in the lower half. Sulphur (and Sr) has a similar distribution to Ca whereas Fe, Si, Al and Ti distributions are antipathetic to those of the alkaline earth metals.

Gold behaviour within this profile appears to related to Ca above 0.75m and to Fe below 0.75m. It also appears that the Au distribution is related to the form of the carbonate, being more concentrated in the friable and nodular material than in the massive calcrete. The peak Au concentration (1.44 ppm, sample 4163) is coincident with the Ca maximum (27.9% CaO, or 50% $CaCO_3$), in calcareous clays with carbonate nodules. Separation of the carbonate fraction from this sample resulted in concentrations increasing to 1.50 ppm Au and 33.3% CaO (see Appendix 1). Similarly, Au is contained in carbonates separated from similar, slightly less calcareous material of sample 4164; the bulk sample contained 12% CaO and 1.12 ppm Au and the carbonate separations contained 24.6% CaO and 1.20 ppm Au. Clean separations were not possible, due to the presence of very fine Fe oxides, silica and clay minerals cemented by the carbonates, but the data confirm the association between Au and secondary carbonate.

Chromium, Co, Cu, Ga, Nb, Ni, Pb, Sc, V and Zr concentrations appear to be negatively correlated with Ca. Phosphorus, Ce, La, Mn, Y and Zn concentrations are higher at the surface and decrease with depth, although Mn appears to be enriched in some massive carbonate samples.

Figure 4: Distribution of elements in Profile 4161. (following pages)

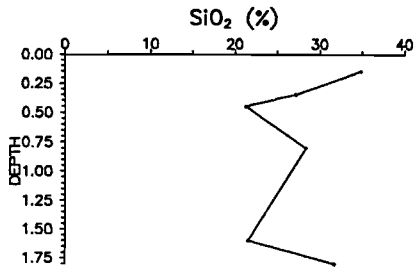
SiO2 (%)
0 10 20 30 40
DEPTH
0.00 0.25 0.50 0.75 1.00 1.25 1.50 1.75

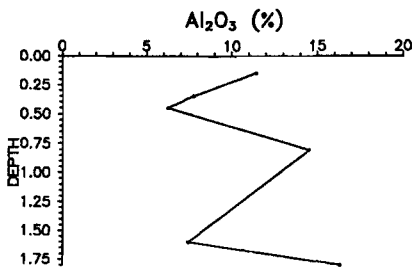
Al2O3 (%)
0 5 10 15 20
DEPTH
0.00 0.25 0.50 0.75 1.00 1.25 1.50 1.75

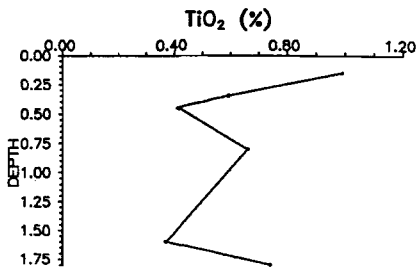
TiO2 (%)
0.00 0.40 0.80 1.20
DEPTH
0.00 0.25 0.50 0.75 1.00 1.25 1.50 1.75

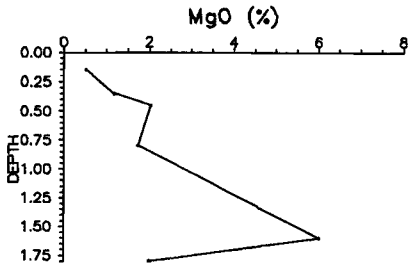
MgO (%)
0 2 4 6 8
DEPTH
0.00 0.25 0.50 0.75 1.00 1.25 1.50 1.75

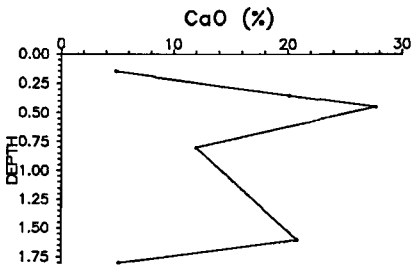
CaO (%)
0 10 20 30
DEPTH
0.00 0.25 0.50 0.75 1.00 1.25 1.50 1.75

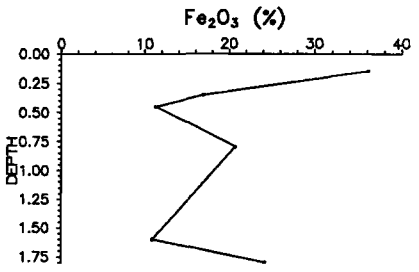
Fe2O3 (%)
0 10 20 30 40
DEPTH
0.00 0.25 0.50 0.75 1.00 1.25 1.50 1.75

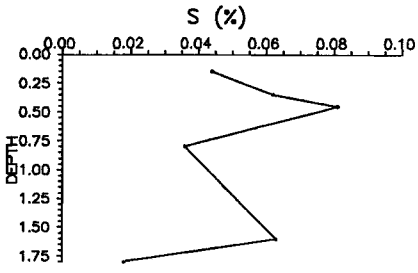
S (%)
0.00 0.02 0.04 0.06 0.08 0.10
DEPTH
0.00 0.25 0.50 0.75 1.00 1.25 1.50 1.75

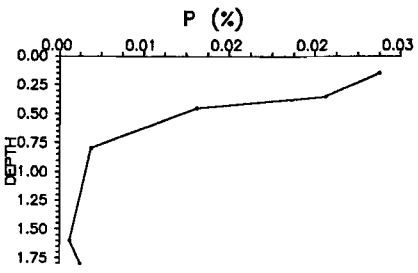
P (%)
0.00 0.01 0.02 0.02 0.03
DEPTH
0.00 0.25 0.50 0.75 1.00 1.25 1.50 1.75

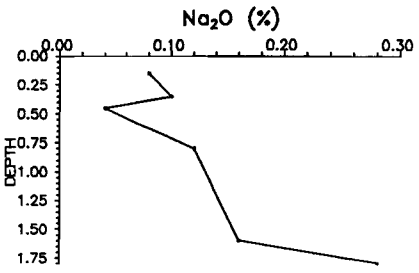
Na2O (%)
0.00 0.10 0.20 0.30
DEPTH
0.00 0.25 0.50 0.75 1.00 1.25 1.50 1.75

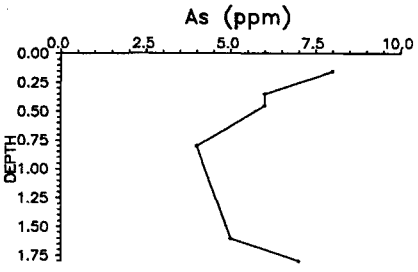
As (ppm)
0.0 2.5 5.0 7.5 10.0
DEPTH
0.00 0.25 0.50 0.75 1.00 1.25 1.50 1.75

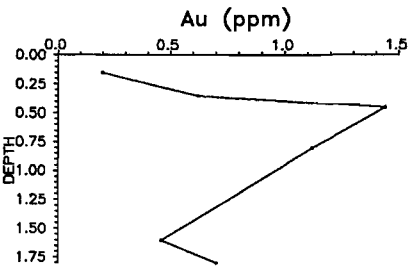
Au (ppm)
0.0 0.5 1.0 1.5
DEPTH
0.00 0.25 0.50 0.75 1.00 1.25 1.50 1.75

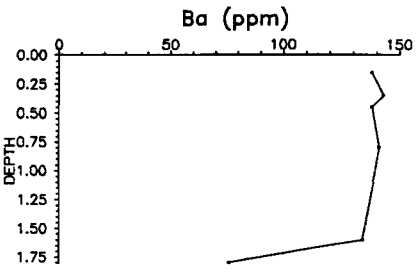
Ba (ppm)
0 50 100 150
DEPTH
0.00 0.25 0.50 0.75 1.00 1.25 1.50 1.75

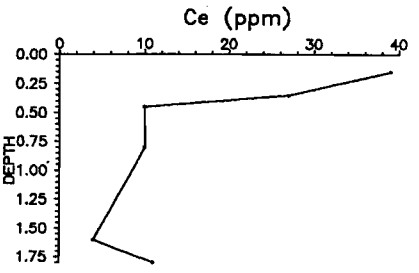
Ce (ppm)
0 10 20 30 40
DEPTH
0.00 0.25 0.50 0.75 1.00 1.25 1.50 1.75

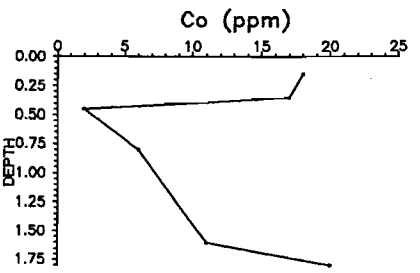
Co (ppm)
0 5 10 15 20 25
DEPTH
0.00 0.25 0.50 0.75 1.00 1.25 1.50 1.75

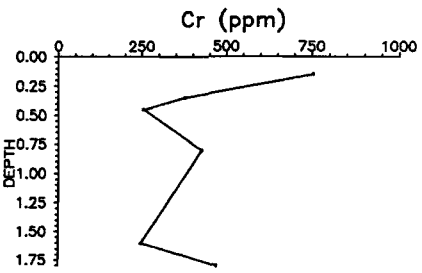
Cr (ppm)
0 250 500 750 1000
DEPTH
0.00 0.25 0.50 0.75 1.00 1.25 1.50 1.75

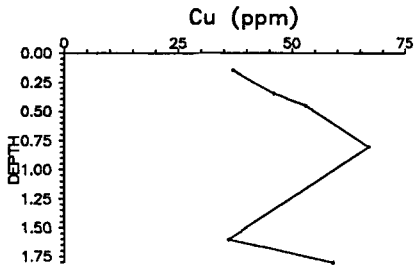
Cu (ppm)
0
25
50
75
DEPTH
0.00
0.25
0.50
0.75
1.00
1.25
1.50
1.75

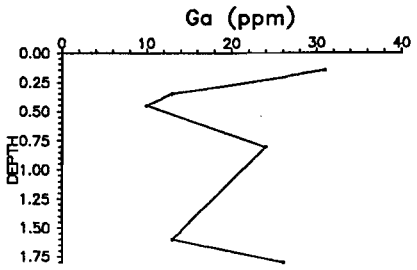
Ga (ppm)
0
10
20
30
40
DEPTH
0.00
0.25
0.50
0.75
1.00
1.25
1.50
1.75

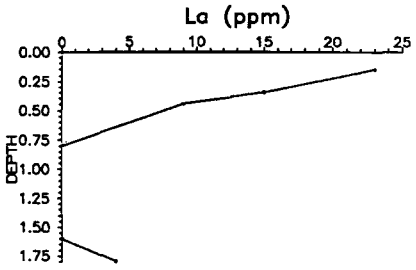
La (ppm)
0
5
10
15
20
25
DEPTH
0.00
0.25
0.50
0.75
1.00
1.25
1.50
1.75

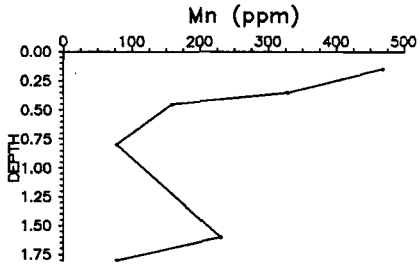
Mn (ppm)
0
100
200
300
400
500
DEPTH
0.00
0.25
0.50
0.75
1.00
1.25
1.50
1.75

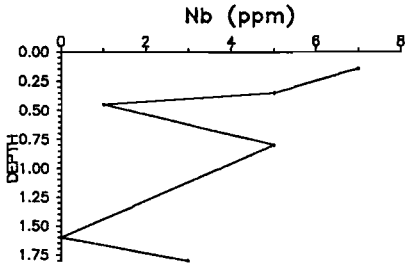
Nb (ppm)
0
2
4
6
8
DEPTH
0.00
0.25
0.50
0.75
1.00
1.25
1.50
1.75

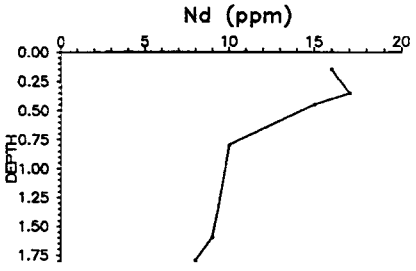
Nd (ppm)
0
5
10
15
20
DEPTH
0.00
0.25
0.50
0.75
1.00
1.25
1.50
1.75

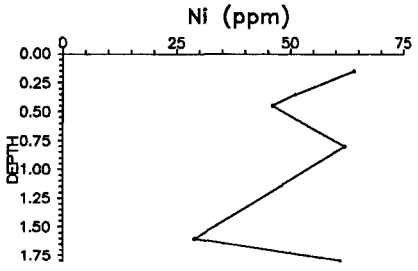
Ni (ppm)
0
25
50
75
DEPTH
0.00
0.25
0.50
0.75
1.00
1.25
1.50
1.75

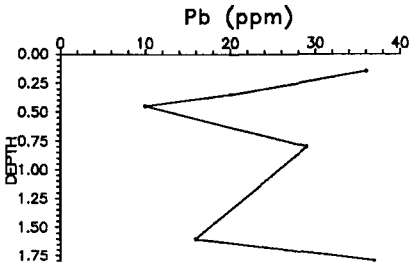
Pb (ppm)
0
10
20
30
40
DEPTH
0.00
0.25
0.50
0.75
1.00
1.25
1.50
1.75

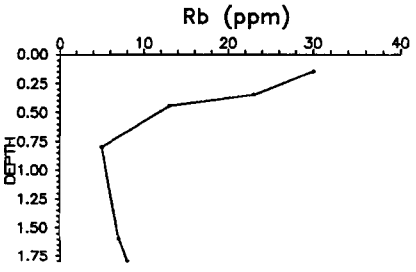
Rb (ppm)
0
10
20
30
40
DEPTH
0.00
0.25
0.50
0.75
1.00
1.25
1.50
1.75

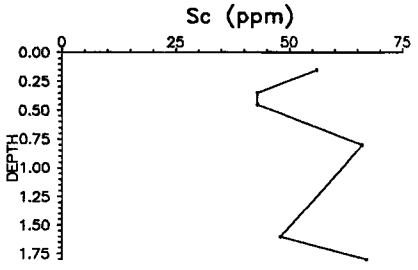
Sc (ppm)
0
25
50
75
DEPTH
0.00
0.25
0.50
0.75
1.00
1.25
1.50
1.75

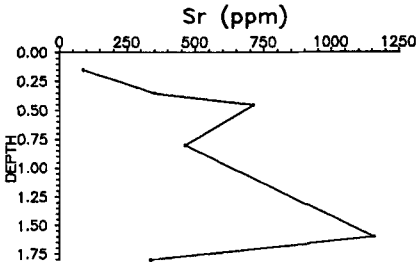
Sr (ppm)
0
250
500
750
1000
1250
DEPTH
0.00
0.25
0.50
0.75
1.00
1.25
1.50
1.75

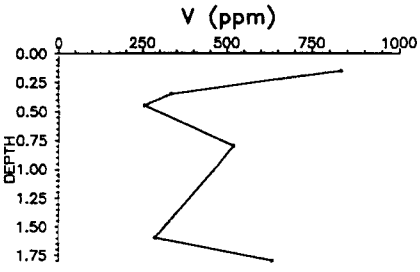
V (ppm)
0
250
500
750
1000
DEPTH
0.00
0.25
0.50
0.75
1.00
1.25
1.50
1.75

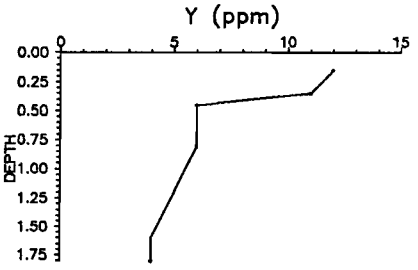
Y (ppm)
0
5
10
15
DEPTH
0.00
0.25
0.50
0.75
1.00
1.25
1.50
1.75

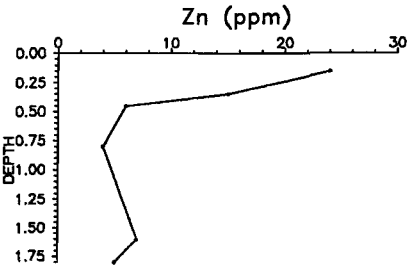
Zn (ppm)
0
10
20
30
DEPTH
0.00
0.25
0.50
0.75
1.00
1.25
1.50
1.75

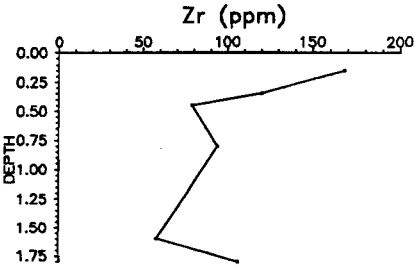
Zr (ppm)
0
50
100
150
200
DEPTH
0.00
0.25
0.50
0.75
1.00
1.25
1.50
1.75

3.1.3 Profile 4169 (10400E 12735N)

Depth (m)	Field description
0-0.2	Red calcareous loam; some large (>5 cm) fragmented calcrete nodules and Fe oxide-rich pisoliths
0.2-0.3	Red loam with Fe oxide-rich pisoliths and large (>5 cm) calcareous nodules
0.3-0.4	Large carbonate nodules in light brown calcareous clay matrix
0.4-1.2	Calcareous nodules with Fe oxide-rich pisoliths in calcareous clay matrix
1.1-1.8	Fe oxide-rich pisoliths, pseudo-bedded in carbonate matrix

Carbonate (predominantly calcite) is present throughout the profile, particularly in the large nodules. Magnesium is present in small quantities in the nodules but in larger amounts in the matrix in the lower part of the profile. Sulphur distribution is related more to Ca than to Mg. There is an antipathetic relationship between Al, Ti and Fe and the alkaline earth metals. In general, the fluctuating abundances reflect variations in the proportions of ferruginous nodules to calcareous matrix within each sample. However, the Au distribution is not obviously related to any one particular phase, and the peak value (1.4 ppm) occurs at about 1.3m.

Cobalt, Cr, Cu, Ga, La, Nb, Ni, Pb, Sc and V show strong (and P, Ce, Rb, Y and Zn weak) negative associations with the distribution of the alkaline earth metal elements. These elements may be associated with clay or iron oxide phases within the soil or just represent a dilution effect caused by the carbonate. Manganese decreases with increasing depth.

Figure 4: Distribution of elements in Profile 4169. (following pages)

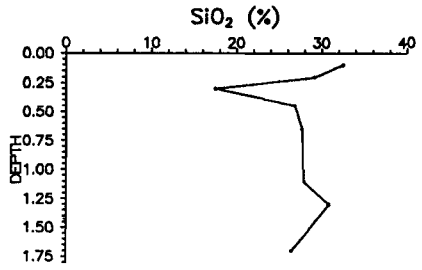
SiO2 (%)
0
10
20
30
40
DEPTH
0.00
0.25
0.50
0.75
1.00
1.25
1.50
1.75

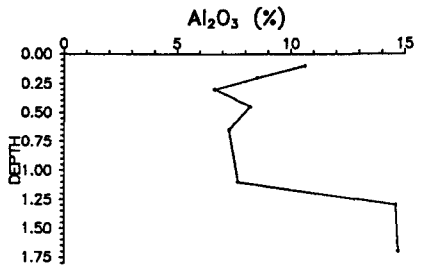
Al2O3 (%)
0
5
10
15
DEPTH
0.00
0.25
0.50
0.75
1.00
1.25
1.50
1.75

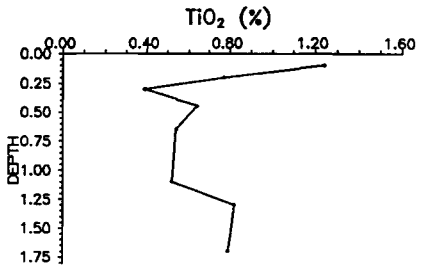
TiO2 (%)
0.00
0.40
0.80
1.20
1.60
DEPTH
0.00
0.25
0.50
0.75
1.00
1.25
1.50
1.75

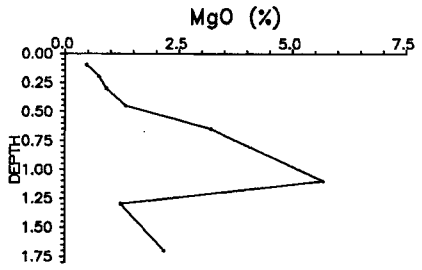
MgO (%)
0.0
2.5
5.0
7.5
DEPTH
0.00
0.25
0.50
0.75
1.00
1.25
1.50
1.75

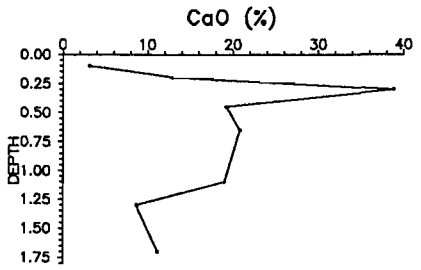
CaO (%)
0
10
20
30
40
DEPTH
0.00
0.25
0.50
0.75
1.00
1.25
1.50
1.75

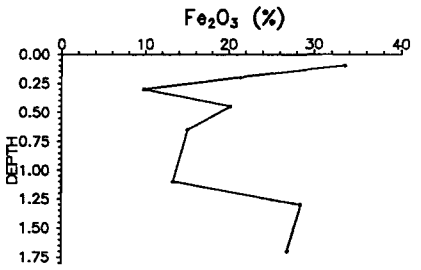
Fe2O3 (%)
0
10
20
30
40
DEPTH
0.00
0.25
0.50
0.75
1.00
1.25
1.50
1.75

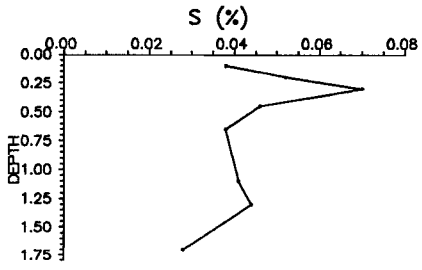
S (%)
0.00
0.02
0.04
0.06
0.08
DEPTH
0.00
0.25
0.50
0.75
1.00
1.25
1.50
1.75

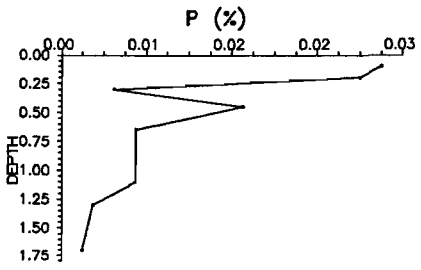
P (%)
0.00
0.01
0.02
0.02
0.03
DEPTH
0.00
0.25
0.50
0.75
1.00
1.25
1.50
1.75

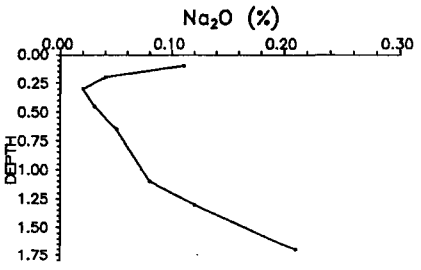
Na2O (%)
0.00
0.10
0.20
0.30
DEPTH
0.00
0.25
0.50
0.75
1.00
1.25
1.50
1.75

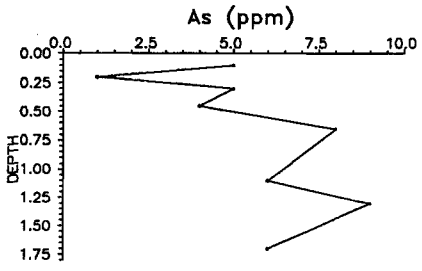
As (ppm)
0.0
2.5
5.0
7.5
10.0
DEPTH
0.00
0.25
0.50
0.75
1.00
1.25
1.50
1.75

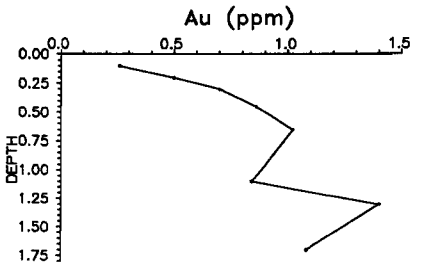
Au (ppm)
0.0
0.5
1.0
1.5
DEPTH
0.00
0.25
0.50
0.75
1.00
1.25
1.50
1.75

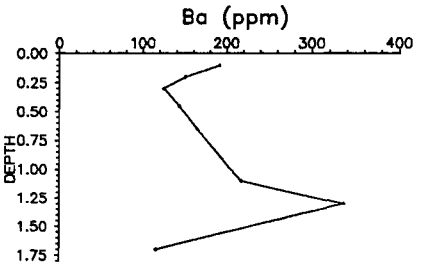
Ba (ppm)
0
100
200
300
400
DEPTH
0.00
0.25
0.50
0.75
1.00
1.25
1.50
1.75

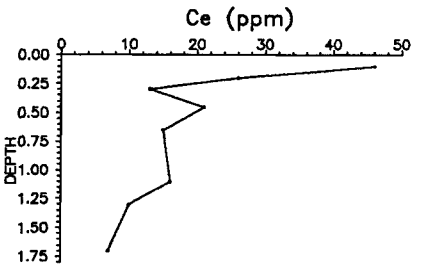
Ce (ppm)
0
10
20
30
40
50
DEPTH
0.00
0.25
0.50
0.75
1.00
1.25
1.50
1.75

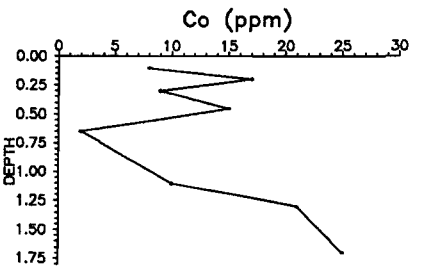
Co (ppm)
0
5
10
15
20
25
30
DEPTH
0.00
0.25
0.50
0.75
1.00
1.25
1.50
1.75

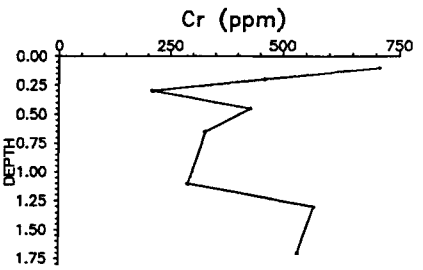
Cr (ppm)
0
250
500
750
DEPTH
0.00
0.25
0.50
0.75
1.00
1.25
1.50
1.75

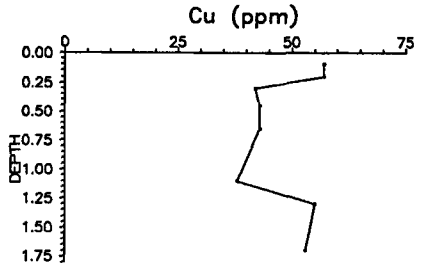
Cu (ppm)
0
25
50
75
DEPTH
0.00
0.25
0.50
0.75
1.00
1.25
1.50
1.75

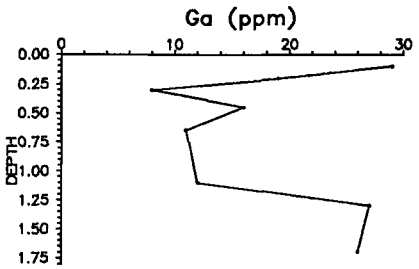
Ga (ppm)
0
10
20
30
DEPTH
0.00
0.25
0.50
0.75
1.00
1.25
1.50
1.75

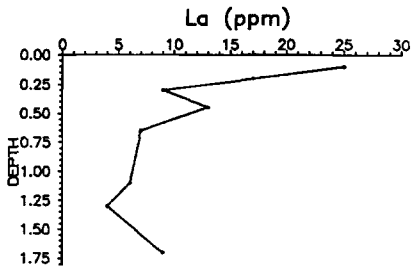
La (ppm)
0
5
10
15
20
25
30
DEPTH
0.00
0.25
0.50
0.75
1.00
1.25
1.50
1.75

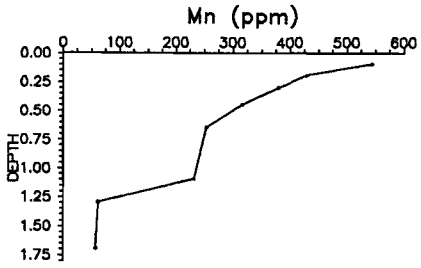
Mn (ppm)
0
100
200
300
400
500
600
DEPTH
0.00
0.25
0.50
0.75
1.00
1.25
1.50
1.75

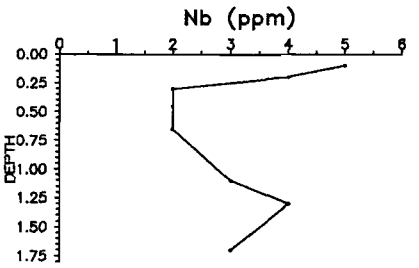
Nb (ppm)
0
1
2
3
4
5
6
DEPTH
0.00
0.25
0.50
0.75
1.00
1.25
1.50
1.75

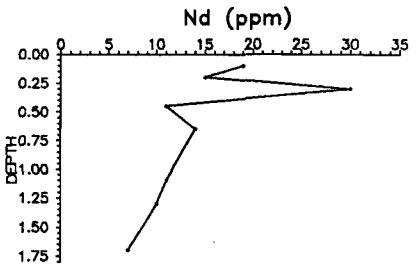
Nd (ppm)
0
5
10
15
20
25
30
35
DEPTH
0.00
0.25
0.50
0.75
1.00
1.25
1.50
1.75

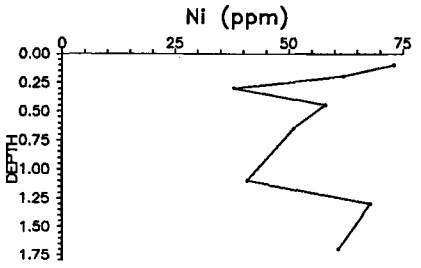
Ni (ppm)
0
25
50
75
DEPTH
0.00
0.25
0.50
0.75
1.00
1.25
1.50
1.75

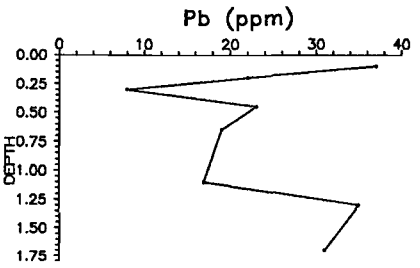
Pb (ppm)
0
10
20
30
40
DEPTH
0.00
0.25
0.50
0.75
1.00
1.25
1.50
1.75

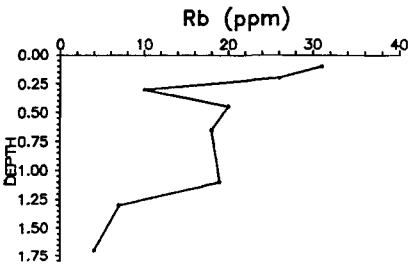
Rb (ppm)
0
10
20
30
40
DEPTH
0.00
0.25
0.50
0.75
1.00
1.25
1.50
1.75

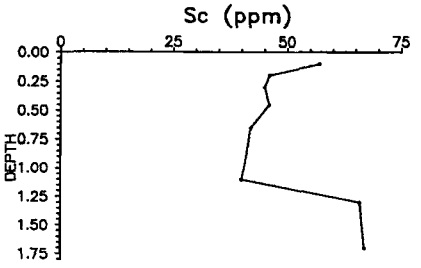
Sc (ppm)
0
25
50
75
DEPTH
0.00
0.25
0.50
0.75
1.00
1.25
1.50
1.75

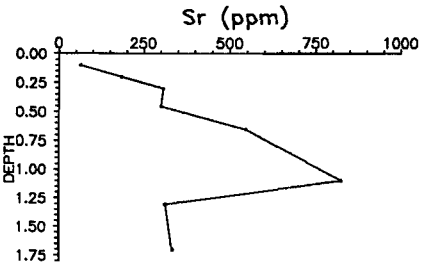
Sr (ppm)
0
250
500
750
1000
DEPTH
0.00
0.25
0.50
0.75
1.00
1.25
1.50
1.75

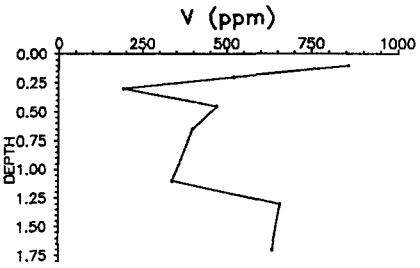
V (ppm)
0
250
500
750
1000
DEPTH
0.00
0.25
0.50
0.75
1.00
1.25
1.50
1.75

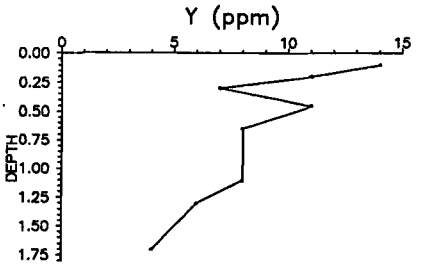
Y (ppm)
0
5
10
15
DEPTH
0.00
0.25
0.50
0.75
1.00
1.25
1.50
1.75

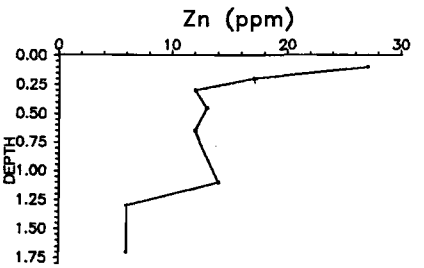
Zn (ppm)
0
10
20
30
DEPTH
0.00
0.25
0.50
0.75
1.00
1.25
1.50
1.75

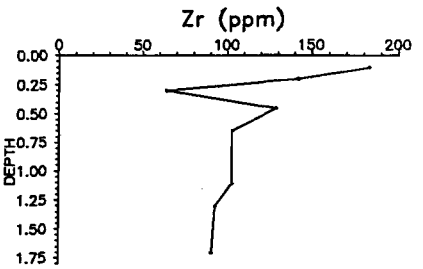
Zr (ppm)
0
50
100
150
200
DEPTH
0.00
0.25
0.50
0.75
1.00
1.25
1.50
1.75

3.1.4 Profile 4177 (10400E 12730N)

Depth (m)	Field description
0-0.2	Red loam; Fe oxide-rich pisoliths; occasional calcareous nodules
0.2-0.4	Transition to nodular calcrete
0.4-0.7	Light brown calcareous loam and calcrete nodules; some Fe-rich pisoliths
0.7-1.2	Fe oxide-rich pisoliths in clay- and carbonate-rich matrix
1.2-1.4	Pseudo-bedded pisoliths with carbonate in sub-horizontal partings

Carbonate is a major component of this profile with Ca concentrations (as calcite) peaking at 0.5m. Magnesium is less abundant but has a similar distribution. This is suggestive of low-Mg calcite or minor dolomite not detected by XRD. With depth, Si and P concentrations decrease, and Al, Na and S concentrations increase. Iron contents gradually decrease with depth with the lowest concentration in the carbonate-rich zone.

The abundance of Au steadily increases with depth and has a maximum of 1.68 ppm near the base of the profile. It does not show, however, clear associations with either Ca or Fe. Separation of samples from within the profile with higher carbonate content (4178C to 4181C, see Appendix 1) significantly decreased the Au concentration. However, sample 4180F, separated from the bulk sample and having a higher Fe content, did not contain more Au than the equivalent sample with high carbonate (4180C). These discrepancies may be due to the different analytical procedures used for the bulk samples and the separations, or illustrate that the Au is preferentially held within fine matrix materials that could not readily be separated, rather than in indurated Ca-Mg carbonates and Fe oxides. The data do, however, demonstrate the associations between Au and both of these mineral phases.

Barium, Sc and Sr concentrations increase and Mn, Nb, Rb, Zn and Zr decrease with greater depth. Arsenic, Ce, Co, Cr, Ga, Nd, Ti, V and Y show some associations with Fe. The associations of the other trace elements are not clear.

Figure 5: Distribution of elements in Profile 4177. (following pages)

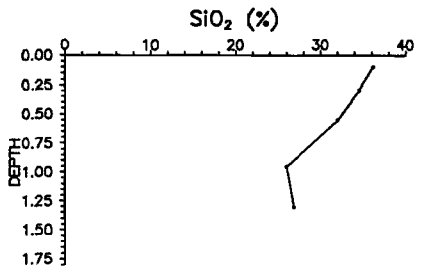
SiO2 (%)
0 10 20 30 40
DEPTH
0.00 0.25 0.50 0.75 1.00 1.25 1.50 1.75

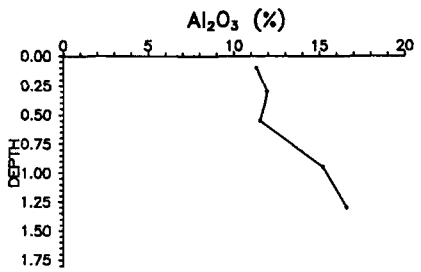
Al2O3 (%)
0 5 10 15 20
DEPTH
0.00 0.25 0.50 0.75 1.00 1.25 1.50 1.75

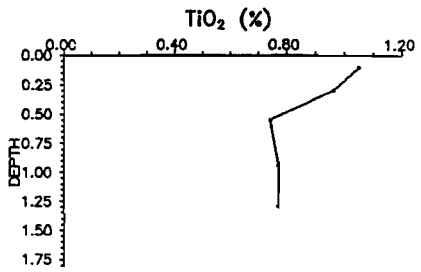
TiO2 (%)
0.00 0.40 0.80 1.20
DEPTH
0.00 0.25 0.50 0.75 1.00 1.25 1.50 1.75

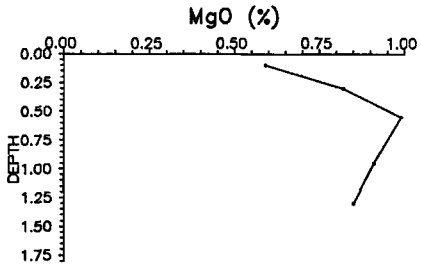
MgO (%)
0.00 0.25 0.50 0.75 1.00
DEPTH
0.00 0.25 0.50 0.75 1.00 1.25 1.50 1.75

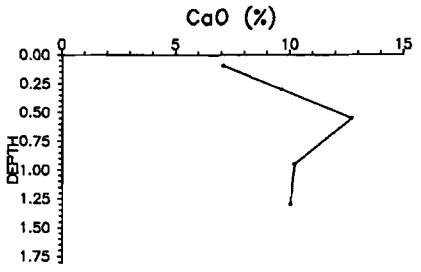
CaO (%)
0 5 10 15
DEPTH
0.00 0.25 0.50 0.75 1.00 1.25 1.50 1.75

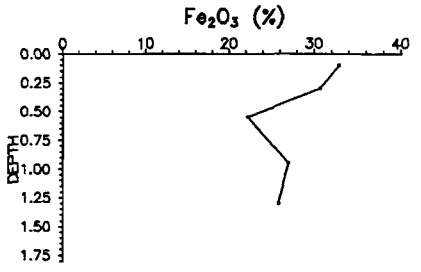
Fe2O3 (%)
0 10 20 30 40
DEPTH
0.00 0.25 0.50 0.75 1.00 1.25 1.50 1.75

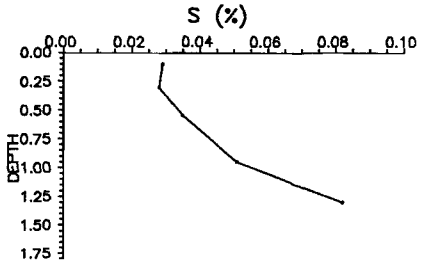
S (%)
0.00 0.02 0.04 0.06 0.08 0.10
DEPTH
0.00 0.25 0.50 0.75 1.00 1.25 1.50 1.75

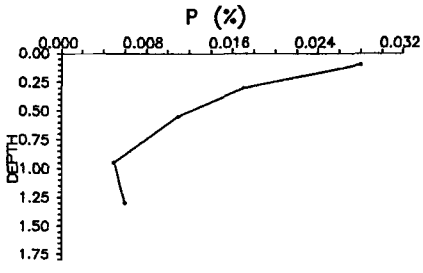
P (%)
0.000 0.008 0.016 0.024 0.032
DEPTH
0.00 0.25 0.50 0.75 1.00 1.25 1.50 1.75

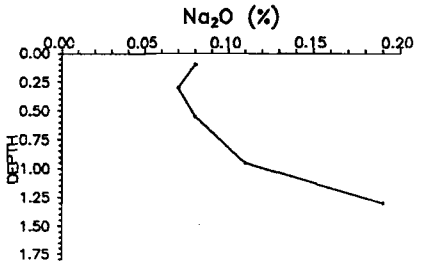
Na2O (%)
0.00 0.05 0.10 0.15 0.20
DEPTH
0.00 0.25 0.50 0.75 1.00 1.25 1.50 1.75

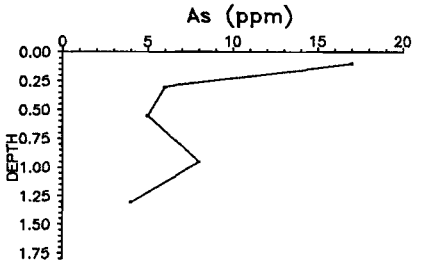
As (ppm)
0 5 10 15 20
DEPTH
0.00 0.25 0.50 0.75 1.00 1.25 1.50 1.75

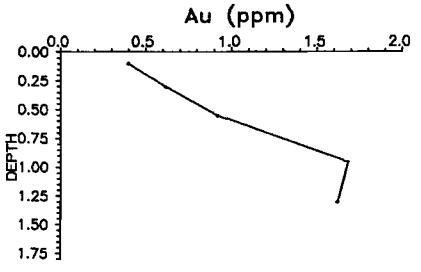
Au (ppm)
0.0 0.5 1.0 1.5 2.0
DEPTH
0.00 0.25 0.50 0.75 1.00 1.25 1.50 1.75

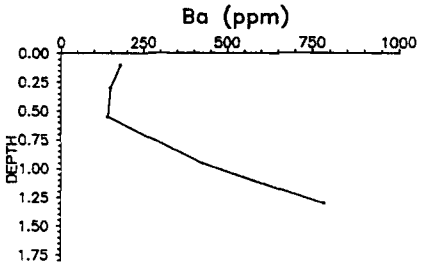
Ba (ppm)
0 250 500 750 1000
DEPTH
0.00 0.25 0.50 0.75 1.00 1.25 1.50 1.75

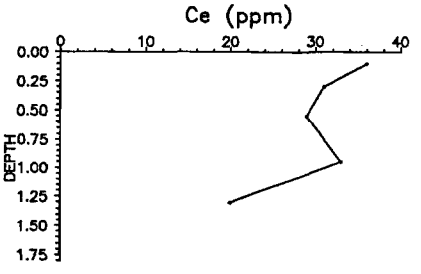
Ce (ppm)
0 10 20 30 40
DEPTH
0.00 0.25 0.50 0.75 1.00 1.25 1.50 1.75

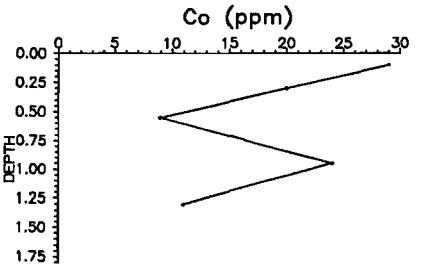
Co (ppm)
0 5 10 15 20 25 30
DEPTH
0.00 0.25 0.50 0.75 1.00 1.25 1.50 1.75

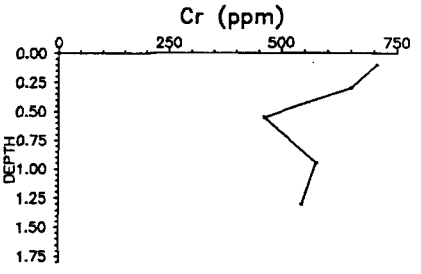
Cr (ppm)
0 250 500 750
DEPTH
0.00 0.25 0.50 0.75 1.00 1.25 1.50 1.75

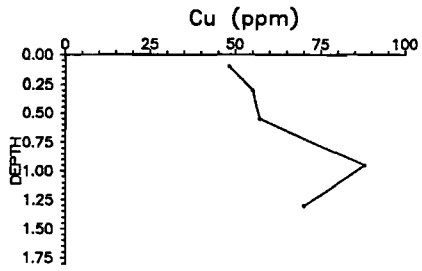
Cu (ppm)
0
25
50
75
100
DEPTH
0.00
0.25
0.50
0.75
1.00
1.25
1.50
1.75

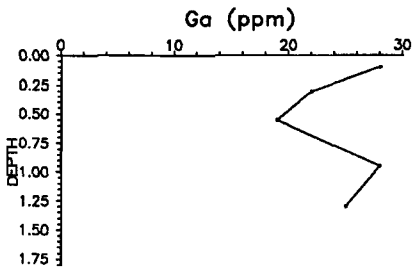
Ga (ppm)
0
10
20
30
DEPTH
0.00
0.25
0.50
0.75
1.00
1.25
1.50
1.75

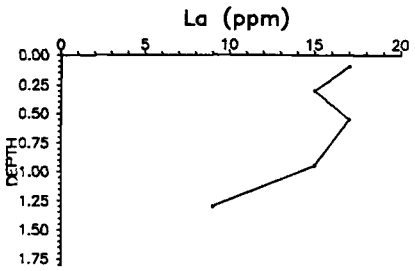
La (ppm)
0
5
10
15
20
DEPTH
0.00
0.25
0.50
0.75
1.00
1.25
1.50
1.75

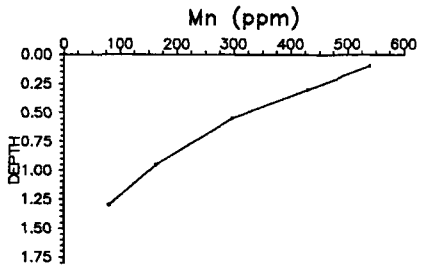
Mn (ppm)
0
100
200
300
400
500
600
DEPTH
0.00
0.25
0.50
0.75
1.00
1.25
1.50
1.75

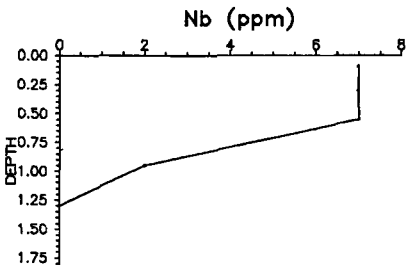
Nb (ppm)
0
2
4
6
8
DEPTH
0.00
0.25
0.50
0.75
1.00
1.25
1.50
1.75

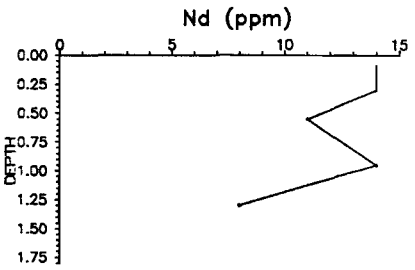
Nd (ppm)
0
5
10
15
DEPTH
0.00
0.25
0.50
0.75
1.00
1.25
1.50
1.75

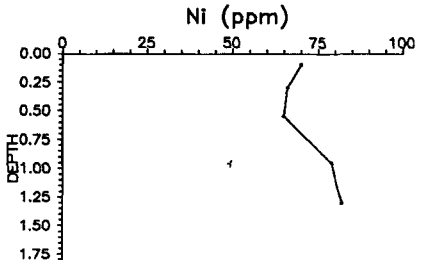
Ni (ppm)
0
25
50
75
100
DEPTH
0.00
0.25
0.50
0.75
1.00
1.25
1.50
1.75

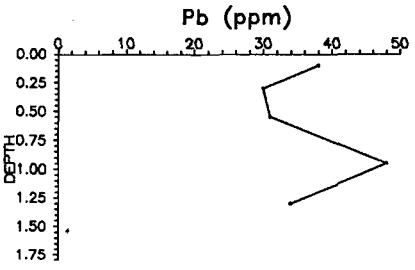
Pb (ppm)
0
10
20
30
40
50
DEPTH
0.00
0.25
0.50
0.75
1.00
1.25
1.50
1.75

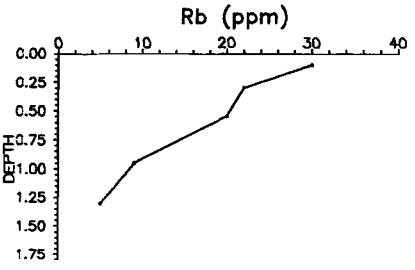
Rb (ppm)
0
10
20
30
40
DEPTH
0.00
0.25
0.50
0.75
1.00
1.25
1.50
1.75

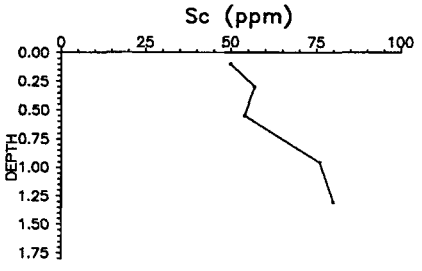
Sc (ppm)
0
25
50
75
100
DEPTH
0.00
0.25
0.50
0.75
1.00
1.25
1.50
1.75

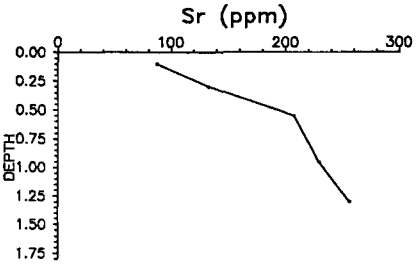
Sr (ppm)
0
100
200
300
DEPTH
0.00
0.25
0.50
0.75
1.00
1.25
1.50
1.75

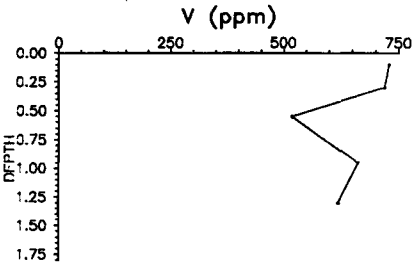
V (ppm)
0
250
500
750
DEPTH
0.00
0.25
0.50
0.75
1.00
1.25
1.50
1.75

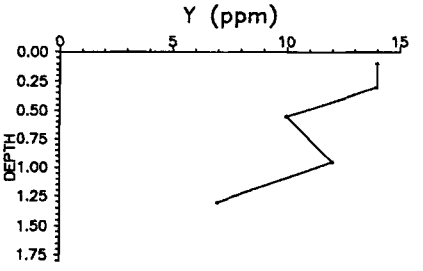
Y (ppm)
0
5
10
15
DEPTH
0.00
0.25
0.50
0.75
1.00
1.25
1.50
1.75

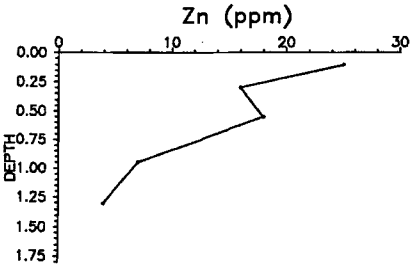
Zn (ppm)
0
10
20
30
DEPTH
0.00
0.25
0.50
0.75
1.00
1.25
1.50
1.75

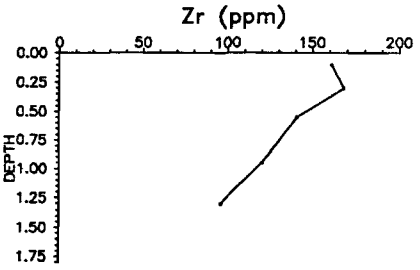
Zr (ppm)
0
50
100
150
200
DEPTH
0.00
0.25
0.50
0.75
1.00
1.25
1.50
1.75

3.1.5 Profile 4201 (10320E 12700N)

This profile was sub-sampled from a RC drill hole at one metre intervals from 0 to 15m. The top three metres are dominated by carbonate enrichment in which a calcite-rich zone appears to overlie a dolomite-rich zone. Gibbsite (reflected in the distribution of Al) sharply increases from the surface to be one of the principal minerals present at 5m, situated beneath the carbonate zone. Below this horizon, quartz, kaolinite and Fe oxide minerals dominate the samples to 15m depth. There is a major zone of goethite and hematite occurring in the middle to the lower half of the profile, which is reflected as the maximum Fe concentration.

Gold is associated with Fe in the upper part of the profile, with maxima at 2.5m (2.04 ppm) and 5.5m (1.53 ppm). Concentrations below 8 metres are background (<0.01 ppm) and are not associated with Fe. There is no apparent association with carbonate.

Chromium, Cu, V and Zr have a general association with Fe in the profile, although, with Ti and Ni, tend to be concentrated with Al in the gibbsite horizon. Manganese decreases with increasing depth, although a local maximum at 10m is coincident with maxima for Cr and V. Barium is associated with the Ca and Mg close to the top of the profile, probably as secondary barite.

Figure 7: Distribution of elements in Profile 4201. (following page)

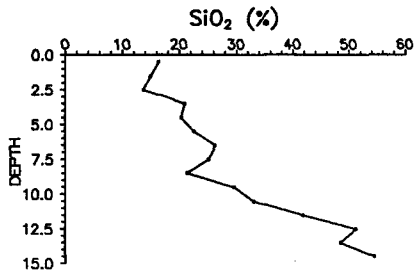
SiO2 (%)
0 10 20 30 40 50 60
DEPTH
0.0 2.5 5.0 7.5 10.0 12.5 15.0

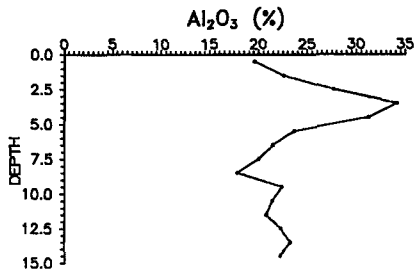
Al2O3 (%)
0 5 10 15 20 25 30 35
DEPTH
0.0 2.5 5.0 7.5 10.0 12.5 15.0

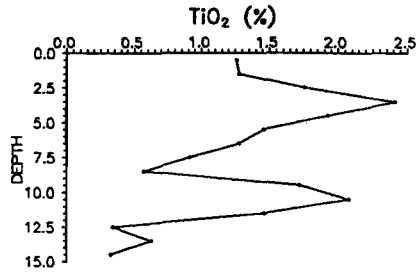
TiO2 (%)
0.0 0.5 1.0 1.5 2.0 2.5
DEPTH
0.0 2.5 5.0 7.5 10.0 12.5 15.0

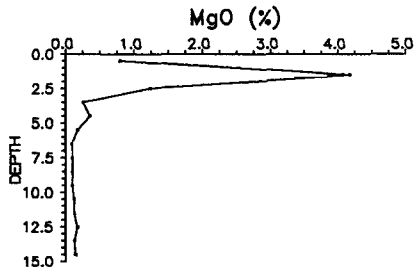
MgO (%)
0.0 1.0 2.0 3.0 4.0 5.0
DEPTH
0.0 2.5 5.0 7.5 10.0 12.5 15.0

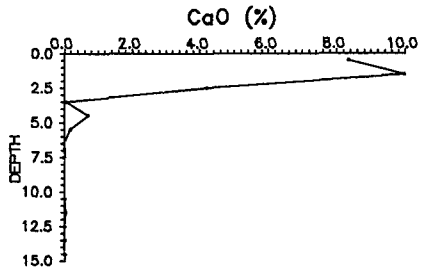
CaO (%)
0.0 2.0 4.0 6.0 8.0 10.0
DEPTH
0.0 2.5 5.0 7.5 10.0 12.5 15.0

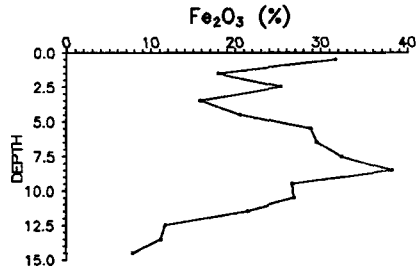
Fe2O3 (%)
0 10 20 30 40
DEPTH
0.0 2.5 5.0 7.5 10.0 12.5 15.0

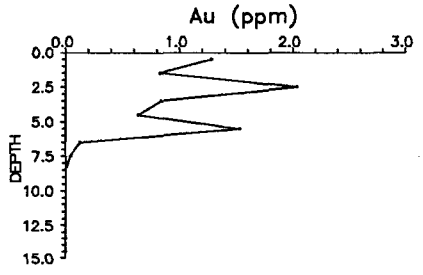
Au (ppm)
0.0 1.0 2.0 3.0
DEPTH
0.0 2.5 5.0 7.5 10.0 12.5 15.0

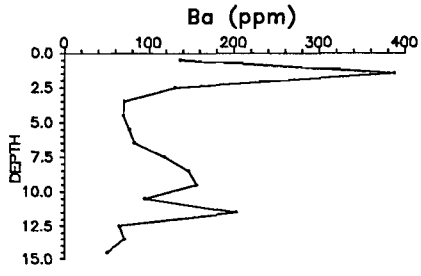
Ba (ppm)
0 100 200 300 400
DEPTH
0.0 2.5 5.0 7.5 10.0 12.5 15.0

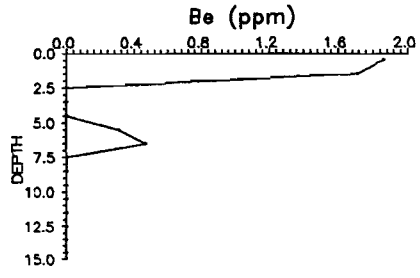
Be (ppm)
0.0 0.4 0.8 1.2 1.6 2.0
DEPTH
0.0 2.5 5.0 7.5 10.0 12.5 15.0

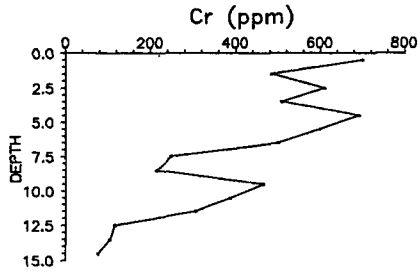
Cr (ppm)
0 200 400 600 800
DEPTH
0.0 2.5 5.0 7.5 10.0 12.5 15.0

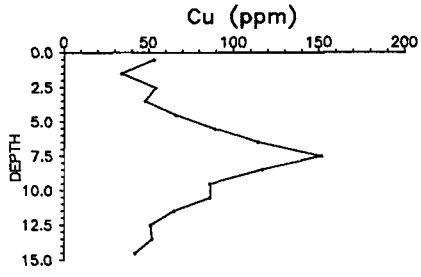
Cu (ppm)
0 50 100 150 200
DEPTH
0.0 2.5 5.0 7.5 10.0 12.5 15.0

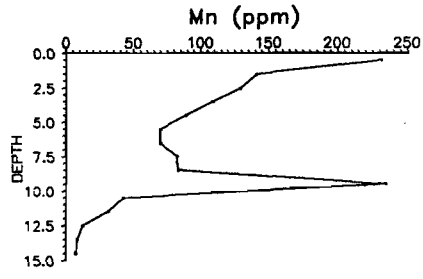
Mn (ppm)
0 50 100 150 200 250
DEPTH
0.0 2.5 5.0 7.5 10.0 12.5 15.0

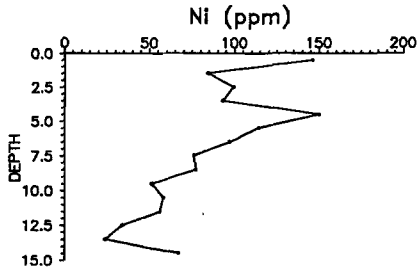
Ni (ppm)
0 50 100 150 200
DEPTH
0.0 2.5 5.0 7.5 10.0 12.5 15.0

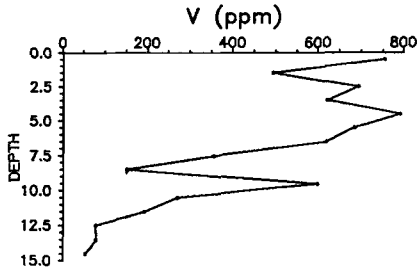
V (ppm)
0 200 400 600 800
DEPTH
0.0 2.5 5.0 7.5 10.0 12.5 15.0

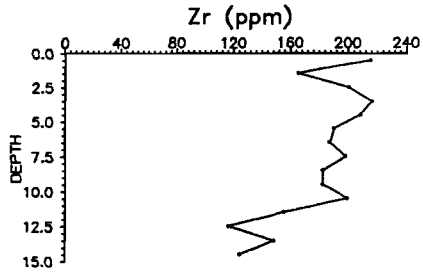
Zr (ppm)
0 40 80 120 160 200 240
DEPTH
0.0 2.5 5.0 7.5 10.0 12.5 15.0

3.1.6 Profile 4246 (10425E 12725N)

This profile was sub-sampled from a RC drill hole at one metre intervals from 0m to 14m and is dominated by hematite and goethite. Quartz abundance is low in the upper part of the profile but increases with depth. Kaolinite is moderately abundant throughout the profile. There is little carbonate present.

Silicon contents increase with depth and have a distribution that is strongly antipathetic to that of Fe. Iron is abundant in the profile and has sharp maxima at 8.5m and 12.5m associated with hematite and goethite. Iron concentrations are generally greater in the top 5m of the profile. Alkaline earth metal concentrations are low throughout the profile, although some Ca may be associated with carbonate near the surface.

The Au distribution is appears strongly related to that of Fe, particularly in the lower part of the profile. The highest Au value occurs near the surface (1.88 ppm), but three other maxima in the profile are coincident with those of Fe.

Chromium, Cu, Mn, Ni, V and Zr distributions are highly correlated and are broadly similar to that of Fe. Barium, Mn and Ni concentrations are greatest near the surface.

Figure 8: Distribution of elements in Profile 4246. (following page)

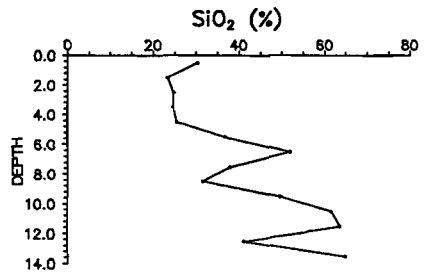
SiO2 (%)
0 20 40 60 80
DEPTH
0.0 2.0 4.0 6.0 8.0 10.0 12.0 14.0

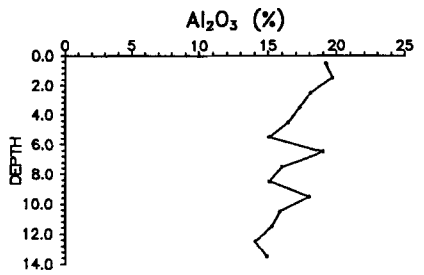
Al2O3 (%)
0 5 10 15 20 25
DEPTH
0.0 2.0 4.0 6.0 8.0 10.0 12.0 14.0

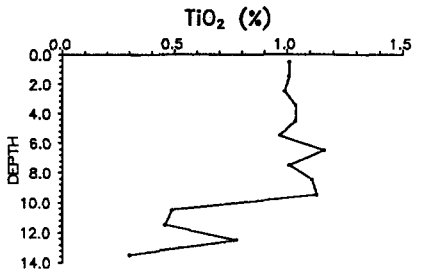
TiO2 (%)
0.0 0.5 1.0 1.5
DEPTH
0.0 2.0 4.0 6.0 8.0 10.0 12.0 14.0

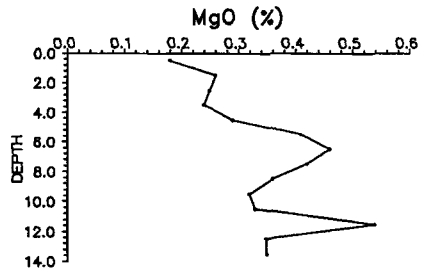
MgO (%)
0.0 0.1 0.2 0.3 0.4 0.5 0.6
DEPTH
0.0 2.0 4.0 6.0 8.0 10.0 12.0 14.0

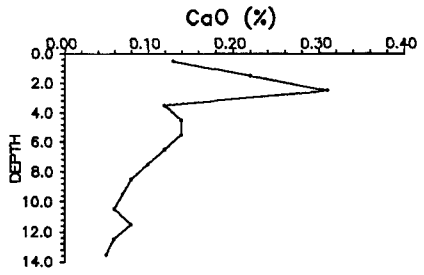
CaO (%)
0.00 0.10 0.20 0.30 0.40
DEPTH
0.0 2.0 4.0 6.0 8.0 10.0 12.0 14.0

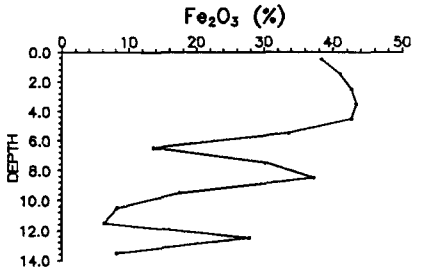
Fe2O3 (%)
0 10 20 30 40 50
DEPTH
0.0 2.0 4.0 6.0 8.0 10.0 12.0 14.0

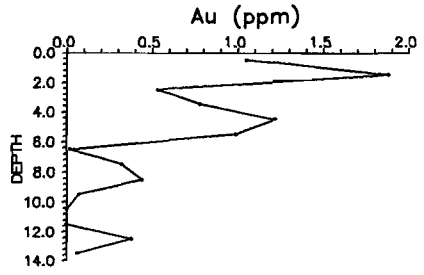
Au (ppm)
0.0 0.5 1.0 1.5 2.0
DEPTH
0.0 2.0 4.0 6.0 8.0 10.0 12.0 14.0

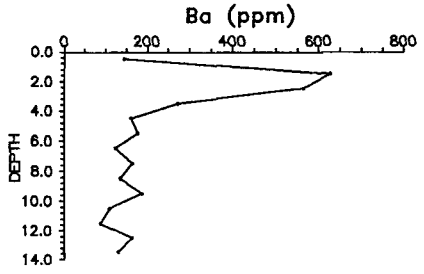
Ba (ppm)
0 200 400 600 800
DEPTH
0.0 2.0 4.0 6.0 8.0 10.0 12.0 14.0

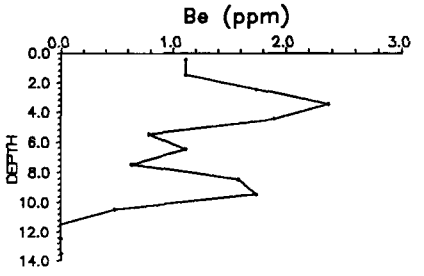
Be (ppm)
0.0 1.0 2.0 3.0
DEPTH
0.0 2.0 4.0 6.0 8.0 10.0 12.0 14.0

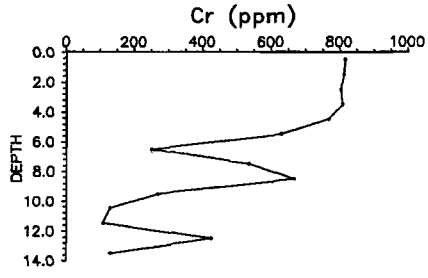
Cr (ppm)
0 200 400 600 800 1000
DEPTH
0.0 2.0 4.0 6.0 8.0 10.0 12.0 14.0

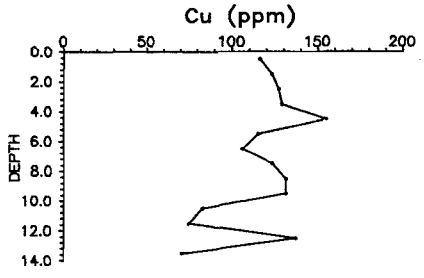
Cu (ppm)
0 50 100 150 200
DEPTH
0.0 2.0 4.0 6.0 8.0 10.0 12.0 14.0

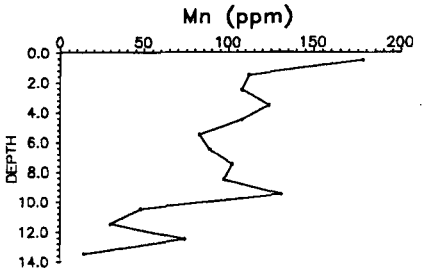
Mn (ppm)
0 50 100 150 200
DEPTH
0.0 2.0 4.0 6.0 8.0 10.0 12.0 14.0

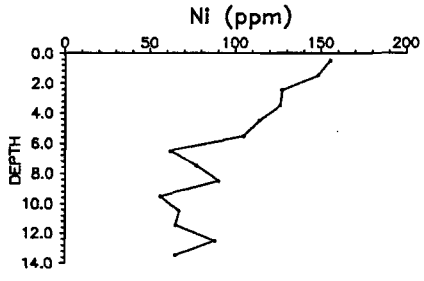
Ni (ppm)
0 50 100 150 200
DEPTH
0.0 2.0 4.0 6.0 8.0 10.0 12.0 14.0

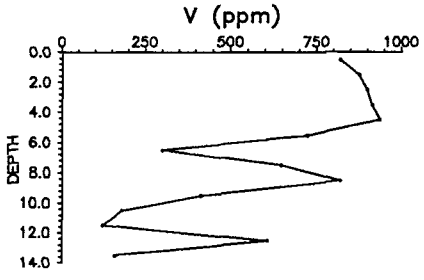
V (ppm)
0 250 500 750 1000
DEPTH
0.0 2.0 4.0 6.0 8.0 10.0 12.0 14.0

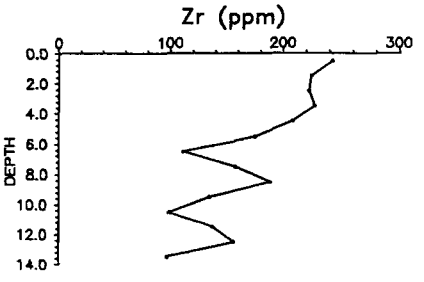
Zr (ppm)
0 100 200 300
DEPTH
0.0 2.0 4.0 6.0 8.0 10.0 12.0 14.0

3.1.7 Traverses

Two traverses were sampled from drill cuttings at 0-1m (topsoil) and 3-4m (subsoil). The two traverses are sufficiently similar in their elemental distribution to be discussed as one, although the Fe contents of the subsoil samples from 12725N (closer to mineralization than 12700N) are significantly higher. This is an important consideration when reporting upon the distribution of minor elements because Fe (as secondary iron oxides) appears to be a major geochemical control. Profile 4246 is located at 12725N and results from these samples (Section 3.1.6) can be referred to for comparative purposes.

Major minerals identified include quartz, kaolinite, goethite, calcite, dolomite, gypsum, feldspar, hematite, gibbsite, smectite, albite, talc, anatase, tremolite and muscovite. Other unidentified, poorly crystalline clay minerals were also present.

The topsoils are carbonate-rich in the western and extreme eastern regions of the traverse and are most carbonate-poor around 10400E (near the centre). The carbonate distribution is best described by those of Ca and Mg, which occur predominantly as calcite and dolomite. Iron occurs within hematite and goethite. There is a general antipathetic relationship between the distributions of Ca and Fe. Silicon values tend to be greater in the carbonate-rich areas and probably represent local accumulations of detrital quartz in the loamy soils. Aluminium concentrations are greatest in the centre of the traverse (at about 10300N) and may relate either to Al substitution in the goethite or hematite or, more probably, local concentrations of gibbsite.

Gold shows some association with Fe although the highest concentration (3.79 ppm at 10475E 12725N) does not appear to be related to any one particular mineral phase. The lowest Au concentrations (0.1 to 0.3 ppm) are found in the most western and eastern samples.

There is a strong correlation between Cr (and to a lesser extent Cu, Ni, V and Zr) and Fe. These elements (except Zr) are probably adsorbed onto secondary iron oxides contained within the lateritic nodules. Zirconium is probably present as fine zircon grains cemented by the Fe oxides or in the sandy matrix.

There is a marked difference in the composition of the subsoil compared to the topsoil. Carbonates from the subsoil are generally much lower in Ca than those from the topsoil. This difference is less pronounced for Mg, suggesting some to be associated with clay minerals as well as in carbonates. Aluminium concentrations are appreciably higher in the subsoil, particularly in the western portion of the traverse, and are probably associated with greater accumulations of kaolinite. The eastern part of the traverse is siliceous whereas the western part is more ferruginous.

The strength of the Au anomaly in the subsoil is weaker than that in the generally more calcareous topsoil, although the distribution is similar; the highest Au concentration, (3.79 ppm), however, occurs at 10475E 12725N in a carbonate-poor, highly ferruginous topsoil sample.

Of the minor and trace elements, the distribution of Cr, V, Zr and Ni in the subsoil shows similarities with that of the topsoil, being related to the distribution of Fe. Copper abundances are similar at both depths, but tend to be slightly higher in the subsoil in the west portion of the profile and, with some elevated Ni concentrations, may be associated with the appearance of tremolite. Some topsoil enrichment relative to the subsoil is found for Mn and Ba.

Figure 9a: Distribution of elements from traverse 12700N.

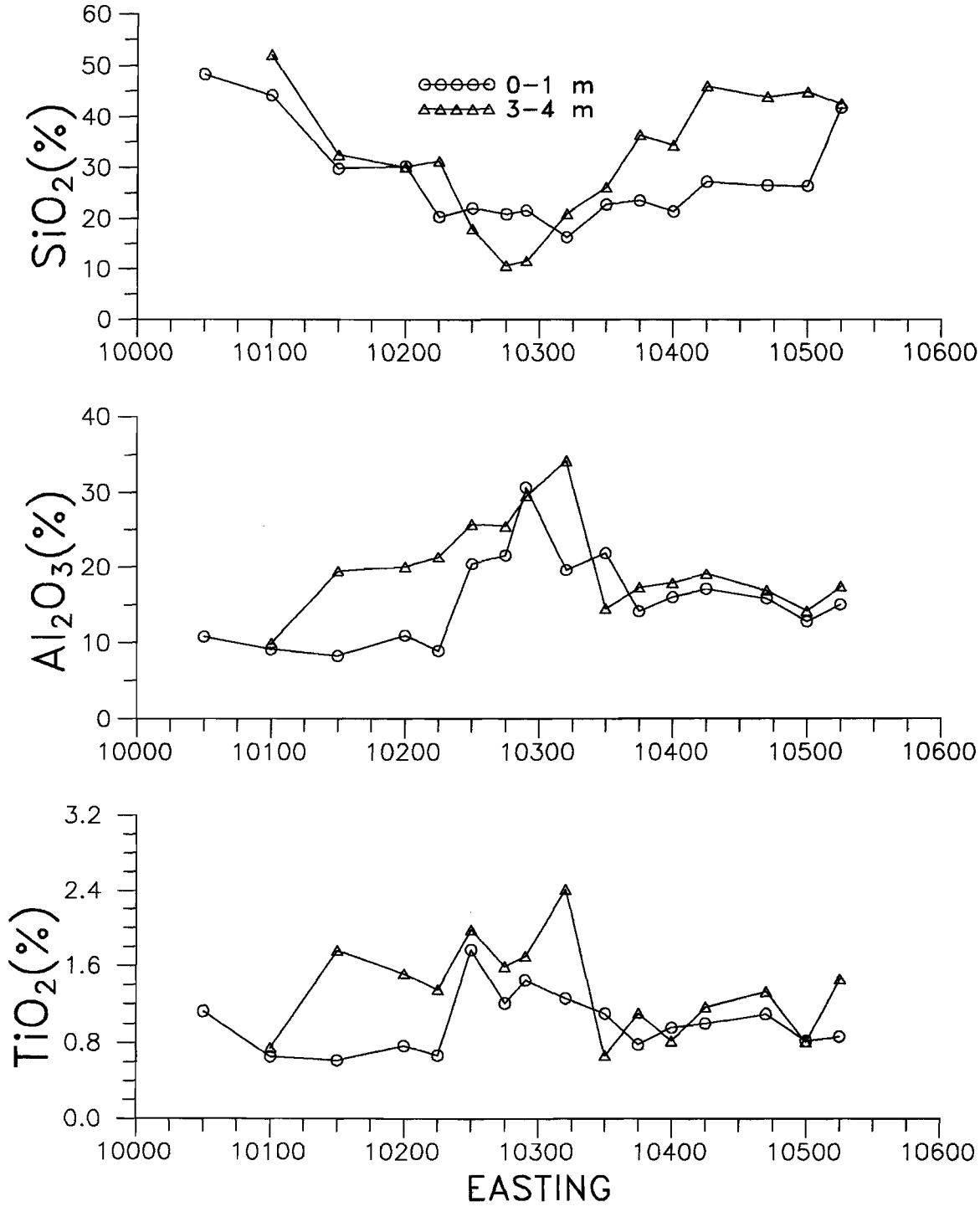

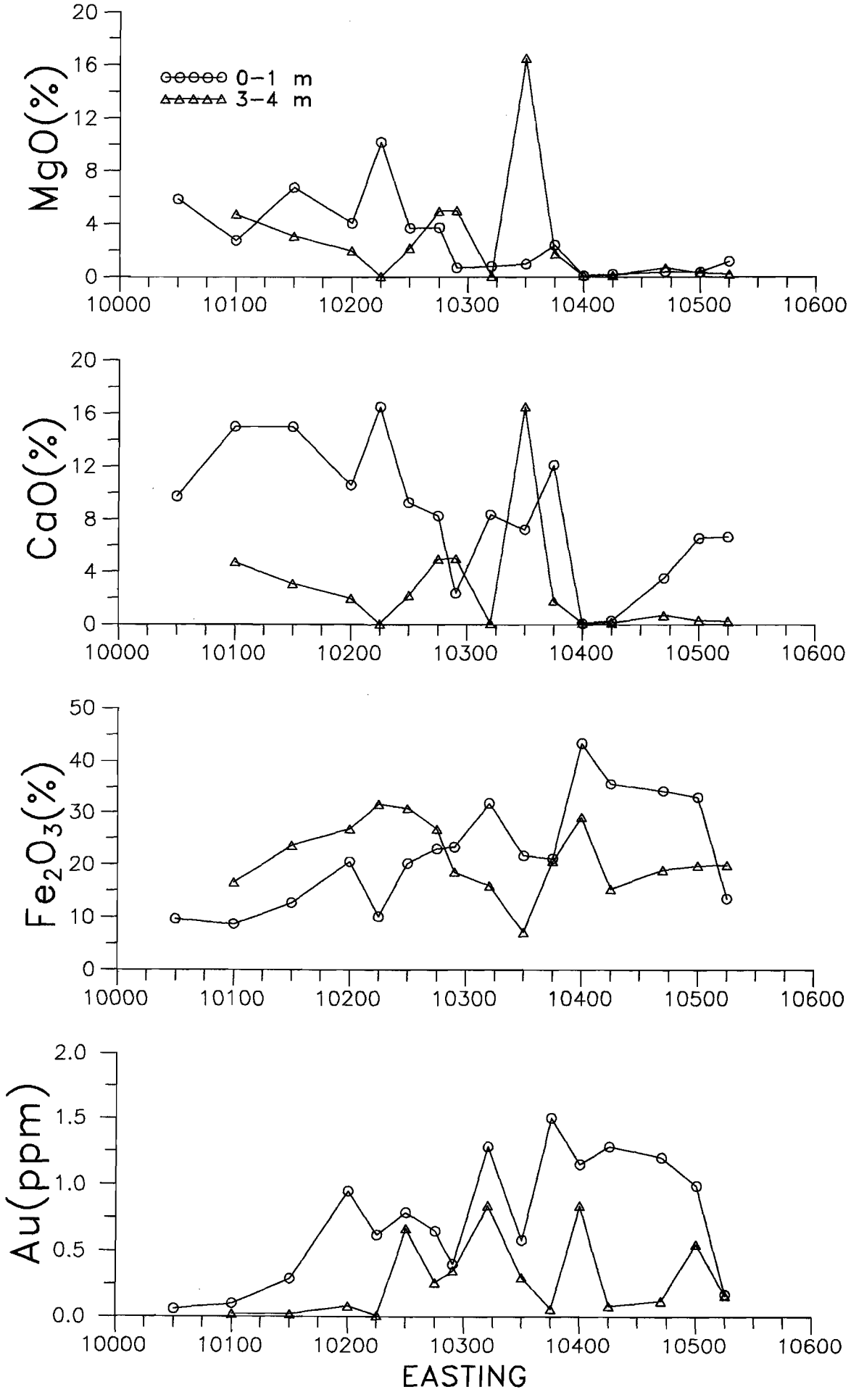
MgO(%)
0–1 m
3–4 m
CaO(%)
Fe_2O_3(%)
Au(ppm)
EASTING
10000
10100
10200
10300
10400
10500
10600

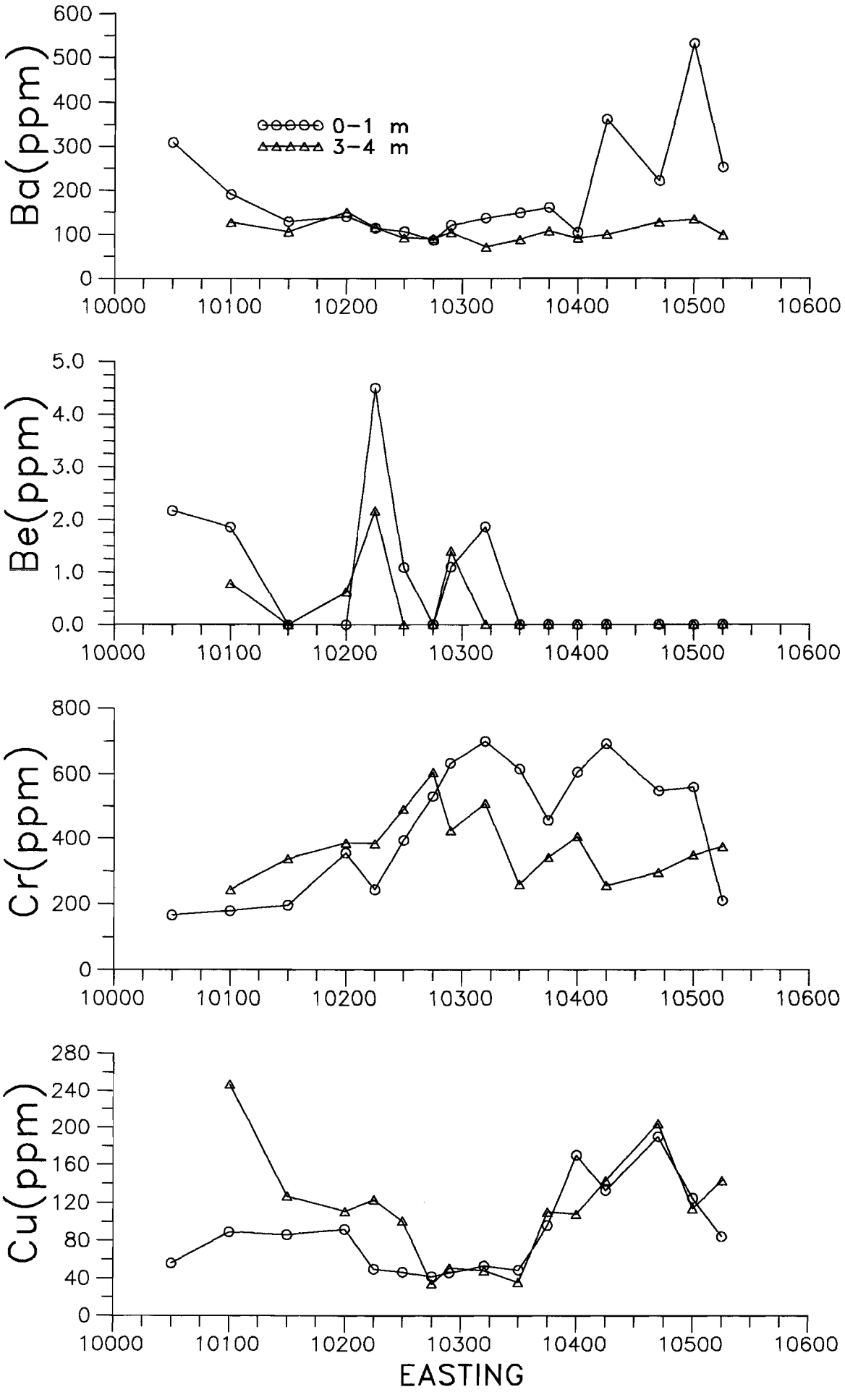
Ba(ppm)
600
500
400
300
200
100
0
0-1 m
3-4 m
10000
10100
10200
10300
10400
10500
10600
Be(ppm)
5.0
4.0
3.0
2.0
1.0
0.0
Cr(ppm)
800
600
400
200
0
Cu(ppm)
280
240
200
160
120
80
40
0
EASTING

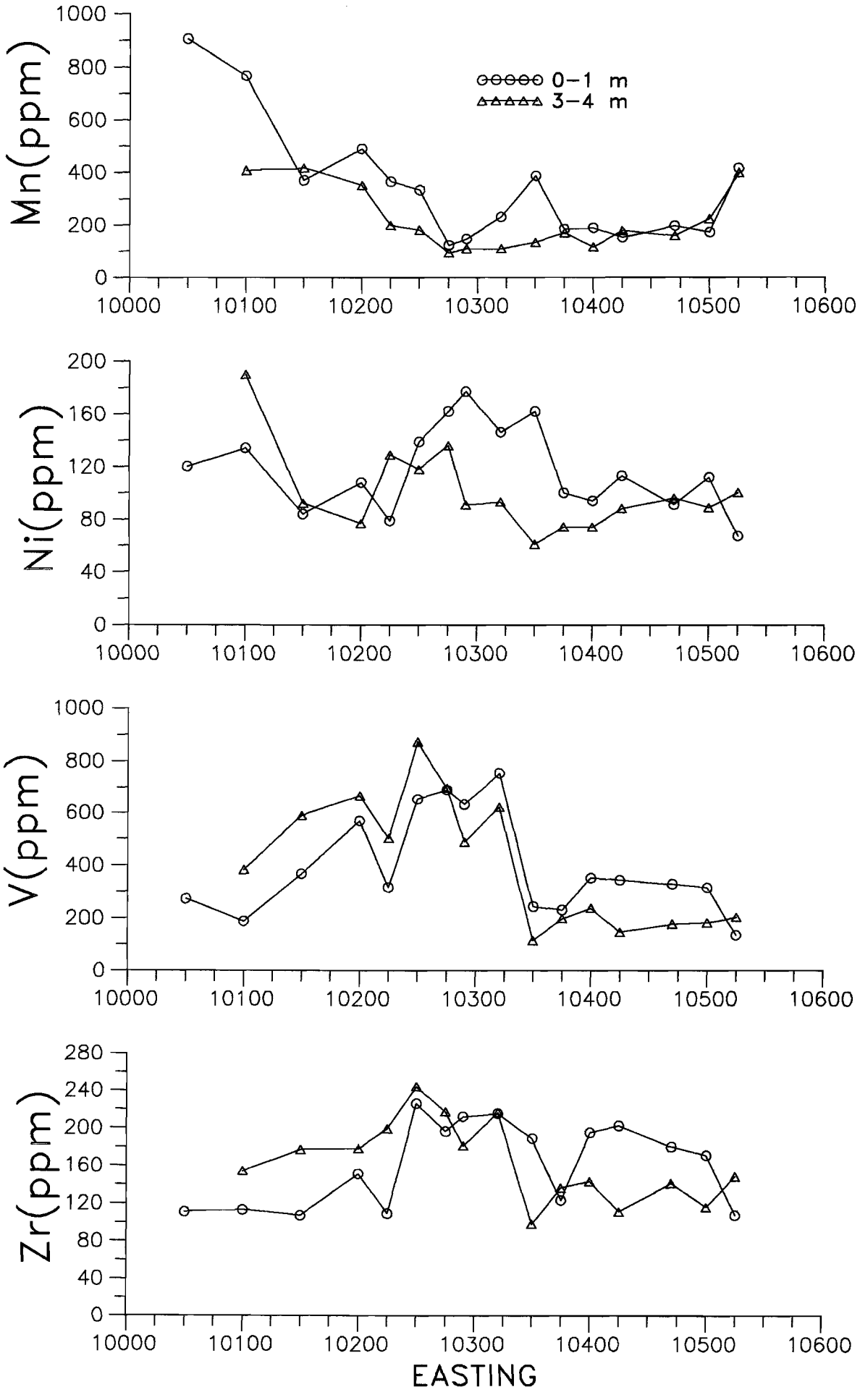
Mn(ppm)
1000
800
600
400
200
0
0-1 m
3-4 m
10000
10100
10200
10300
10400
10500
10600
Ni(ppm)
200
160
120
80
40
0
V(ppm)
Zr(ppm)
280
240
EASTING

Figure 9b: Distribution of elements from traverse 12725N.

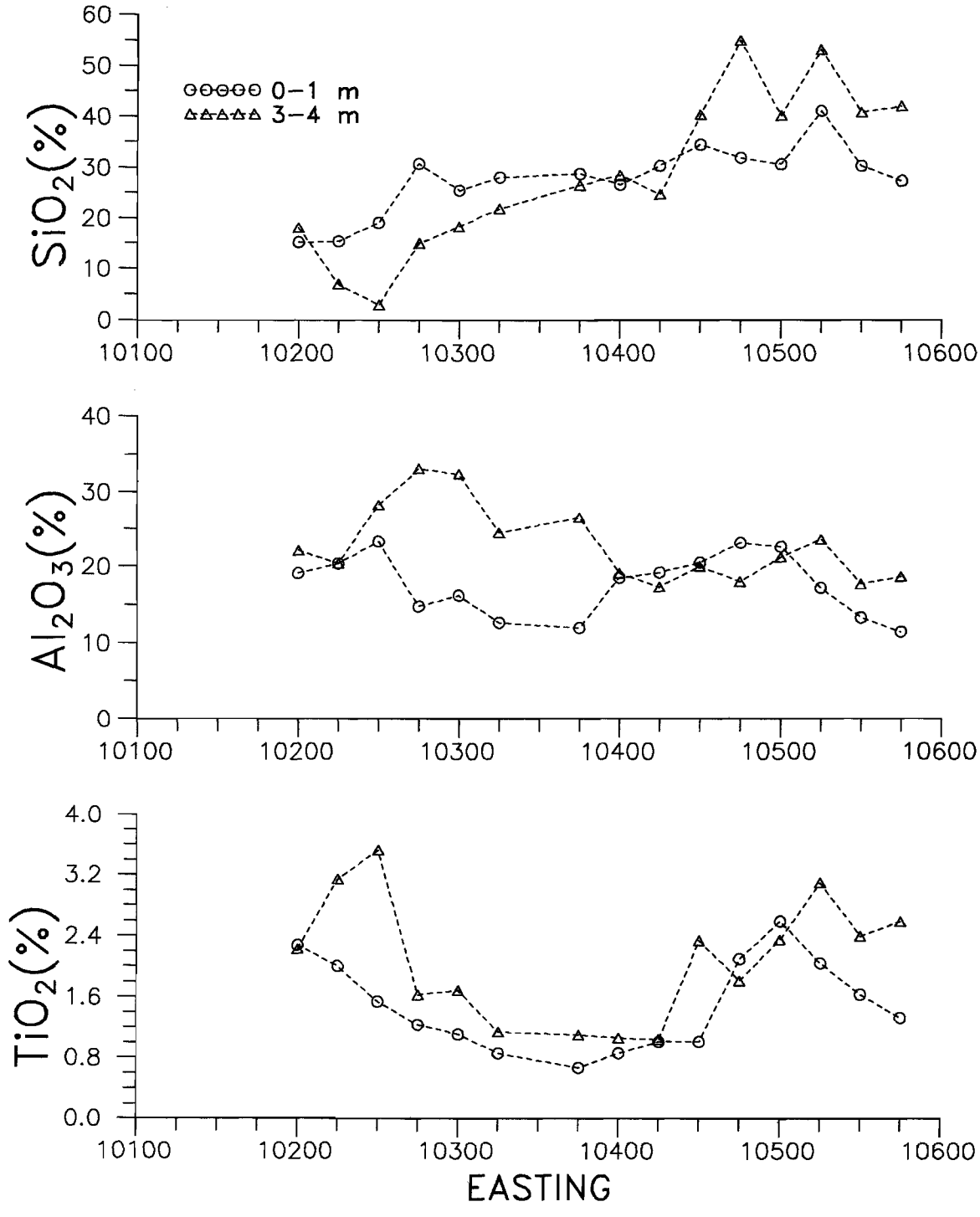

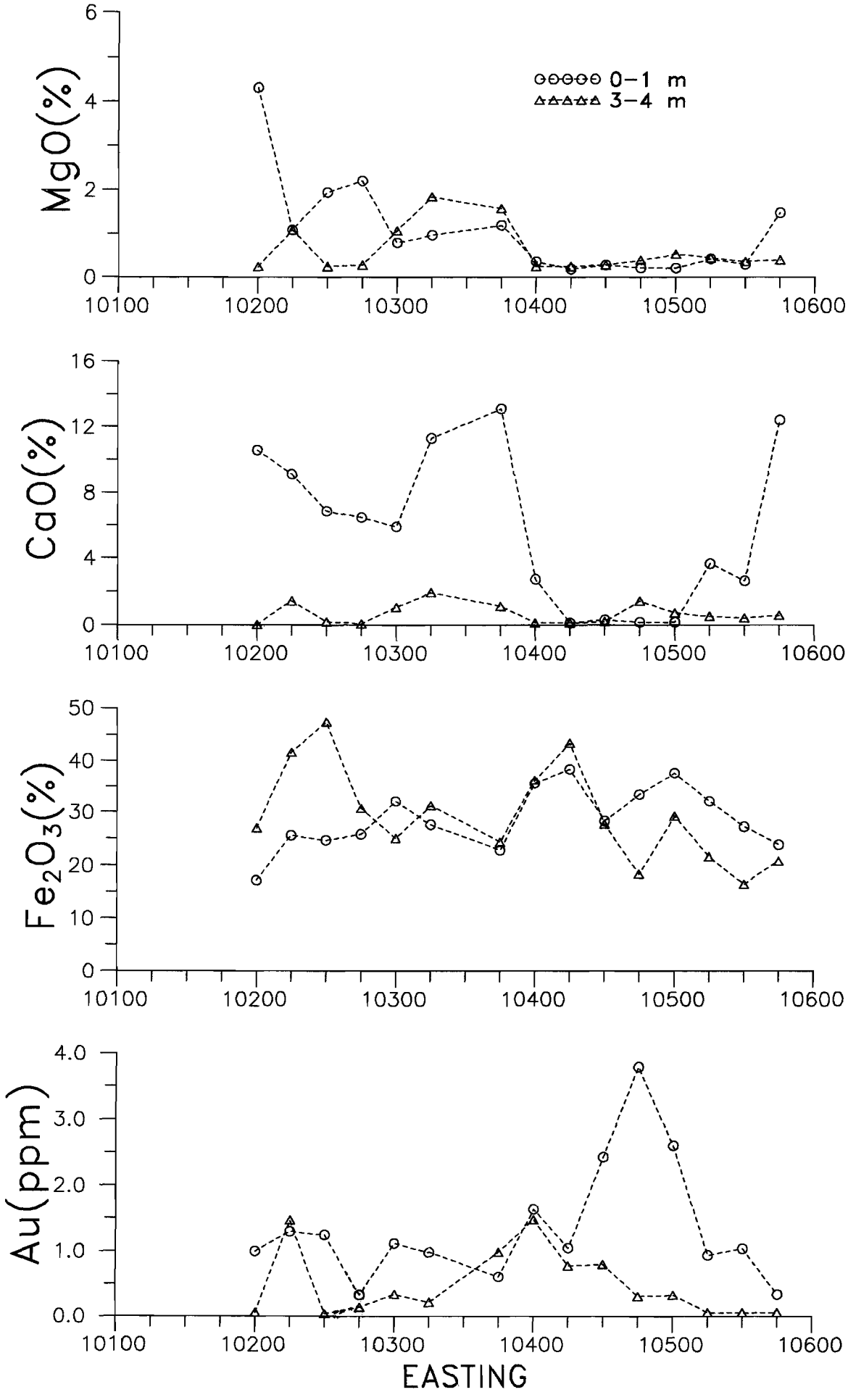
MgO(%)
0-1 m
3-4 m
CaO(%)
Fe_2O_3(%)
Au(ppm)
EASTING
10100
10200
10300
10400
10500
10600

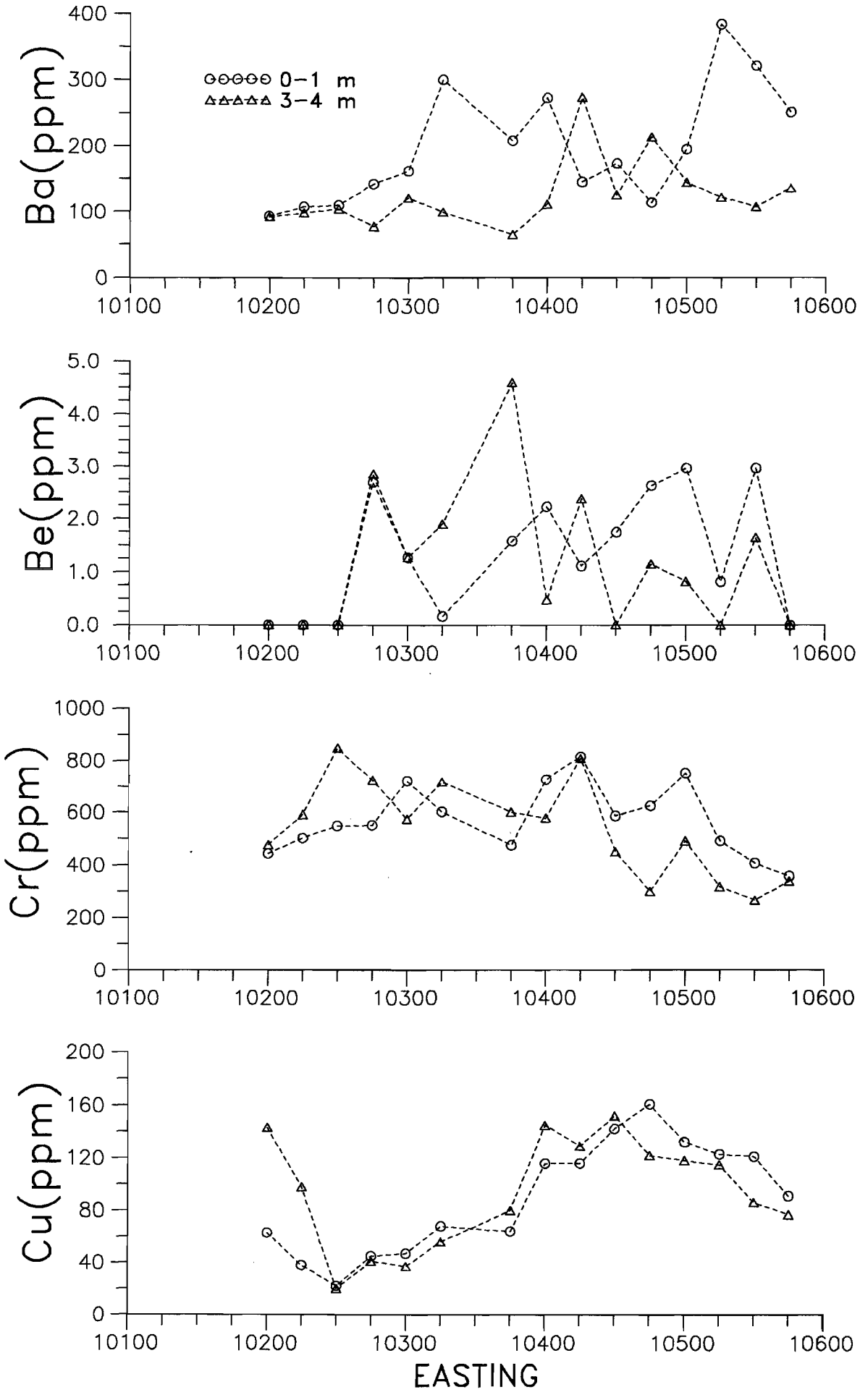
Ba(ppm)
0-1 m
3-4 m
400
300
200
100
0
Be(ppm)
5.0
4.0
3.0
2.0
1.0
0.0
Cr(ppm)
1000
800
600
400
200
0
Cu(ppm)
200
160
120
80
40
0
10100
10200
10300
10400
10500
10600
EASTING

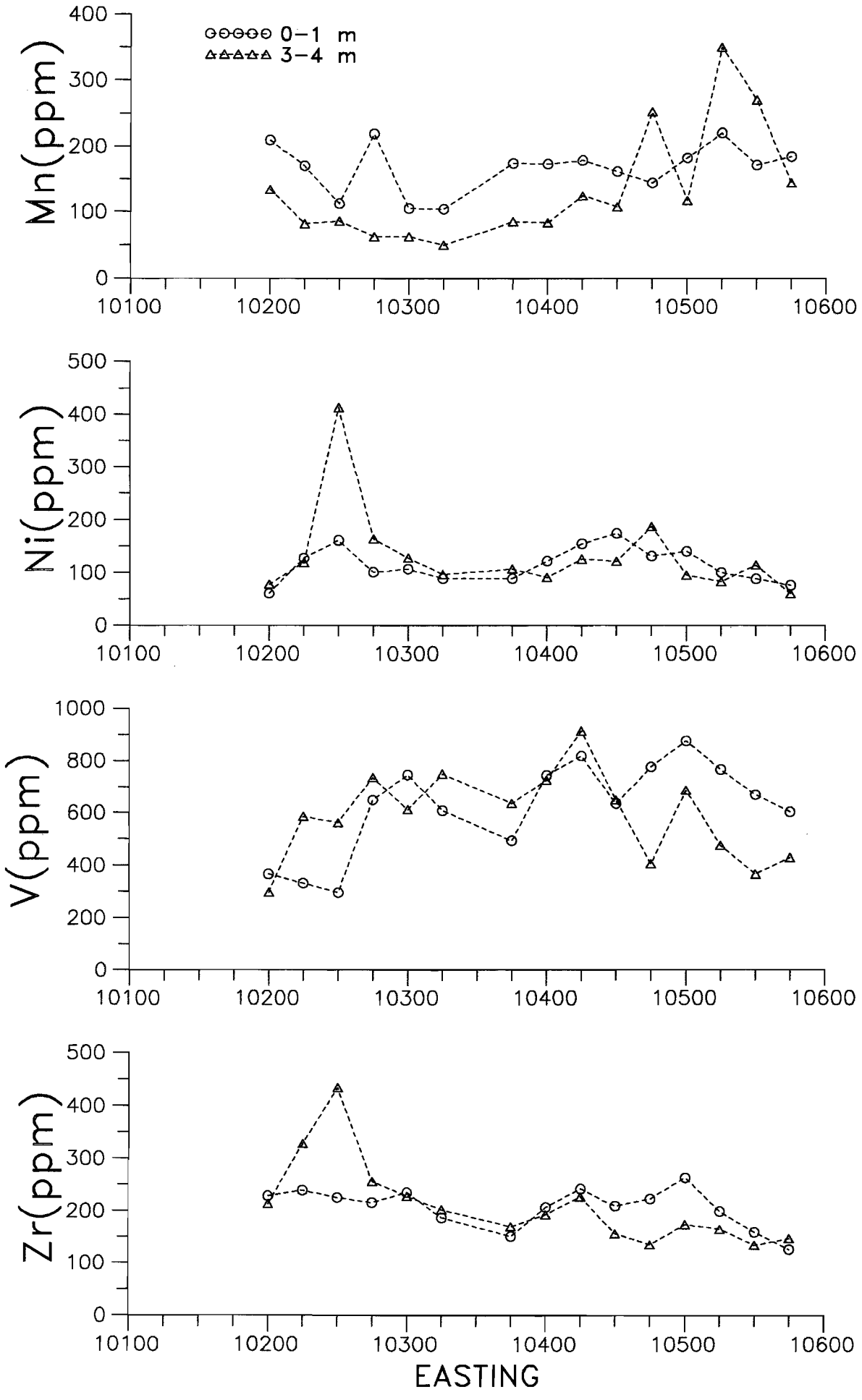
0–1 m
3–4 m
Mn(ppm)
Ni(ppm)
V(ppm)
Zr(ppm)
0
100
200
300
400
500
600
800
1000
10100
10200
10300
10400
10500
10600
EASTING

3.2 Lady Gladys

Each profile is a short (2.0 - 2.5 m) section through the pisolitic and nodular ferruginous and upper mottled zones of the deep lateritic regolith which have been invaded and possibly partly replaced by the precipitation of pedogenic carbonates. The latter act as diluents to the concentrations of Fe, Al, Si and other elements held within pre-existing minerals, such as the Fe and Al oxides, clays and quartz and other resistates.

3.2.1 Profile 4283 (10014E 9406N)

Depth (m)	Field description
0-0.15	Brown calcareous loam; carbonate nodules at the base
0.15-0.5	White calcrete around Fe oxide nodules; top of horizon delineated by a thin (5 mm) layer of indurated, laminated carbonate
0.5-1.0	Transition to orange brown clays, less carbonate
1.0-1.5	Ferruginous fragments to 5 cm, clay matrix; pink carbonate
1.5-2.0	Ferruginous nodules in orange brown clay
2.0-2.5	Orange brown clays, with some Fe oxide-rich nodules

The profile is dominated by Fe oxides, with considerable quantities of carbonate present close to the surface. Quartz is not abundant. Silicon concentrations are low, averaging about 20% (as SiO_2) and are negatively correlated with Fe, Ca and Mg. Calcium concentrations are particularly abundant at the surface, as calcite; there is an additional maximum at about 1.25m, coincident with Mg and the occurrence of dolomite. Aluminium concentrations increase with depth, as the material becomes clay-rich, with a maximum (coincident with Ca and Mg) associated with gibbsite. Iron concentrations are high, present mainly as goethite. Titanium is particularly abundant at 0.75 m (8%) where some of it is present as anatase and rutile, and the remainder may be associated with goethite. Phosphorus distribution decreases sharply from the surface and is probably correlated with organic material.

Gold is abundant in the calcareous upper 1.75 m, where it is associated with Fe, Ca or Mg, but then decreases sharply to less than 0.5 ppm in ferruginous but Ca-poor material. The highest Au concentration (2.10 ppm) occurs in a thin (1-5 mm), almost continuous layer of finely laminated, calcite-rich carbonate at the base of the soil at about 0.15 m depth (sample 4280C, Appendix 2). Dolomitic nodules and segregations in the profile from 0.0-0.15 m (4283C), 0.15-0.50 m (4281C) and 1.00-1.50 m (4282C) have lower Au contents (0.5-0.9 ppm Au), and inspection of the data suggests a possible relationship with the Fe contents of the carbonates. A siliceous, slightly more ferruginous fraction of the soil (4283F), poorer in carbonate, has an intermediate Au content (0.7 ppm). These data imply that Au is concentrated in an environment characterized by high Ca-Mg carbonate contents, but that it is not necessarily associated with a particular mineral phase.

The distributions of As, Ba, Co, Nd, Sc and Sr are positively correlated with Ca and Mg, whereas Ce, Cr, Cu, Ga, Ni and V concentrations are associated with Fe. Copper, Ga, La, Mn, Nb, V and Zr maxima are strongly related to that of Ti but are probably associated with Fe oxide minerals.

Figure 10: Distribution of elements in Profile 4283. (following pages)

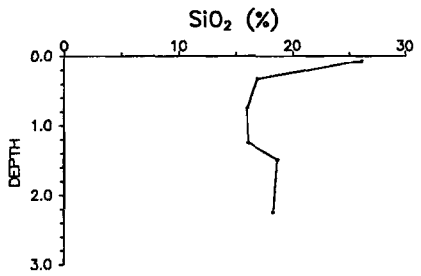
SiO2 (%)
0
10
20
30
DEPTH
0.0
1.0
2.0
3.0

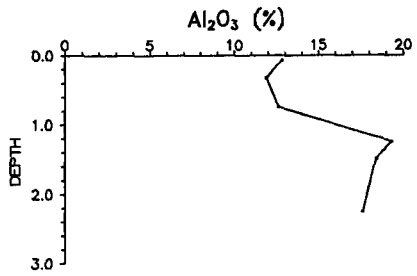
Al2O3 (%)
0
5
10
15
20
DEPTH
0.0
1.0
2.0
3.0

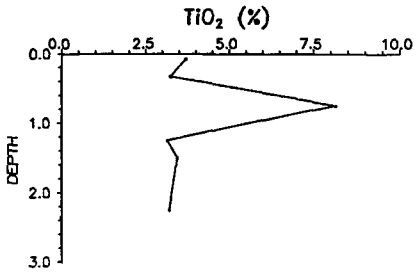
TiO2 (%)
0.0
2.5
5.0
7.5
10.0
DEPTH
0.0
1.0
2.0
3.0

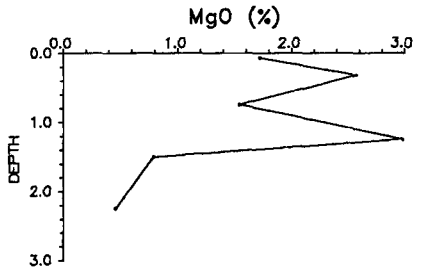
MgO (%)
0.0
1.0
2.0
3.0
DEPTH
0.0
1.0
2.0
3.0

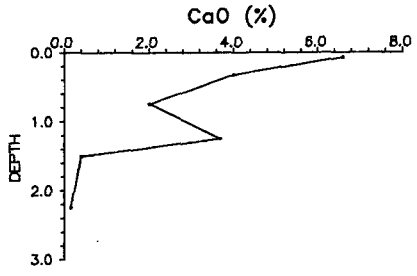
CaO (%)
0.0
2.0
4.0
6.0
8.0
DEPTH
0.0
1.0
2.0
3.0

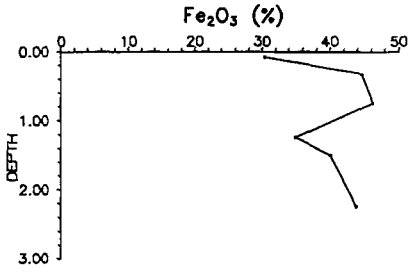
Fe2O3 (%)
0
10
20
30
40
50
DEPTH
0.00
1.00
2.00
3.00

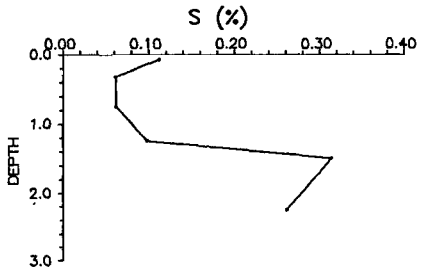
S (%)
0.00
0.10
0.20
0.30
0.40
DEPTH
0.0
1.0
2.0
3.0

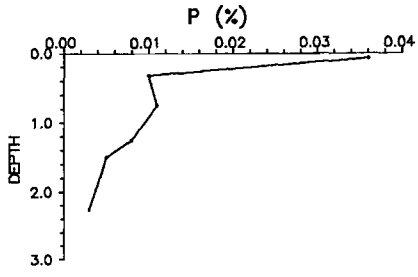
P (%)
0.00
0.01
0.02
0.03
0.04
DEPTH
0.0
1.0
2.0
3.0

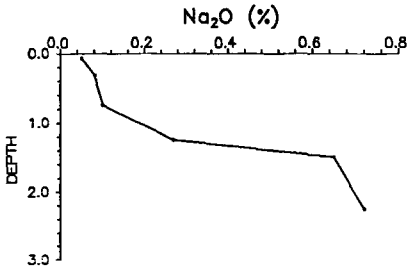
Na2O (%)
0.0
0.2
0.4
0.6
0.8
DEPTH
0.0
1.0
2.0
3.0

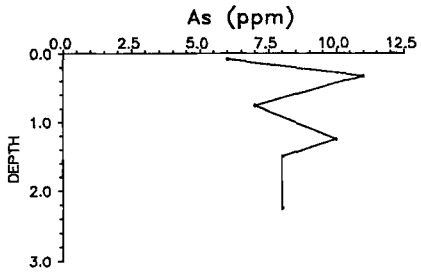
As (ppm)
0.0
2.5
5.0
7.5
10.0
12.5
DEPTH
0.0
1.0
2.0
3.0

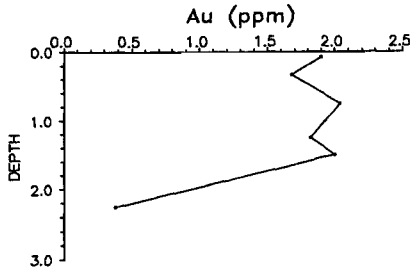
Au (ppm)
0.0
0.5
1.0
1.5
2.0
2.5
DEPTH
0.0
1.0
2.0
3.0

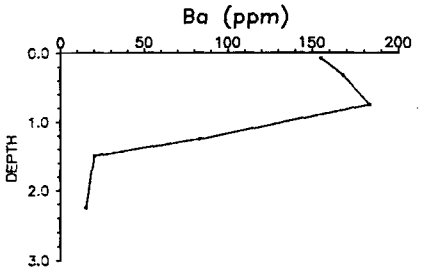
Ba (ppm)
0
50
100
150
200
DEPTH
0.0
1.0
2.0
3.0

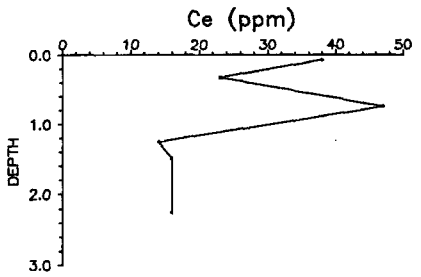
Ce (ppm)
0
10
20
30
40
50
DEPTH
0.0
1.0
2.0
3.0

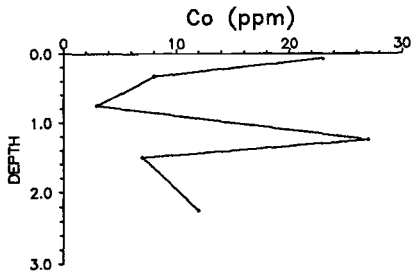
Co (ppm)
0
10
20
30
DEPTH
0.0
1.0
2.0
3.0

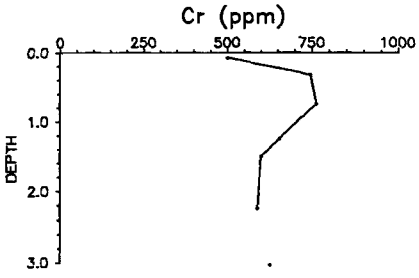
Cr (ppm)
0
250
500
750
1000
DEPTH
0.0
1.0
2.0
3.0

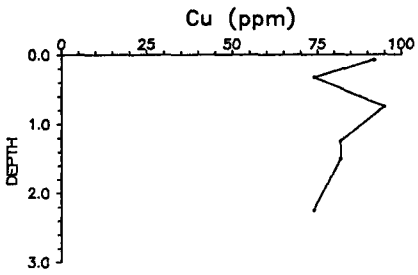
Cu (ppm)
0
25
50
75
100
DEPTH
0.0
1.0
2.0
3.0

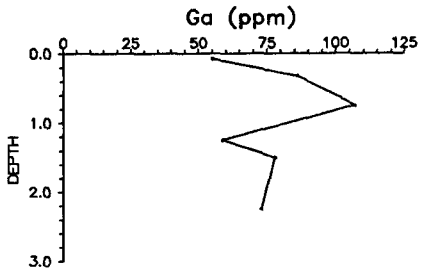
Ga (ppm)
0
25
50
75
100
125
DEPTH
0.0
1.0
2.0
3.0

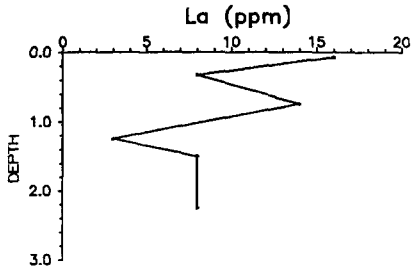
La (ppm)
0
5
10
15
20
DEPTH
0.0
1.0
2.0
3.0

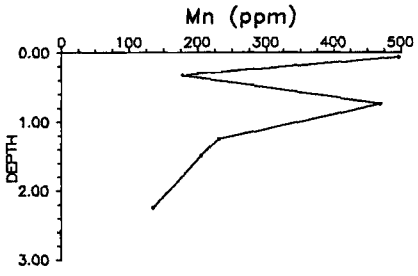
Mn (ppm)
0
100
200
300
400
500
DEPTH
0.00
1.00
2.00
3.00

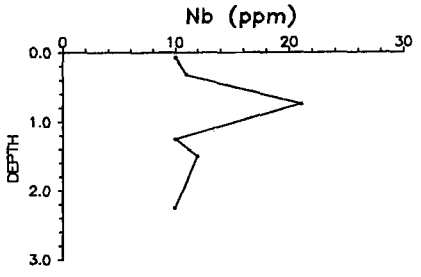
Nb (ppm)
0
10
20
30
DEPTH
0.0
1.0
2.0
3.0

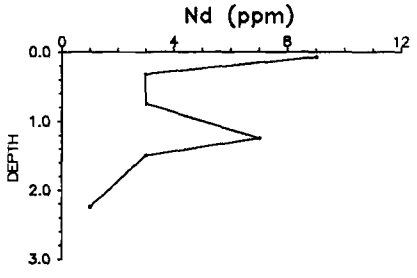
Nd (ppm)
0
4
8
12
DEPTH
0.0
1.0
2.0
3.0

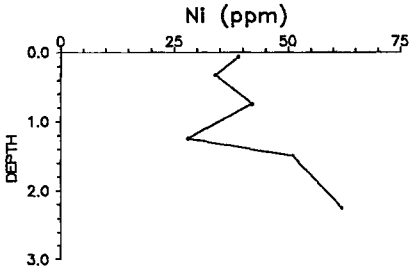
Ni (ppm)
0
25
50
75
DEPTH
0.0
1.0
2.0
3.0

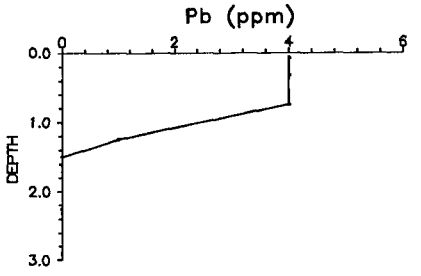
Pb (ppm)
0
2
4
6
DEPTH
0.0
1.0
2.0
3.0

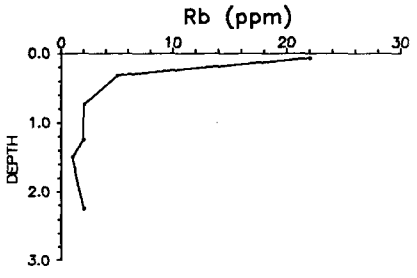
Rb (ppm)
0
10
20
30
DEPTH
0.0
1.0
2.0
3.0

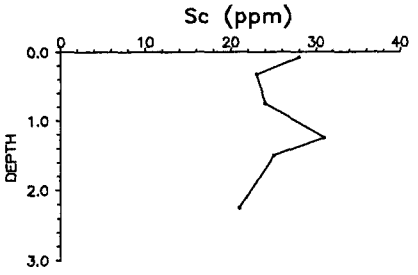
Sc (ppm)
0
10
20
30
40
DEPTH
0.0
1.0
2.0
3.0

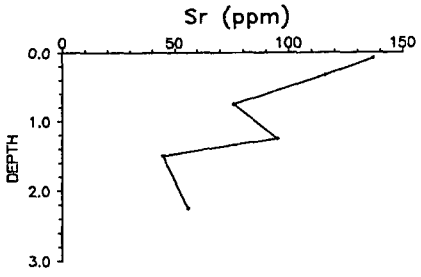
Sr (ppm)
0
50
100
150
DEPTH
0.0
1.0
2.0
3.0

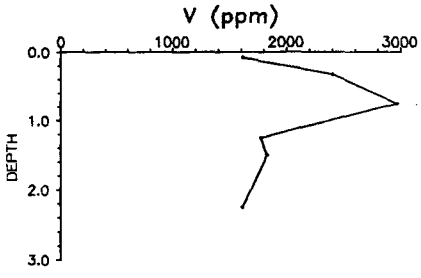
V (ppm)
0
1000
2000
3000
DEPTH
0.0
1.0
2.0
3.0

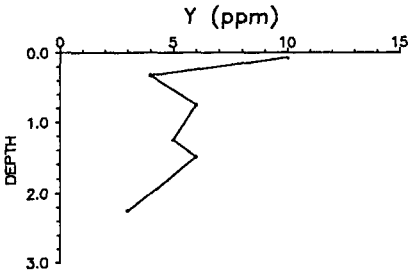
Y (ppm)
0
5
10
15
DEPTH
0.0
1.0
2.0
3.0

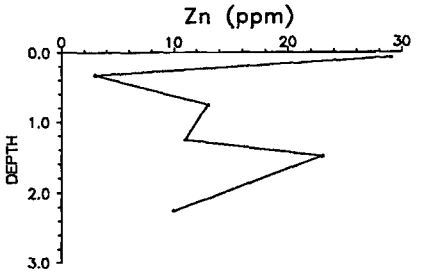
Zn (ppm)
0
10
20
30
DEPTH
0.0
1.0
2.0
3.0

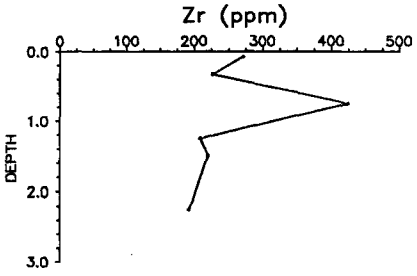
Zr (ppm)
0
100
200
300
400
500
DEPTH
0.0
1.0
2.0
3.0

3.2.2 Profile 4289 (10023E 9400N)

Depth (m)	Field description
0-0.3	Brown calcareous clay loam, with carbonate- and Fe-rich nodules
0.3-0.8	Fe-rich nodules with white carbonate coatings in white calcareous matrix
1.0-1.5	Fe oxide-rich nodules to 5 cm in clay matrix-brown, yellow, some carbonate
1.5-2.5	Fe-rich nodules in yellow brown clays

The top 1.3 m of the profiles are dominated by carbonate minerals (dolomite with minor calcite), with Fe oxide minerals (principally goethite) and gibbsite below. The concentrations of Ca, Mg and Sr, which occur in dolomite, reflect this distribution, with maxima at the base of the soil and gradually decreasing with depth. Titanium and Fe show an antipathetic distribution, being diluted by the carbonates. Silicon content decreases from the surface but increases again below 2m. Aluminium concentrations increase with depth in accordance with the appearance of kaolinite and, in particular, gibbsite. The abundances of S and Na gradually increase with depth, possibly due to the precipitation of evaporite salts with clay minerals. Phosphorus concentrations decrease sharply from the surface and may be associated with organic material.

Gold concentrations decrease with depth, being highest in the carbonate horizon (1.5 to 3 ppm); however, a second maximum (1.48 ppm) is associated with an increase in Fe concentration near the base of the profile.

Chromium, Co, Cu, Ga, Mn, Ni, V, Y and Zr distributions generally follow those of Fe and Ti, whereas As, Ba and La show some similarities with Ca. Lead and Zn are similar to P and decrease sharply from the surface.

Figure 11: Distribution of elements in Profile 4289. (following pages)

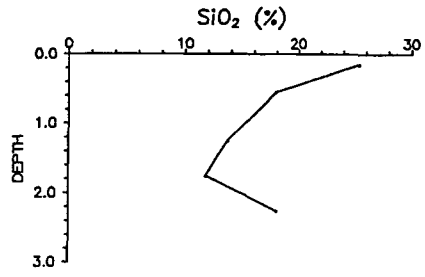
SiO2 (%)
0
10
20
30
0.0
1.0
2.0
3.0
DEPTH

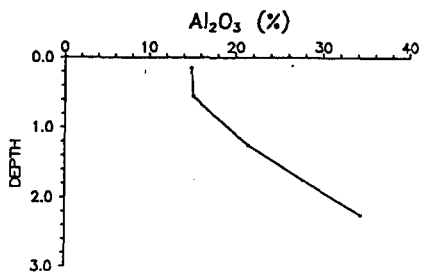
Al2O3 (%)
0
10
20
30
40
0.0
1.0
2.0
3.0
DEPTH

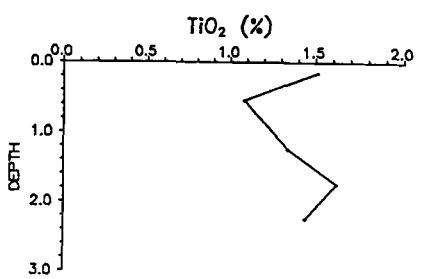
TiO2 (%)
0.0
0.5
1.0
1.5
2.0
0.0
1.0
2.0
3.0
DEPTH

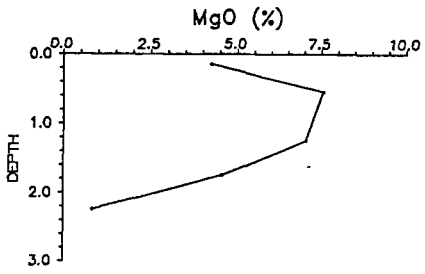
MgO (%)
0.0
2.5
5.0
7.5
10.0
0.0
1.0
2.0
3.0
DEPTH

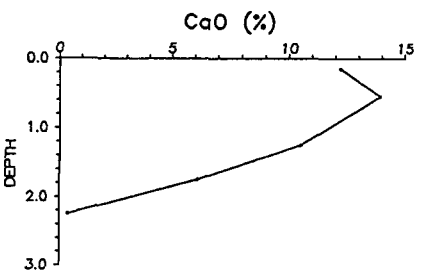
CaO (%)
0
5
10
15
0.0
1.0
2.0
3.0
DEPTH

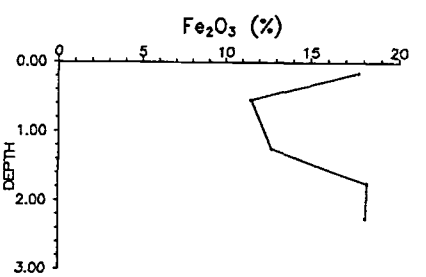
Fe2O3 (%)
0
5
10
15
20
0.00
1.00
2.00
3.00
DEPTH

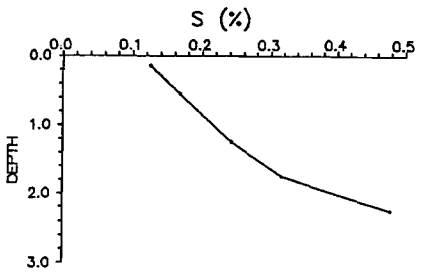
S (%)
0.0
0.1
0.2
0.3
0.4
0.5
0.0
1.0
2.0
3.0
DEPTH

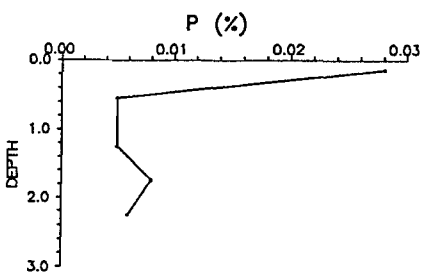
P (%)
0.00
0.01
0.02
0.03
0.0
1.0
2.0
3.0
DEPTH

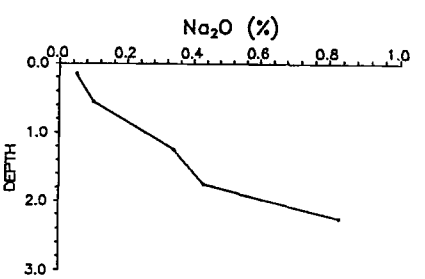
Na2O (%)
0.0
0.2
0.4
0.6
0.8
1.0
0.0
1.0
2.0
3.0
DEPTH

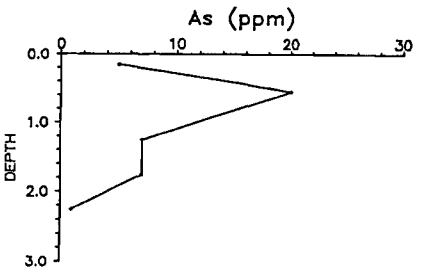
As (ppm)
0
10
20
30
0.0
1.0
2.0
3.0
DEPTH

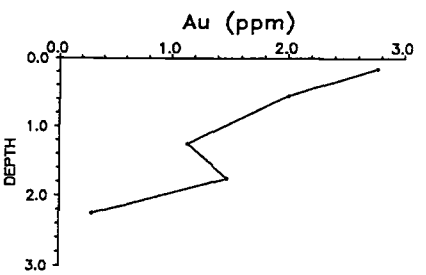
Au (ppm)
0.0
1.0
2.0
3.0
0.0
1.0
2.0
3.0
DEPTH

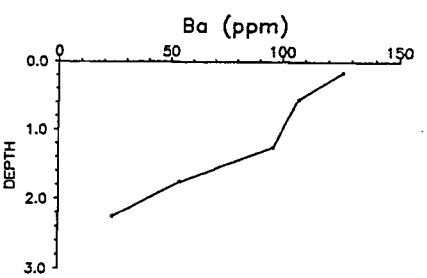
Ba (ppm)
0
50
100
150
0.0
1.0
2.0
3.0
DEPTH

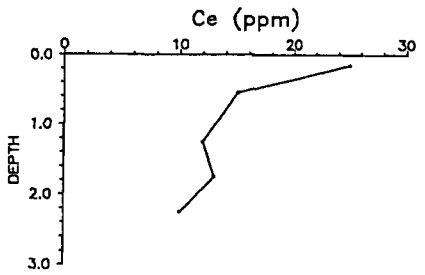
Ce (ppm)
0
10
20
30
0.0
1.0
2.0
3.0
DEPTH

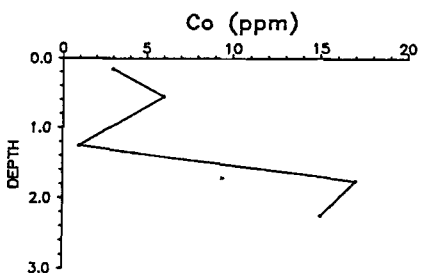
Co (ppm)
0
5
10
15
20
0.0
1.0
2.0
3.0
DEPTH

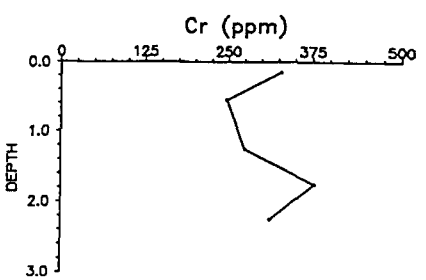
Cr (ppm)
0
125
250
375
500
0.0
1.0
2.0
3.0
DEPTH

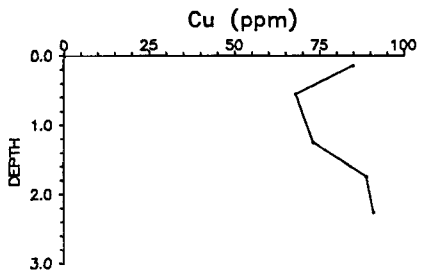
Cu (ppm)
0
25
50
75
100
DEPTH
0.0
1.0
2.0
3.0

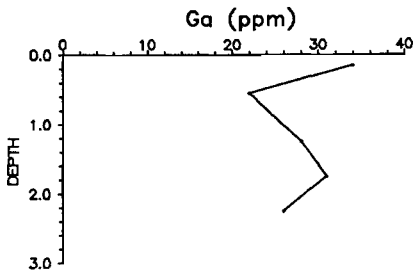
Ga (ppm)
0
10
20
30
40
DEPTH
0.0
1.0
2.0
3.0

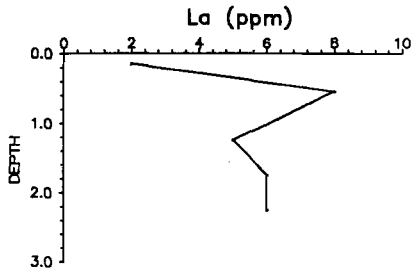
La (ppm)
0
2
4
6
8
10
DEPTH
0.0
1.0
2.0
3.0

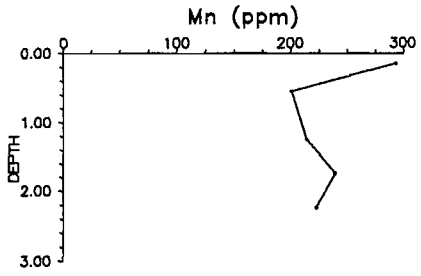
Mn (ppm)
0
100
200
300
DEPTH
0.00
1.00
2.00
3.00

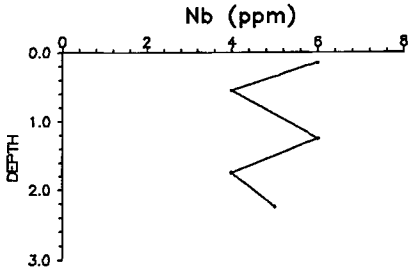
Nb (ppm)
0
2
4
6
8
DEPTH
0.0
1.0
2.0
3.0

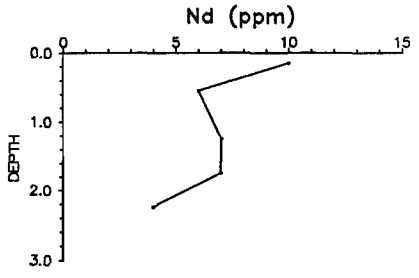
Nd (ppm)
0
5
10
15
DEPTH
0.0
1.0
2.0
3.0

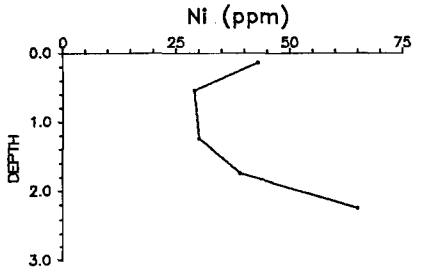
Ni (ppm)
0
25
50
75
DEPTH
0.0
1.0
2.0
3.0

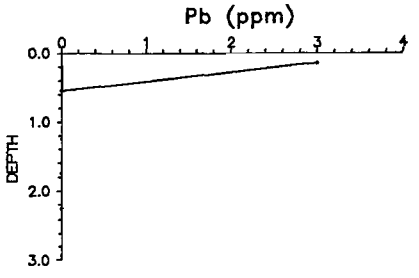
Pb (ppm)
0
1
2
3
4
DEPTH
0.0
1.0
2.0
3.0

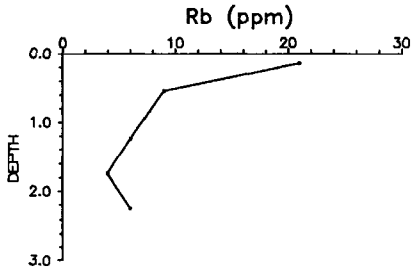
Rb (ppm)
0
10
20
30
DEPTH
0.0
1.0
2.0
3.0

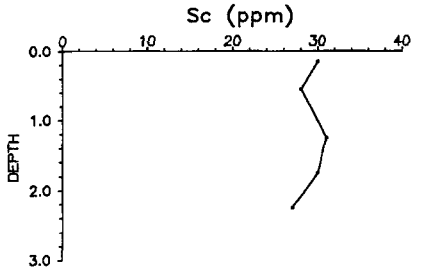
Sc (ppm)
0
10
20
30
40
DEPTH
0.0
1.0
2.0
3.0

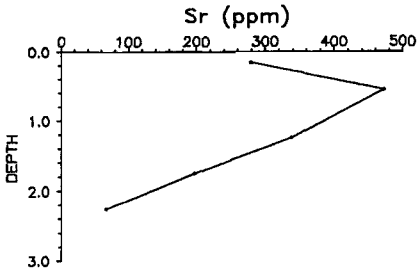
Sr (ppm)
0
100
200
300
400
500
DEPTH
0.0
1.0
2.0
3.0

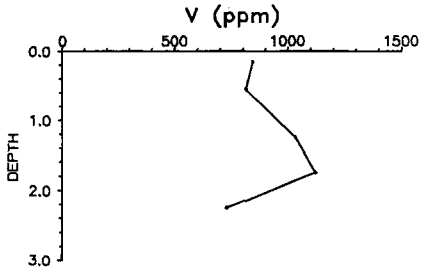
V (ppm)
0
500
1000
1500
DEPTH
0.0
1.0
2.0
3.0

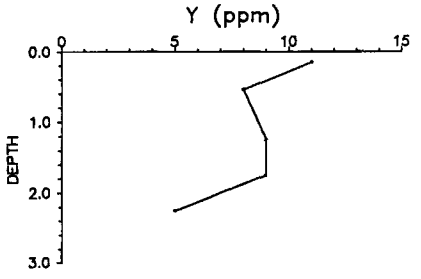
Y (ppm)
0
5
10
15
DEPTH
0.0
1.0
2.0
3.0

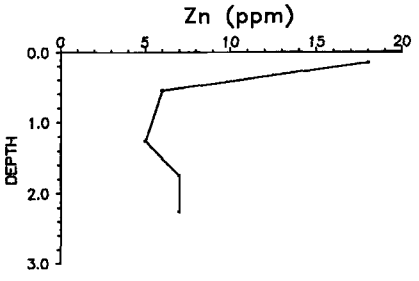
Zn (ppm)
0
5
10
15
20
DEPTH
0.0
1.0
2.0
3.0

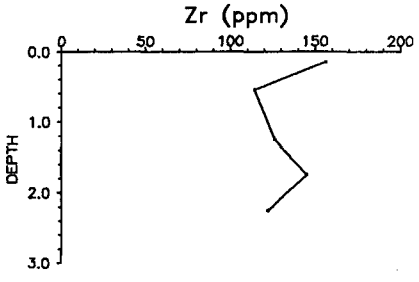
Zr (ppm)
0
50
100
150
200
DEPTH
0.0
1.0
2.0
3.0

3.2.3 Profile 4296 (10033E 9400N)

Depth (m)	Field description
0-0.20	Brown calcareous clay loam
0.2-0.45	Loam with calcrete nodules
0.45-1.0	Laminated calcrete, with calcareous and ferruginous nodules; white carbonate matrix
1.0-1.5	Calcrete nodules with clay-rich matrix; some Fe oxide-rich nodules
1.5-2.0	Fe oxide-rich nodules in yellow brown clay

This profile consists of lateritic nodules and pisoliths invaded by pedogenic carbonates. High concentrations of Ca (>6%), Mg (>4%) and Sr (200-600 ppm) are present throughout the profile, but decline markedly below 1.5m. Iron (and Ti) concentrations are diluted by the carbonate and are greatest at the surface and below 1.5m, where carbonates are less abundant. The carbonates are increasingly dolomitic with depth, and Fe is present mainly as goethite, with minor hematite.

Silicon, present as quartz and kaolinite, decreases in concentration with depth, whereas the concentration of Al, as gibbsite and kaolinite, progressively increases. Some Al at the base of the profile is substituted within goethite. Sulphur and Na contents increase with depth and have, in addition, coincident maxima within the most calcareous material. Some Na is probably present in smectites deeper in the sampled profile. Phosphorus contents decrease sharply decreases from the surface and are probably related to organic material.

Gold distribution is not related to any one particular mineral phase. However, it has maxima of 1.72 ppm at 0.3 m coincident with the Ca maximum, and is also high (1.46 ppm) where Fe (and Al) contents are highest, at the base of the profile. The As distribution is similar to that of Au. Cerium, Cr, Ga, Nb, Nd, Ni and V distributions are similar to that of Fe. Close to the surface, concentrations of Mn, Pb, Rb and Zn, like P, decrease markedly, but at depth follow Fe. The La content decreases steadily with depth.

Figure 12: Distribution of elements in Profile 4296. (following pages)

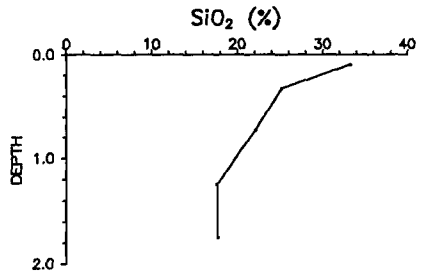
SiO_2 (%)
0
10
20
30
40
DEPTH
0.0
1.0
2.0

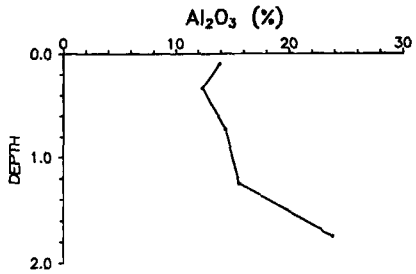
Al_2O_3 (%)
0
10
20
30
DEPTH
0.0
1.0
2.0

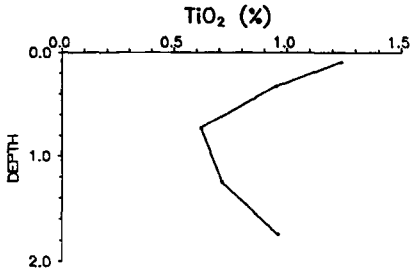
TiO_2 (%)
0.0
0.5
1.0
1.5
DEPTH
0.0
1.0
2.0

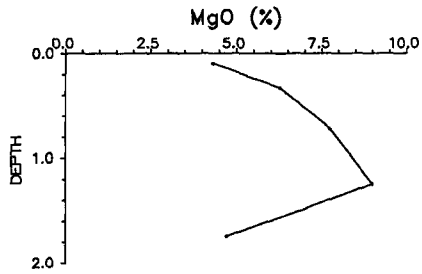
MgO (%)
0.0
2.5
5.0
7.5
10.0
DEPTH
0.0
1.0
2.0

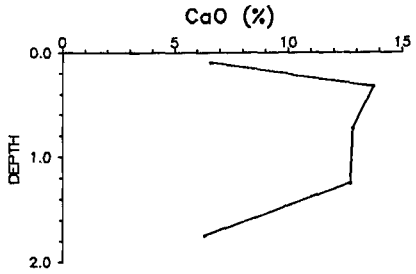
CaO (%)
0
5
10
15
DEPTH
0.0
1.0
2.0

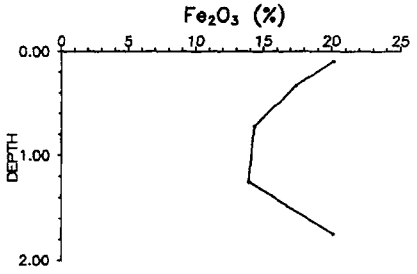
Fe_2O_3 (%)
0
5
10
15
20
25
DEPTH
0.00
1.00
2.00

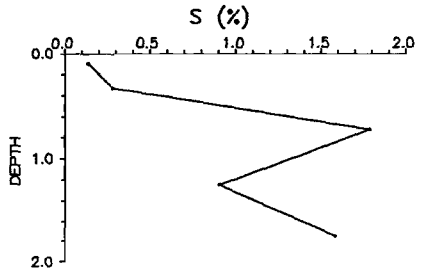
S (%)
0.0
0.5
1.0
1.5
2.0
DEPTH
0.0
1.0
2.0

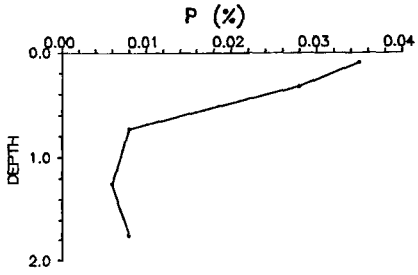
P (%)
0.00
0.01
0.02
0.03
0.04
DEPTH
0.0
1.0
2.0

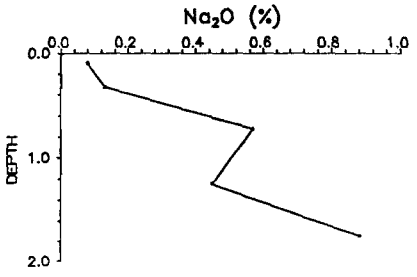
Na_2O (%)
0.0
0.2
0.4
0.6
0.8
1.0
DEPTH
0.0
1.0
2.0

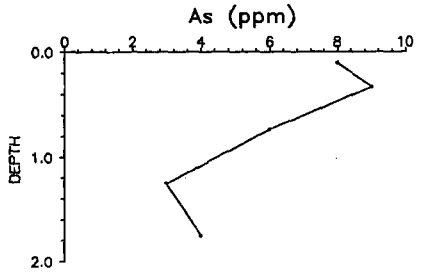
As (ppm)
0
2
4
6
8
10
DEPTH
0.0
1.0
2.0

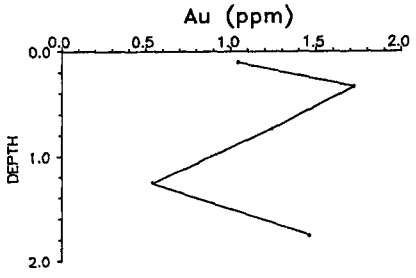
Au (ppm)
0.0
0.5
1.0
1.5
2.0
DEPTH
0.0
1.0
2.0

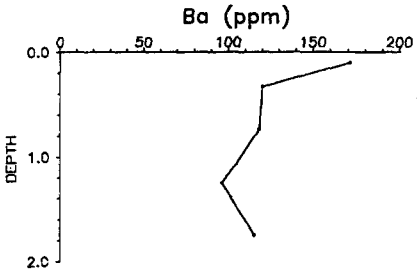
Ba (ppm)
0
50
100
150
200
DEPTH
0.0
1.0
2.0

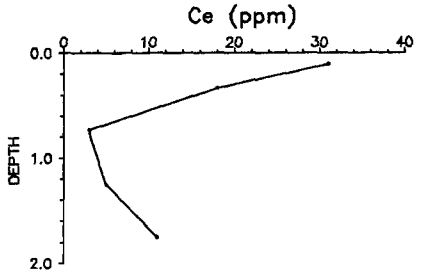
Ce (ppm)
0
10
20
30
40
DEPTH
0.0
1.0
2.0

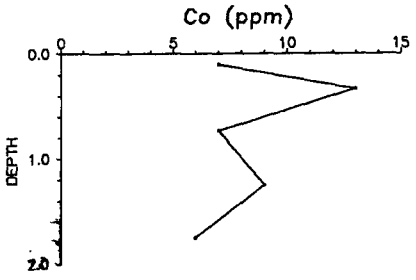
Co (ppm)
0
5
10
15
DEPTH
0.0
1.0
2.0

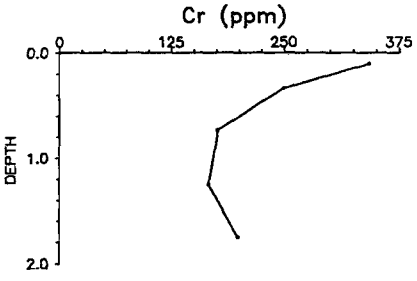
Cr (ppm)
0
125
250
375
DEPTH
0.0
1.0
2.0

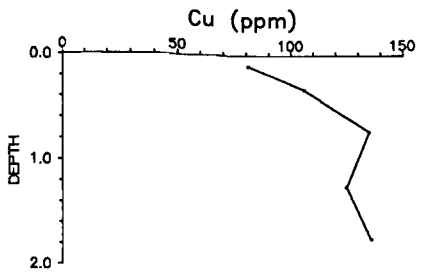
Cu (ppm)
0
50
100
150
0.0
1.0
2.0
DEPTH

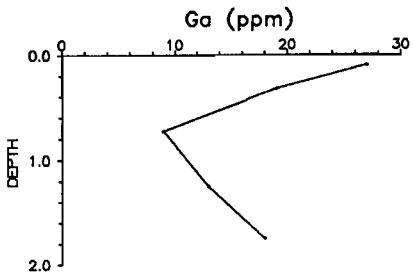
Ga (ppm)
0
10
20
30
0.0
1.0
2.0
DEPTH

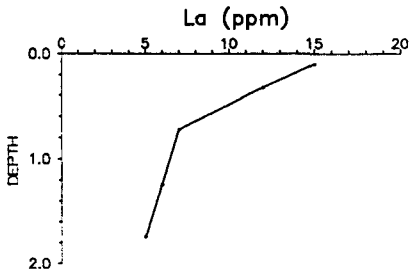
La (ppm)
0
5
10
15
20
0.0
1.0
2.0
DEPTH

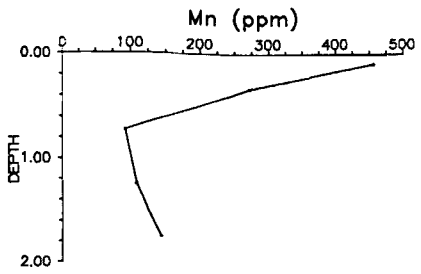
Mn (ppm)
0
100
200
300
400
500
0.00
1.00
2.00
DEPTH

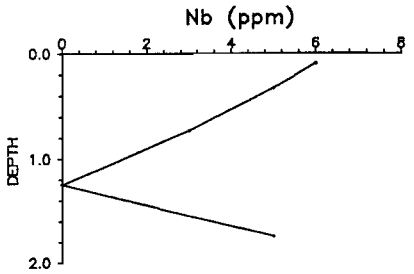
Nb (ppm)
0
2
4
6
8
0.0
1.0
2.0
DEPTH

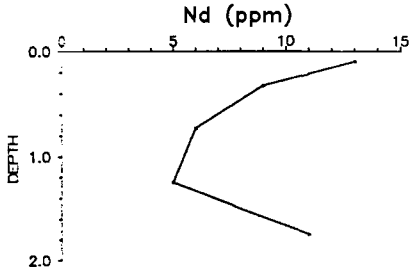
Nd (ppm)
0
5
10
15
0.0
1.0
2.0
DEPTH

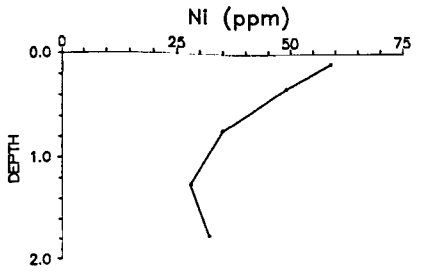
Ni (ppm)
0
25
50
75
0.0
1.0
2.0
DEPTH

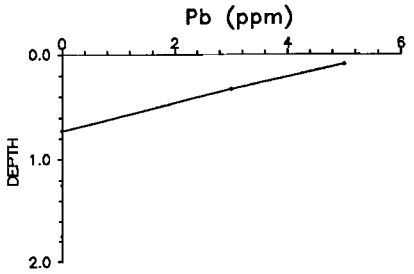
Pb (ppm)
0
2
4
6
0.0
1.0
2.0
DEPTH

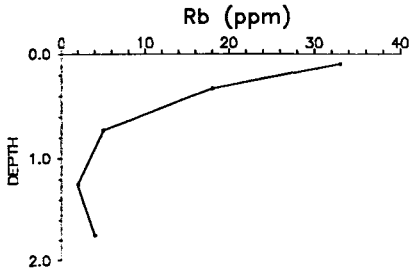
Rb (ppm)
0
10
20
30
40
0.0
1.0
2.0
DEPTH

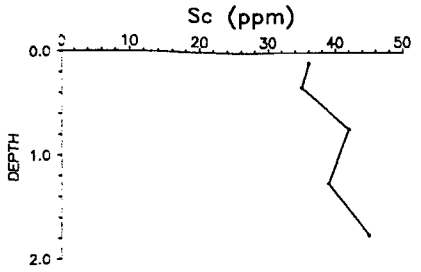
Sc (ppm)
0
10
20
30
40
50
0.0
1.0
2.0
DEPTH

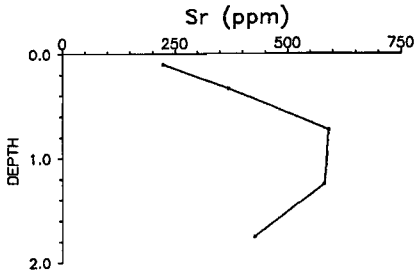
Sr (ppm)
0
250
500
750
0.0
1.0
2.0
DEPTH

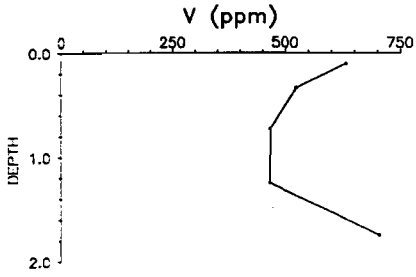
V (ppm)
0
250
500
750
0.0
1.0
2.0
DEPTH

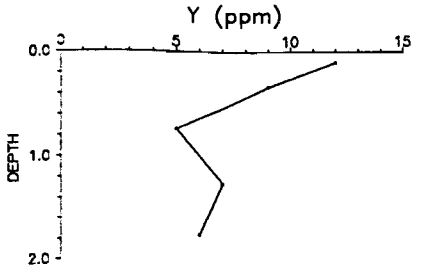
Y (ppm)
0
5
10
15
0.0
1.0
2.0
DEPTH

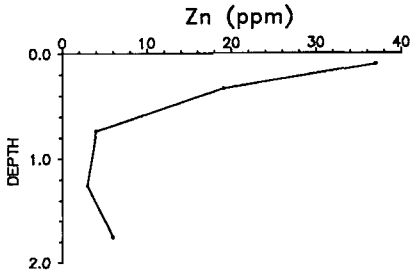
Zn (ppm)
0
10
20
30
40
0.0
1.0
2.0
DEPTH

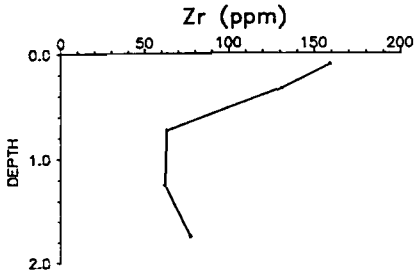
Zr (ppm)
0
50
100
150
200
0.0
1.0
2.0
DEPTH

3.2.4 Profile 4301 (10035E 9408N)

Depth (m)	Field description
0-0.20	Brown loam with calcrete nodules
0.2-0.8	Calcrete nodules (to 10 cm) and Fe oxide-nodules in white to brown calcareous clay matrix
0.8-1.0	Similar to above with more calcareous yellow clay
1.0-1.7 (approx.)	Massive white indurated calcrete enclosing Fe oxide-rich nodules
1.0-1.7 (approx.)	Fe oxide-rich nodules in a yellow-brown clay matrix

This profile is increasingly carbonate-rich with depth (from calcite to dolomite). Quartz, kaolinite and iron oxide minerals decrease with depth, although some Fe oxide-rich nodules (marked as a single point on the distribution diagram) occur at the base of the profile. In consequence, Ca, Mg, Na and Sr concentrations increase, and Si, Al, Ti, Fe, S and P decrease with depth. The distributions of these latter elements are controlled by the presence (or absence) of carbonate or other phases e.g., organic matter, clays. Phosphorus, although strongly correlated with Fe throughout the profile, is present in small amounts in the Fe oxide-rich nodules and, therefore, is probably associated with organic material, as suggested for other profiles in the area.

The profile is calcareous throughout and Au contents are mostly high (>1.2 ppm). The lowest Au content (0.22 ppm) occurs in massive calcrete at the base of the profile, although ferruginous nodules from this horizon contain 1.52 ppm Au. Arsenic (and Nb) contents are low, but have a similar distribution to Au.

Cerium, Co, Cr, Cu, Ga, Ni, V and Zr concentrations decrease with depth and appear to be diluted by carbonate. Barium, La, Mn, Nd, Pb, Rb, Y and Zn concentrations also decrease with depth but, in contrast to the preceding elements, have low concentrations present in the Fe-rich nodules at the base of the profile and, like P, may be related to organic material.

Figure 13: Distribution of elements in Profile 4301. (Solid triangle indicates Fe oxide-rich nodules - sample 4305) (following pages)

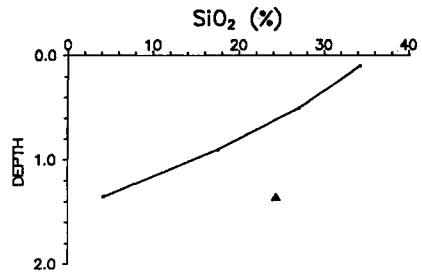
SiO2 (%)
0
10
20
30
40
0.0
1.0
2.0
DEPTH

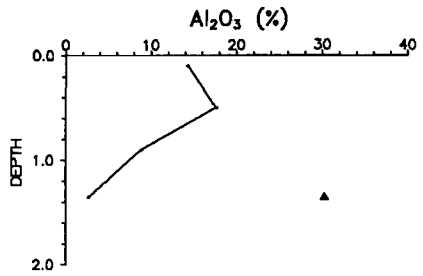
Al2O3 (%)
0
10
20
30
40
0.0
1.0
2.0
DEPTH

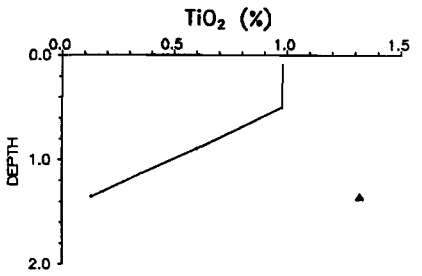
TiO2 (%)
0.0
0.5
1.0
1.5
0.0
1.0
2.0
DEPTH

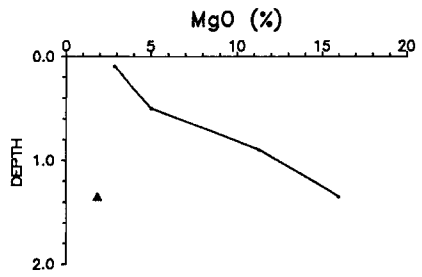
MgO (%)
0
5
10
15
20
0.0
1.0
2.0
DEPTH

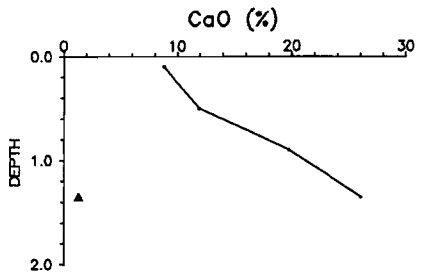
CaO (%)
0
10
20
30
0.0
1.0
2.0
DEPTH

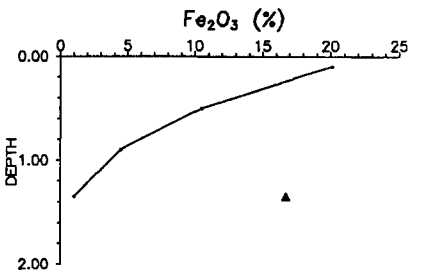
Fe2O3 (%)
0
5
10
15
20
25
0.00
1.00
2.00
DEPTH

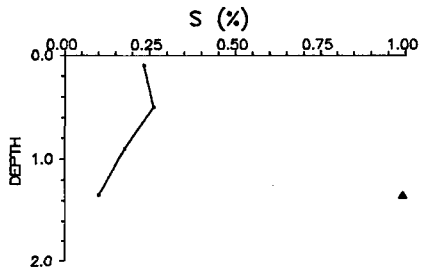
S (%)
0.00
0.25
0.50
0.75
1.00
0.0
1.0
2.0
DEPTH

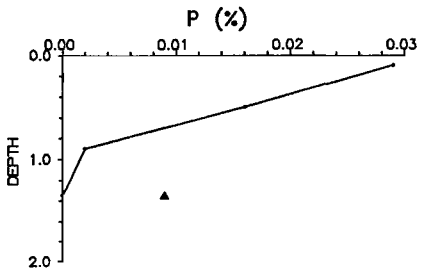
P (%)
0.00
0.01
0.02
0.03
0.0
1.0
2.0
DEPTH

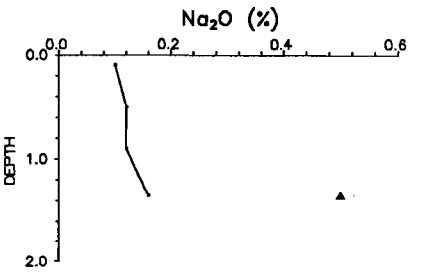
Na2O (%)
0.0
0.2
0.4
0.6
0.0
1.0
2.0
DEPTH

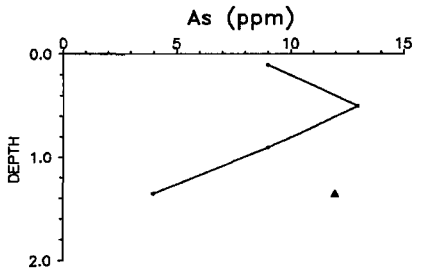
As (ppm)
0
5
10
15
0.0
1.0
2.0
DEPTH

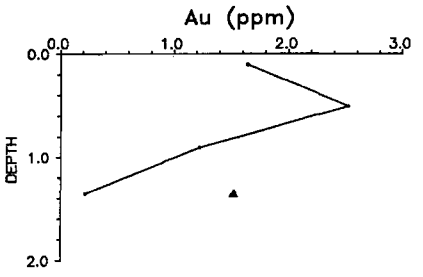
Au (ppm)
0.0
1.0
2.0
3.0
0.0
1.0
2.0
DEPTH

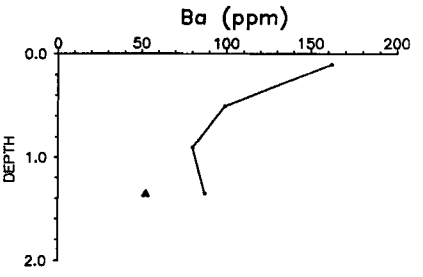
Ba (ppm)
0
50
100
150
200
0.0
1.0
2.0
DEPTH

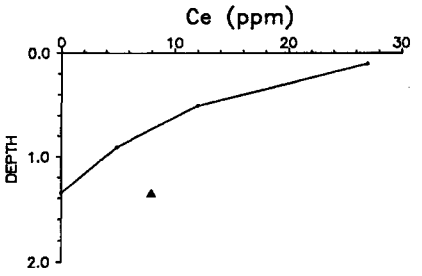
Ce (ppm)
0
10
20
30
0.0
1.0
2.0
DEPTH

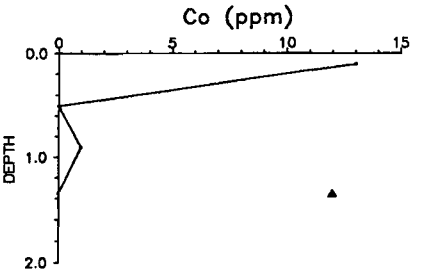
Co (ppm)
0
5
10
15
0.0
1.0
2.0
DEPTH

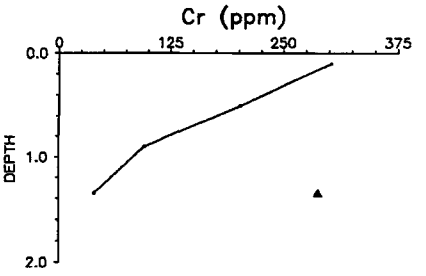
Cr (ppm)
0
125
250
375
0.0
1.0
2.0
DEPTH

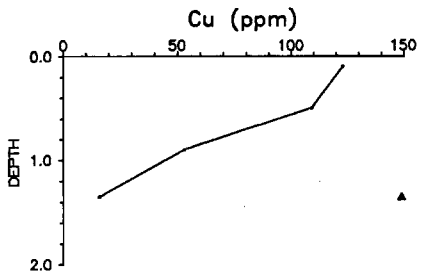
Cu (ppm)
0
50
100
150
0.0
1.0
2.0
DEPTH

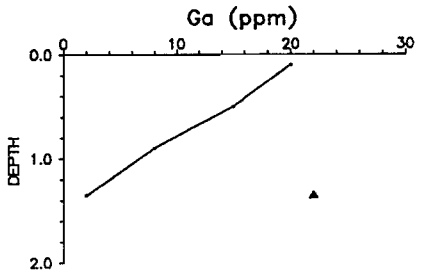
Ga (ppm)
0
10
20
30
0.0
1.0
2.0
DEPTH

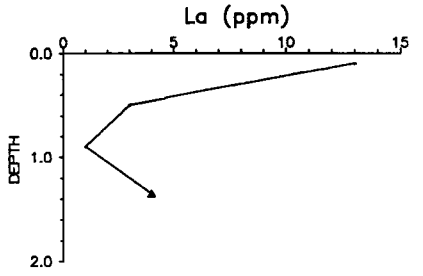
La (ppm)
0
5
10
15
0.0
1.0
2.0
DEPTH

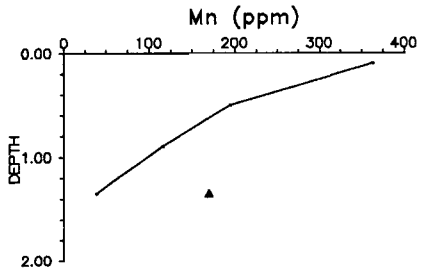
Mn (ppm)
0
100
200
300
400
0.00
1.00
2.00
DEPTH

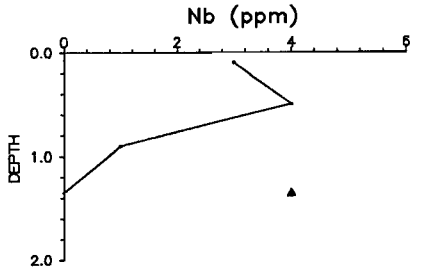
Nb (ppm)
0
2
4
6
0.0
1.0
2.0
DEPTH

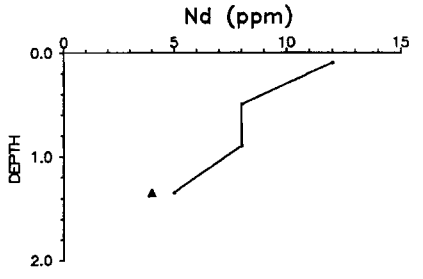
Nd (ppm)
0
5
10
15
0.0
1.0
2.0
DEPTH

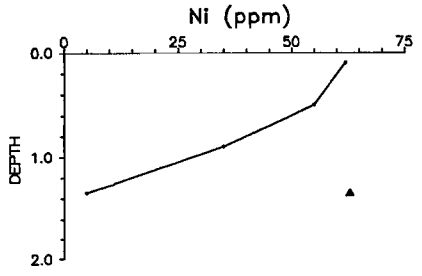
Ni (ppm)
0
25
50
75
0.0
1.0
2.0
DEPTH

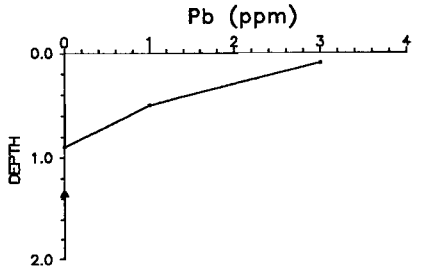
Pb (ppm)
0
1
2
3
4
0.0
1.0
2.0
DEPTH

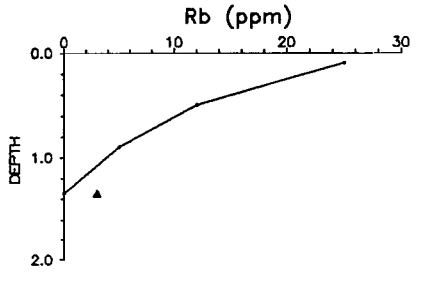
Rb (ppm)
0
10
20
30
0.0
1.0
2.0
DEPTH

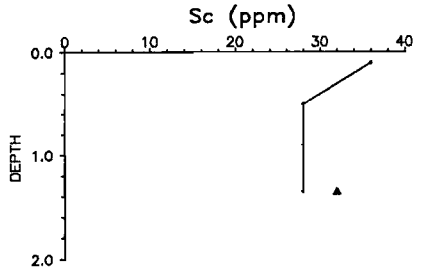
Sc (ppm)
0
10
20
30
40
0.0
1.0
2.0
DEPTH

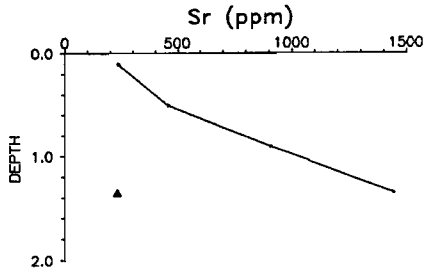
Sr (ppm)
0
500
1000
1500
0.0
1.0
2.0
DEPTH

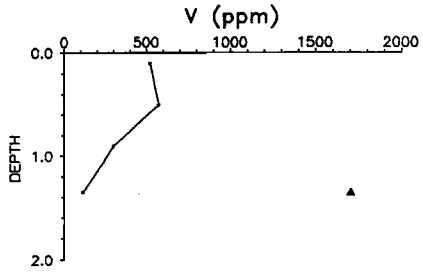
V (ppm)
0
500
1000
1500
2000
0.0
1.0
2.0
DEPTH

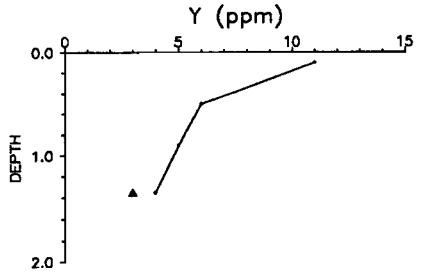
Y (ppm)
0
5
10
15
0.0
1.0
2.0
DEPTH

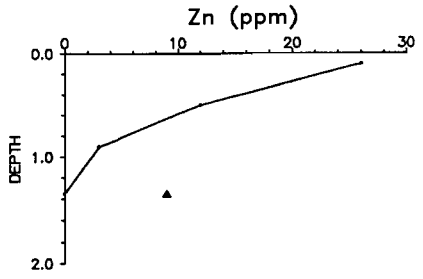
Zn (ppm)
0
10
20
30
0.0
1.0
2.0
DEPTH

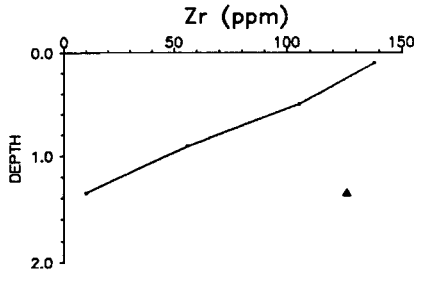
Zr (ppm)
0
50
100
150
0.0
1.0
2.0
DEPTH

4.0 DISCUSSION

The results indicate that Au is present in high concentrations in soils and lateritic gravels at Peach Tree and at Lady Gladys. These materials are commonly carbonate-rich, at least in the top 1 - 2 m, and gold is present in both the calcareous and ferruginous fractions. At Peach Tree, in addition, higher, more localized, concentrations of Au have been intersected by drilling at greater depths in a ferruginous saprolite beneath a leached zone. These concentrations are assumed to represent weathered primary mineralization, possibly secondarily enriched.

The surface enrichment of Au is fairly typical for profiles found throughout the Yilgarn Block and has been attributed to weathering associated, firstly, with warm, humid conditions during the early Tertiary and, secondly, with a later, more arid phase (e.g., Butt, 1989). The former humid climates were probably equivalent to those prevailing in the present wetter savannas and caused the widespread development of lateritic regoliths characterized by surficial ferruginous zones overlying deep, clay-rich saprolites. The later arid to semi-arid climates, which still prevail, have resulted in modifications to the pre-existing profile due to the development of acid and highly saline groundwaters, a general lowering of water-tables and changes to, and slowing of, chemical weathering. Some Fe accumulation in the saprolite can be related to precipitation at old water-table levels. More importantly, the excess of evaporation over precipitation has led to the accumulation of normally mobile alkaline earth elements as carbonates in the near-surface.

The present distribution of Au at Mulline can be related to these major climatic events:

1. Some of the Au is associated with the Fe accumulations, particularly the lateritic gravels and, presumably, has been subject to similar chemical controls. Under the luxuriant growth generated by humid tropical conditions during the Tertiary, Au may be mobilized as organic complexes (Gray, 1989), precipitated with Fe oxides and retained within the laterite, mostly as fine particles of secondary Ag-poor gold. Larger grains encapsulated within the lateritic nodules, noted at Bardoc (Freyssinet and Butt, 1988) but not identified in this study, are of residual primary Au.

2. At both Peach Tree and Lady Gladys, as at other sites in the southern Yilgarn Block, a significant proportion of Au in the surface horizons is associated with accumulations of pedogenic carbonate. The nature of the association is not very clear, but inspection of the data suggests it to be most significant in the top 0.5m. Below this depth, the association with Fe becomes increasingly important. The relationship between Au and Ca may be chemical or may merely represent a zone where the two elements accumulate independently by a physically driven process related to their proximity to the surface, e.g., percolation of rainfall followed by evaporation and precipitation. Results from laboratory studies suggests that this Au is highly mobile and probably occurs as organic complexes (Gray et al., 1990a; Gray et al., 1990b).

The distribution of Au in the surface horizons is controlled by the relative importance of the two associations, i.e., with lateritic Fe oxides and with pedogenic carbonates, and interpretation of the data must take these two influences into account. In general, the addition of pedogenic carbonate to a soil horizon dilutes the abundance of other, pre-existing components. This feature is observable, for example, in the distributions of Fe and trace elements, including Au, contained within the lateritic Fe oxides. The abundances of elements associated with the carbonates (e.g., Ca, Mg, Sr, Ba) are, of course, increased. For Au, accumulation in the carbonate horizon generally offsets the dilution of Au in the Fe oxides, such that there is a net increase in Au abundance. There is thus no simple correlation between the abundance of Au with either Fe or

Ca. This differs from the relationships observed at Mt. Hope and Panglo, where the carbonates generally did not occur within lateritic horizons and hence the Au-Fe oxide association was absent.

It is worth speculating on the origin of the secondary carbonates in the regolith. There are several possible direct or indirect sources of the Ca, including rock weathering, groundwater, vegetation, aeolian dust and rainfall (either dissolved or as aerosols), each of which may contribute to some extent. The CO_2 component of the carbonate is probably derived from respiration by plant roots and microorganisms. Production of CO_2 will be greatest slightly below the surface and in the root zone (rhizosphere), typically within the top metre of the soil profile.

The carbonate nearer the surface takes the form of coatings or friable aggregates which partly make up the loamy soil matrix. Their fine texture is suggestive of recently formed and (re-) mobilized material. Vegetation may be partly responsible for cycling and re-cycling of this Ca from lower in the profile to the surface, since Ca is an important nutrient. Eucalypt ash from Panglo, for example, contains up to 30 wt% Ca (Lintern and Scott, 1990). The Ca is returned to the soil as leachates during rainfall, by the fall of litter and as the vegetation dies and decays. Carbonate situated lower in the profile tends to be indurated and either nodular or weakly layered and appears to represent the accumulation of carbonate derived from the re-working of more friable material. The layering or pseudo-bedding evident at Peach Tree is due to preferential infiltration and precipitation of carbonate along sub-horizontal partings within the lateritic gravels. Some of this layered carbonate may be derived laterally, for example from the source represented by the massive carbonates that form the bar across the trench.

The origin of the massive carbonates of the bar in the trench at Peach Tree is uncertain. The E-W strike and massive nature suggest the bar to be related to an underlying primary structure, but the carbonates are clearly secondary and enclose lateritic pisoliths. In areas of residual soil at Mt Pleasant, where fresh rocks occur within 3m of the surface, primary carbonate alteration can be seen to be reworked close to the surface and to merge into the pedogenic carbonate horizon (Lawrance, 1991). At Peach Tree, however, the depth of weathering is much greater and any carbonate associated with primary mineralization would be expected to be leached throughout most of the regolith. Accordingly, if there is a relationship between the surface occurrence of the carbonates and primary structures, it is probably due to those structures resulting in zones providing preferential evaporation or evapo-transpiration pathways through the regolith. More generally, the areal distribution of the carbonates and, indeed, that of the gold, suggests a relationship with a particular primary unit, possibly either carbonate alteration associated with mineralization or the host rocks, centred approximately about the strike of the bar. Study of the deeper regolith and of the primary mineralization and host rocks is required to establish these relationships.

5.0 SUMMARY AND IMPLICATIONS FOR EXPLORATION

Field and geochemical observations suggest there is a complex relationship between the distributions of lateritic materials, carbonates and gold at Mulline which can be summarized as follows:

1. The gold anomaly/resource is contained within the lateritic gravels and duricrusts; it occurs where carbonates are also present in the profile, but is not confined to the calcareous horizons.

2. The carbonates are most abundant centrally within the low mound formed by the lateritic materials and have a spatial relationship with the distribution of gold. The lateritic gravels may be partly protected from erosion by carbonate cementation.

3. Gold is present in both carbonate-rich and Fe oxide-rich soils and gravels and there are no simple correlations between their abundances. The carbonates possibly dilute the initial Au content of the lateritic materials but have themselves been Au enriched. The association between Au and Ca is strongest in the top 0.5m, where carbonates are more abundant and occur as coatings and within the soil matrix. In comparison, the much stronger associations between Au and Ca found at Mt. Hope and Panglo are in materials in which carbonates are in this form but in which there is no additional Au-Fe association.

4. Clear associations between other elements and mineral phases are difficult to recognize because of the effects of dilution by secondary carbonate.

The implications of these results for exploration are similar to those derived from research at Mt. Hope and Panglo. Because Au accumulates preferentially in the carbonate horizon, this horizon should be sampled if present. Carbonates occurring in the friable matrix and as coatings, usually in the top metre, appear to be concentrate Au more than nodular and massive forms slightly deeper in the profile, hence shallow augering remains a suitable sampling technique However, carbonate has only a limited distribution close to the Menzies Line, hence calcareous and non-calcareous soils must be distinguished, because the latter will tend to have much lower background and threshold values. The results also confirm the importance of lateritic gravels as sample media, for they also offer the potential of a multi-element expression of mineralization. However, they too are not present over the whole terrain and, if collected as part of a soil sample, the response may be influenced by the presence of carbonates. Accordingly, it is unlikely that a single sample type (e.g., calcareous soil, lateritic pisoliths) can be collected to give satisfactory coverage at either regional or detailed scales. Sampling and interpreation procedures, therefore, have to take into account the varying distributions of calcareous and/or lateritic media and different criteria must be established for assessing the data, including those pertaining to samples which contain neither calcareous nor ferruginous components in significant amounts.

6.0 ACKNOWLEDGEMENTS

The sponsors of AMIRA Project P241 are thanked for their support and in particular, R.W. Howard of Pancontinental Mining Ltd, for supplying maps and sections relating to the area. We are indebted to the staff at CSIRO for their assistance, particularly J.F. Crabb and R.J. Bilz (sample preparation), M.K.W. Hart (XRF), J.E. Wildman (ICP), A.K. Howe and M.J. Willing (AAS), and A.D. Vartesi and C.R. Steel (drafting). We also acknowledge C.W. Dornan for his valuable assistance with XRD interpretation. A.Z. Gedeon is thanked for his assistance in the initial stages of the study, particularly for sample separations and XRD interpretation.

7.0 REFERENCES

Aplin, T.E.H., 1975. The vegetation of Western Australia. Western Australian Yearbook No.14. W.A. Government Printer, Perth, 570 pp.

Butt, C.R.M., 1989. Genesis of supergene gold deposits in the lateritic regolith of the Yilgarn Block, Western Australia. In: R.R. Keays, W.R.H. Ramsay and D.I. Groves (Editors), The geology of gold deposits: the perspective in 1988. Economic Geology Monograph 6, Economic Geology, New Haven, pp. 460-470.

Butt, C.R.M., Horwitz, R.C. and Mann, A.W., 1977. Uranium occurrences in calcrete and associated sediments in Western Australia. Report FP16, CSIRO Australia, Division of Mineralogy, Floreat Park, pp. 67.

Diels, L., 1906. Die Pflanzenwelt von West-Australien sudlich des Wendekreises. Vegn. Erde 7, Leipzig.

Freyssinet, P. and Butt, C.R.M., 1988. Morphology and geochemistry of gold in a lateritic profile, Bardoc mine, Western Australia. Restricted Report, MG 59R. CSIRO Australia, Division of Exploration Geoscience, Perth, 19 pp. (Unpublished).

Geological Survey, 1969. 1:250,000 Geological Series - Explanatory Notes, Kalgoorlie, Sheet SH/51 M.J.B. Kriewaldt (Compiler). Bureau of Mineral Resources, Canberra, 18 pp.

Geological Survey, 1990. Geology and mineral resources of Western Australia. Memoir 3. Geological Survey of Western Australia, Perth, 827 pp.

Gray D.G., 1989. The aqueous chemistry of gold in the weathering environment. Restricted Report, 4R. CSIRO Australia, Division of Exploration Geoscience, Perth, 65 pp. (Unpublished).

Gray, D.G., Lintern, M.J. and Longman, G.D., 1990a. Chemistry of gold in some Western Australian soils. Restricted Report, 126R. CSIRO Australia, Division of Exploration Geoscience, Perth, 62 pp. (Unpublished).

Gray, D.G., Lintern, M.J. and Longman, G.D., 1990b. Chemistry of gold-humic interactions. Restricted Report 128R. CSIRO Australia, Division of Exploration Geoscience, Perth, 32pp. (Unpublished).

Lawrance, L.M., 1991. Distribution of gold and ore-associated elements within lateritic weathering profiles of the Yilgarn Block, Western Australia. PhD. thesis, Univ. of Western Australia, Perth, Australia, 416 pp. (Unpublished).

Lintern, M.J., Mann, A.W. and Longman, G.D., 1988. The determination of gold by anodic stripping voltammetry. Analytica Chimica Acta, 209: 193-203.

Lintern, M.J., 1989. Study of the distribution of gold in soils at Mt. Hope, Western Australia. Restricted Report 24R. CSIRO Australia, Division of Exploration Geoscience, Perth, 17 pp. (Unpublished).

Lintern, M.J. and Scott, K.M., 1990. The distribution of gold and other elements in soils and vegetation at Panglo, Western Australia. Restricted Report 129R. CSIRO Australia, Division of Exploration Geoscience, Perth, 50 pp. (Unpublished).

Mann, A.W. and Horwitz, R.C., 1979. Groundwater calcrete deposits in Australia: some observations from Western Australia. Journal of the Geological Society of Australia. 26: 293-303.

8.0 APPENDICES

1. Peach Tree entire chemical data set (tabulated).
2. Lady Gladys entire chemical data set (tabulated).

3a. Comparison of 0-1m composite chemical data distribution between 12700N and 12725N (plotted).

3b. Comparison of 3-4m composite chemical data distribution between 12700N and 12725N (plotted).

Data disk enclosed with files in EXCEL (.XLS) and ASCII (.TXT) formats.

1. Peach Tree entire chemical data set.

TYPE	NUMBER	EAST	NORTH	DEPTH	SiO2 % (icp)	AL2O3 % (icp)	TiO2 % (xrf)	MgO % (icp)	CaO % (icp)	Fe2O3 % (icp)	S % (xrf)	P % (xrf)	Na2O % (xrf)	Ag ppm (xrf)	As ppm (xrf)	Au ppm (aav)	Ba ppm (xrf)	Be ppm (icp)	Bi ppm (xrf)	Cd ppm (xrf)	Ce ppm (xrf)	Co ppm (xrf)	Cr ppm (xrf)	Cs ppm (xrf)
	4150	10400	12771	0.30	31.8	14.40	1.40	0.21	0.24	43.90	0.016	0.035	0.08	0	23	0.22	233	0.4	5	0	47	11	995	0
	4151	10400	12771	0.50	29.2	8.13	0.36	1.00	25.50	8.27	0.108	0.014	0.16	1	2	1.20	324	1.5	2	3	18	11	200	0
	4152	10400	12765	0.45	26.5	16.30	1.31	0.27	0.32	46.00	0.015	0.021	0.03	0	15	0.58	293	0.0	2	0	50	8	1098	1
	4153	10400	12765	0.75	21.1	11.70	0.62	1.15	16.20	24.60	0.079	0.010	0.06	0	15	1.40	265	0.9	0	0	21	5	471	0
	4154	10400	12757	0.15	32.4	11.50	1.09	0.47	6.56	35.10	0.042	0.025	0.10	0	16	0.30	205	1.3	1	0	36	24	779	0
	4155	10400	12757	0.20	23.8	8.58	0.70	1.05	19.10	24.50	0.081	0.010	0.07	0	2	0.38	196	1.0	1	0	18	9	474	0
Profile	4156	10400	12750	0.40	35.1	11.00	1.02	0.86	7.56	33.40	0.043	0.035	0.07	0	5	0.28	172	0.5	3	1	31	13	670	0
4156	4157	10400	12750	0.60	29.3	9.20	0.73	2.39	16.60	24.00	0.050	0.015	0.03	1	6	0.48	169	2.0	0	0	25	5	471	0
	4158	10400	12750	0.95	21.3	7.32	0.53	5.37	22.20	17.10	0.055	0.006	0.07	0	6	0.86	193	3.6	2	0	12	8	347	0
	4159	10400	12750	1.20	24.8	15.50	1.23	1.07	3.78	37.10	0.022	0.005	0.11	0	13	0.92	165	2.3	2	0	17	15	842	0
	4160	10400	12750	1.50	25.1	15.60	1.28	0.55	4.28	36.80	0.020	0.001	0.17	0	11	0.48	76	1.1	3	0	13	12	803	0
Profile	4161	10400	12744	0.30	34.8	11.40	1.13	0.52	4.90	36.10	0.044	0.030	0.08	3	8	0.20	184	2.2	3	1	39	18	797	0
4161	4162	10400	12744	0.50	27.1	7.74	0.60	1.18	20.10	16.90	0.062	0.025	0.10	0	6	0.62	143	5.2	0	0	27	17	343	0
	4163	10400	12744	0.50	21.2	6.25	0.43	2.03	27.70	11.30	0.081	0.013	0.04	0	6	1.44	129	3.8	0	0	10	2	243	0
	4164	10400	12744	0.90	28.3	14.50	0.77	1.73	12.00	20.70	0.036	0.003	0.12	0	4	1.12	135	1.7	3	0	10	6	439	0
	4165	10400	12744	1.70	21.5	7.46	0.44	6.00	20.80	10.90	0.063	0.001	0.16	0	5	0.46	126	3.1	1	2	4	11	260	0
	4166	10400	12744	1.90	31.7	16.30	0.86	2.00	5.18	24.20	0.018	0.002	0.28	1	7	0.70	72	2.7	3	0	11	20	498	0
	4167	10400	12743	1.00	15.2	5.57	0.38	4.77	26.50	8.80	0.071	0.002	0.05	3	4	0.90	159	3.1	1	0	2	4	203	0
	4168	10400	12742	1.00	21.5	5.77	0.49	3.01	21.10	13.40	0.056	0.009	0.03	0	9	1.06	133	1.7	0	2	15	0	316	0
Profile	4169	10400	12735	0.20	32.5	10.60	1.24	0.47	3.18	33.50	0.038	0.030	0.11	0	5	0.26	191	0.0	0	0	46	8	832	0
4169	4170	10400	12735	0.40	29.1	8.51	0.77	0.75	12.90	21.40	0.052	0.028	0.04	0	1	0.50	150	1.0	2	1	26	17	513	0
	4171	10400	12735	0.30	17.5	6.64	0.39	0.91	38.80	9.78	0.070	0.005	0.02	0	5	0.70	125	1.4	1	0	13	9	193	0
	4172	10400	12735	0.50	26.8	8.21	0.64	1.33	19.20	20.20	0.046	0.017	0.03	0	4	0.86	143	0.0	3	2	21	15	428	0
	4173	10400	12735	0.80	27.7	7.27	0.54	3.21	20.80	15.00	0.038	0.007	0.05	0	8	1.02	164	0.0	1	0	15	2	331	0
	4174	10400	12735	1.20	27.9	7.67	0.52	5.68	19.00	13.30	0.041	0.007	0.08	3	6	0.84	217	0.0	0	0	16	10	308	0
	4175	10400	12735	1.50	30.8	14.60	0.82	1.23	8.74	28.40	0.044	0.003	0.12	1	9	1.40	336	0.0	0	2	10	21	586	0
	4176	10400	12735	1.80	26.4	14.70	0.79	2.18	11.20	26.90	0.028	0.002	0.21	0	6	1.08	116	0.0	0	0	7	25	561	0
Profile	4177	10400	12730	0.20	36.2	11.30	1.05	0.59	7.06	32.80	0.029	0.028	0.08	1	17	0.40	179	0.0	2	0	36	29	706	0
4177	4178	10400	12730	0.40	34.5	11.90	0.96	0.82	9.62	30.60	0.028	0.017	0.07	0	6	0.62	149	0.0	0	0	31	20	651	0
	4179	10400	12730	0.70	32.0	11.50	0.74	0.99	12.70	22.20	0.035	0.011	0.08	0	5	0.92	142	0.0	5	1	29	9	462	0
	4180	10400	12730	1.20	26.0	15.20	0.77	0.91	10.20	27.00	0.051	0.005	0.11	4	8	1.68	423	0.0	0	0	33	24	575	0
	4181	10400	12730	1.40	26.9	16.60	0.77	0.85	10.00	25.80	0.082	0.006	0.19	0	4	1.62	782	0.0	2	0	20	11	545	0
	4182	10400	12725	0.15	35.7	14.80	1.26	0.38	1.05	36.60	0.016	0.023	0.05	0	9	0.56	162	0.0	1	1	59	38	862	0
	4183	10400	12725	0.30	25.0	16.40	1.01	0.44	3.57	36.40	0.012	0.012	0.03	0	16	1.84	100	0.0	3	0	82	39	829	0
	4184	10400	12712	0.30	34.7	20.00	1.49	0.11	0.11	30.10	0.025	0.013	0.01	1	3	0.66	82	0.0	2	0	29	34	730	0
	4185	10400	12700	0.30	26.3	15.60	0.97	0.10	0.13	43.10	0.038	0.016	0.00	0	4	1.18	51	0.0	3	0	26	29	526	0

TYPE	NUMBER	Cu ppm (xrf)	Ga ppm (xrf)	Ge ppm (xrf)	In ppm (xrf)	La ppm (xrf)	Mn ppm (xrf)	Mo ppm (xrf)	Nb ppm (xrf)	Nd ppm (xrf)	Ni ppm (xrf)	Pb ppm (xrf)	Rb ppm (xrf)	Sb ppm (xrf)	Sc ppm (xrf)	Se ppm (xrf)	Sn ppm (xrf)	Sr ppm (xrf)	V ppm (xrf)	W ppm (xrf)	Y ppm (xrf)	Zn ppm (xrf)	Zr ppm (xrf)
	4150	45	40	2	4	23	203	5	7	22	86	37	21	0	75	5	1	19	1090	2	15	23	184
	4151	50	11	1	4	15	145	0	4	18	52	6	14	0	43	4	0	314	180	0	16	11	65
	4152	77	42	1	1	26	147	5	8	25	108	49	19	0	99	3	0	22	1200	5	15	17	164
	4153	83	24	2	3	7	117	2	0	17	71	25	12	1	63	1	0	282	463	2	13	12	95
	4154	52	29	3	0	15	344	3	4	17	82	36	26	3	55	0	0	95	785	6	12	23	181
	4155	56	18	2	0	7	363	3	6	15	61	24	17	0	48	1	0	286	495	4	9	11	117
Profile	4156	43	26	2	0	18	420	5	5	17	62	29	28	0	50	0	0	135	678	0	12	33	175
4156	4157	57	18	1	1	9	315	3	4	14	55	21	21	0	50	0	3	409	483	1	11	12	134
	4158	47	14	0	2	9	181	2	5	12	44	20	16	0	49	0	0	802	385	0	10	6	95
	4159	82	39	0	0	6	94	4	5	11	79	42	8	0	95	2	1	221	970	4	7	6	138
	4160	73	34	2	2	8	84	5	7	6	86	38	5	0	94	3	0	156	954	9	4	2	134
Profile	4161	37	31	2	0	23	468	0	7	16	64	36	30	1	56	2	0	89	832	2	12	24	168
4161	4162	46	13	1	0	15	327	1	5	17	51	20	23	1	43	0	0	351	334	5	11	15	120
	4163	53	10	1	0	9	158	1	1	15	46	10	13	1	43	1	0	712	254	1	6	6	79
	4164	67	24	0	0	0	77	3	5	10	62	29	5	0	66	0	2	462	518	0	6	4	94
	4165	36	13	0	0	0	230	2	0	9	29	16	7	1	48	0	0	1158	285	0	4	7	58
	4166	59	26	2	1	4	78	2	3	8	61	37	8	0	67	0	0	337	632	2	4	5	106
	4167	41	8	0	1	6	169	1	3	11	32	8	7	1	46	1	5	1083	236	2	7	6	61
	4168	45	11	1	0	12	220	4	3	17	45	15	17	0	45	0	2	673	347	0	10	11	93
Profile	4169	54	29	0	0	25	544	3	5	19	73	37	31	1	57	2	0	65	857	3	14	27	183
4169	4170	54	19	0	0	17	428	2	4	15	62	22	26	0	46	0	0	185	520	4	11	17	142
	4171	36	8	1	5	9	380	2	2	30	38	8	10	0	45	0	2	308	193	1	7	12	64
	4172	53	16	1	3	13	316	1	2	11	58	23	20	2	46	4	0	301	470	1	11	13	129
	4173	44	11	1	2	7	254	3	2	14	51	19	18	0	42	2	0	545	398	3	8	12	103
	4174	42	12	1	0	6	232	2	3	11	41	17	19	0	40	1	0	825	339	0	8	14	103
	4175	65	27	0	0	4	61	0	4	10	68	35	7	2	66	3	0	315	659	0	6	6	93
	4176	61	26	1	0	9	57	0	3	7	61	31	4	0	67	2	0	335	635	3	4	6	91
Profile	4177	58	28	0	0	17	539	3	7	14	70	38	30	1	50	3	0	88	729	0	14	25	161
4177	4178	61	22	0	2	15	430	5	7	14	66	30	22	0	57	3	5	133	720	4	14	16	168
	4179	68	19	2	0	17	296	3	7	11	65	31	20	1	54	1	1	207	518	5	10	18	141
	4180	95	28	0	0	15	163	3	2	14	79	48	9	3	76	2	1	229	662	3	12	7	120
	4181	73	25	1	0	9	81	1	0	8	82	34	5	2	80	4	0	256	620	0	7	4	96
	4182	73	34	2	0	21	418	3	10	22	75	46	24	3	83	3	0	34	955	3	16	32	191
	4183	117	35	0	0	29	226	4	6	30	112	48	10	0	92	2	0	47	925	2	25	14	145
	4184	88	40	0	0	13	106	4	8	13	70	27	15	0	95	2	1	10	1019	6	9	16	177
	4185	178	21	0	0	4	124	1	3	9	60	24	13	0	174	5	1	5	641	8	7	68	110

1. Peach Tree entire chemical data set (cont.).

TYPE	NUMBER	HOLE	EAST	NORTH	DEPTH	SiO2 % (icp)	Al2O3 % (icp)	TiO2 % (icp)	MgO % (icp)	CaO % (icp)	Fe2O3 % (icp)	Au ppm (asv)	Ba ppm (icp)	Be ppm (icp)	Cr ppm (icp)	Cu ppm (icp)	Mn ppm (icp)	Ni ppm (icp)	V ppm (icp)	Zr ppm (icp)
Profile 4201	4201	PTRC32	10320	12700	0.50	16.30	19.60	1.26	0.80	8.35	31.70	1.28	137	1.86	699	53	231	146	754	215
	4202	PTRC32	10320	12700	1.50	15.00	22.60	1.28	4.18	9.97	18.00	0.83	387	1.71	484	34	141	84	493	165
	4203	PTRC32	10320	12700	2.50	13.70	27.70	1.76	1.24	4.21	25.40	2.04	131	0.00	610	54	129	99	693	200
	4204	PTRC32	10320	12700	3.50	21.00	34.20	2.41	0.26	0.06	15.90	0.84	71	0.00	508	48	109	93	621	216
	4205	PTRC32	10320	12700	4.50	20.40	31.30	1.93	0.36	0.71	20.60	0.64	70	0.00	693	66	89	150	792	208
	4206	PTRC32	10320	12700	5.50	22.60	23.70	1.46	0.18	0.18	28.90	1.53	77	0.31	599	89	70	114	684	190
	4207	PTRC32	10320	12700	6.50	26.30	21.50	1.28	0.10	0.00	29.60	0.13	83	0.47	501	114	70	97	619	187
	4208	PTRC32	10320	12700	7.50	25.10	20.00	0.91	0.10	0.00	32.40	0.04	118	0.00	248	151	82	76	356	198
	4209	PTRC32	10320	12700	8.50	21.40	17.80	0.57	0.10	0.00	38.20	0.00	146	0.00	213	116	83	77	151	182
	4210	PTRC32	10320	12700	9.50	29.60	22.40	1.72	0.10	0.00	26.70	0.00	156	0.00	465	86	234	51	597	182
	4211	PTRC32	10320	12700	10.50	33.10	21.40	2.08	0.13	0.01	26.90	0.00	95	0.00	386	86	42	58	271	199
	4212	PTRC32	10320	12700	11.50	41.90	20.80	1.46	0.13	0.04	21.50	0.00	202	0.00	306	65	31	56	192	155
	4213	PTRC32	10320	12700	12.50	51.30	22.30	0.34	0.18	0.01	11.70	0.00	65	0.00	116	51	12	34	78	116
	4214	PTRC32	10320	12700	13.50	48.60	23.30	0.63	0.14	0.01	11.20	0.00	71	0.00	105	52	8	24	79	148
	4215	PTRC32	10320	12700	14.50	54.50	22.20	0.32	0.15	0.01	7.79	0.00	51	0.00	77	42	7	67	54	124
Profile 4246	4246	PTRC42	10425	12725	0.50	30.30	19.20	1.01	0.18	0.13	38.40	1.05	145	1.11	816	116	178	155	818	242
	4247	PTRC42	10425	12725	1.50	23.40	19.70	1.01	0.26	0.22	41.10	1.88	627	1.11	813	123	112	148	874	224
	4248	PTRC42	10425	12725	2.50	24.80	18.10	0.99	0.25	0.31	42.70	0.53	564	1.74	803	127	108	127	898	222
	4249	PTRC42	10425	12725	3.50	24.70	17.30	1.04	0.24	0.12	43.40	0.78	273	2.37	809	129	124	126	913	227
	4250	PTRC42	10425	12725	4.50	25.50	16.50	1.04	0.29	0.14	42.70	1.22	162	1.90	768	155	108	114	936	208
	4251	PTRC42	10425	12725	5.50	36.80	15.10	0.97	0.41	0.14	33.70	0.99	178	0.79	630	115	83	105	723	175
	4252	PTRC42	10425	12725	6.50	51.90	19.00	1.16	0.46	0.12	13.60	0.02	124	1.11	251	106	89	62	302	111
	4253	PTRC42	10425	12725	7.50	37.90	16.00	1.01	0.42	0.10	30.20	0.32	164	0.63	535	123	102	77	645	157
	4254	PTRC42	10425	12725	8.50	31.60	15.10	1.11	0.36	0.08	37.30	0.44	136	1.58	666	131	97	90	818	188
	4255	PTRC42	10425	12725	9.50	49.70	18.00	1.13	0.32	0.07	17.50	0.07	188	1.74	268	131	131	56	413	134
	4256	PTRC42	10425	12725	10.50	61.60	15.90	0.49	0.33	0.06	8.29	0.00	110	0.48	128	83	48	67	181	98
	4257	PTRC42	10425	12725	11.50	63.70	15.30	0.46	0.54	0.08	6.28	0.00	88	0.00	108	75	30	65	123	137
	4258	PTRC42	10425	12725	12.50	41.30	14.10	0.78	0.35	0.06	27.90	0.38	165	0.00	425	137	74	88	606	156
	4259	PTRC42	10425	12725	13.50	64.80	14.90	0.30	0.35	0.05	8.16	0.06	131	0.00	129	71	14	65	161	97
Traverse 12700	4186	PTWR24	10050	12700	0.50	48.30	10.80	1.13	5.85	9.74	9.66	0.06	309	2.17	166	56	906	120	273	111
	4187	PTWR23	10100	12700	0.50	44.20	9.15	0.66	2.75	15.00	8.66	0.10	190	1.86	179	89	767	134	189	113
	4188	PTWR23	10100	12700	3.50	52.10	9.94	0.75	0.94	4.71	16.50	0.02	127	0.78	243	247	407	190	383	154
	4189	PTWR22	10150	12700	0.50	29.70	8.30	0.62	6.73	15.00	12.70	0.29	129	0.00	196	86	370	84	368	107
	4190	PTWR22	10150	12700	3.50	32.50	19.50	1.76	1.93	3.07	23.60	0.02	106	0.00	338	127	417	92	590	177
	4191	PTWR21	10200	12700	0.50	30.30	11.00	0.77	4.06	10.60	20.50	0.95	141	0.00	356	92	491	108	570	151
	4192	PTWR21	10200	12700	3.50	30.10	20.10	1.52	0.91	1.97	26.80	0.08	151	0.62	386	111	352	77	666	178
	4193	PTRC71	10225	12700	0.50	20.40	8.96	0.67	10.20	16.50	10.10	0.62	115	4.50	243	50	366	79	317	109
	4194	PTRC71	10225	12700	3.50	31.30	21.40	1.35	0.30	0.04	31.60	0.01	116	2.17	383	123	199	129	501	199
	4195	PTWR20	10250	12700	0.50	22.10	20.50	1.77	3.68	9.28	20.20	0.79	107	1.09	395	47	335	139	653	226
	4196	PTWR20	10250	12700	3.50	18.00	25.80	1.98	1.10	2.17	30.80	0.67	93	0.00	491	101	182	118	874	244
	4197	PTRC31	10275	12700	0.50	20.90	21.60	1.21	3.75	8.28	23.00	0.65	87	0.00	530	42	123	162	689	196
	4198	PTRC31	10275	12700	3.50	10.60	25.50	1.59	3.78	4.97	26.80	0.26	91	0.00	605	34	93	136	696	217
	4199	PTWR19	10290	12700	0.50	21.60	30.70	1.45	0.70	2.33	23.30	0.40	121	1.09	633	46	148	177	632	212
	4200	PTWR19	10290	12700	3.50	11.60	29.60	1.70	2.94	4.99	18.50	0.35	105	1.40	424	51	110	91	488	181
	4216	PTWR18	10350	12700	0.50	22.80	21.90	1.11	0.97	7.19	21.60	0.58	149	0.00	615	49	388	162	245	189
	4217	PTWR18	10350	12700	3.50	26.20	14.50	0.67	3.47	16.50	7.14	0.30	89	0.00	259	36	134	61	115	98
	4218	PTRC25	10375	12700	0.50	23.50	14.10	0.78	2.39	12.10	21.10	1.50	161	0.00	455	96	184	100	231	123
	4219	PTRC25	10375	12700	3.50	36.40	17.30	1.11	2.15	1.75	20.60	0.06	108	0.00	341	110	170	74	198	136
	4220	PTWR5	10400	12700	0.50	21.40	16.00	0.96	0.09	0.07	43.30	1.15	105	0.00	606	170	190	94	353	195
	4221	PTWR5	10400	12700	3.50	34.40	17.90	0.82	0.14	0.12	29.00	0.84	92	0.00	405	108	116	74	238	143
	4222	PTRC46	10425	12700	0.50	27.20	17.10	1.00	0.22	0.25	35.50	1.28	362	0.00	691	133	153	113	344	202
	4223	PTRC46	10425	12700	3.50	46.00	19.10	1.17	0.43	0.13	15.30	0.08	100	0.00	255	143	178	88	146	111
	4224	PTRC45	10470	12700	0.50	26.50	15.80	1.10	0.39	3.49	34.10	1.20	222	0.00	546	190	197	91	329	180
	4225	PTRC45	10470	12700	3.50	43.90	16.90	1.33	0.71	0.68	18.90	0.12	128	0.00	295	204	159	96	178	141
	4226	PTRC4	10500	12700	0.50	26.40	12.80	0.82	0.37	6.55	32.90	0.99	532	0.00	559	125	173	112	316	171
	4227	PTRC4	10500	12700	3.50	44.90	14.20	0.81	1.08	0.32	19.70	0.55	135	0.00	349	114	224	89	183	116
	4228	PTRC53	10525	12700	0.50	41.70	15.00	0.86	1.20	6.64	13.50	0.17	253	0.00	209	84	416	67	135	107
	4229	PTRC53	10525	12700	3.50	42.50	17.40	1.46	1.19	0.23	19.80	0.16	99	0.00	374	143	397	100	203	148
Traverse 12725	4230	PTRC97	10200	12725	0.50	15.10	19.10	2.28	4.31	10.60	17.20	1.00	93	0.00	444	63	209	60	366	228
	4231	PTRC97	10200	12725	3.50	18.00	22.10	2.23	0.23	0.03	27.00	0.06	92	0.00	478	143	134	77	296	213
	4232	PTRC70	10225	12725	0.50	15.30	20.40	2.00	1.08	9.10	25.60	1.30	107	0.00	503	38	170	127	332	239
	4233	PTRC70	10225	12725	3.50	6.91	20.40	3.14	1.08	1.45	41.60	1.47	98	0.00	592	98	82	119	586	328
	4234	PTRC19	10250	12725	0.50	19.00	23.30	1.54	1.94	6.86	24.70	1.25	110	0.00	550	22	112	161	296	225
	4235	PTRC19	10250	12725	3.50	2.93	28.30	3.52	0.24	0.21	47.40	0.04	104	0.00	849	20	86	413	562	434
	4236	PTRC20	10275	12725	0.50	30.70	14.80	1.24	2.20	6.47	25.80	0.33	142	2.69	552	45	219	101	649	216
	4237	PTRC20	10275	12725	3.50	14.90	33.10	1.63	0.27	0.06	30.70	0.14	77	2.85	725	41	63	164	737	256
	4238	PTRC21	10300	12725	0.50	25.50	16.20	1.11	0.79	5.90	32.10	1.12	162	1.27	722	47	105	107	747	235
	4239	PTRC21	10300	12725	3.50	18.30	32.40	1.69	1.07	1.08	25.10	0.34	121	1.27	576	37	63	128	612	228
	4240	PTRC22	10325	12725	0.50	28.00	12.70	0.86	0.96	11.30	27.60	0.98	300	0.16	603	68	104	89	608	187
	4241	PTRC22	10325	12725	3.50	21.80	24.50	1.14	1.83	1.93	31.20	0.22	99	1.90	718	56	50	97	750	202
	4242	PTRC24	10375	12725	0.50	28.70	12.00	0.67	1.19	13.10	22.90	0.61	208	1.58	476	64	174	89	493	151
	4243	PTRC24	10375	12725	3.50	26.50	26.50	1.10	1.57	1.14	24.40	0.99	65	4.59	601	80	85	107	635	170
	4244	PTRC41	10400	12725	0.50	26.60	18.50	0.86	0.35	2.73	35.60	1.64	272	2.22	728	116	173	122	745	207
	4245	PTRC41	10400	12725	3.50	28.40	19.10	1.06	0.24	0.12	36.20	1.48	111	0.48	580	145	84	91	727	193
	4260	PTRC43	10450	12725	0.50	34.50	20.50	1.01	0.27	0.30	28.30	2.43	173	1.74	587	142	161	174	633	209
	4261	PTRC43	10450	12725	3.50	40.30	20.00	2.34	0.27	0.19	27.70	0.80	125	0.00	451	152	107	121	648	156
	4262	PTRC44	10475	12725	0.50	31.90	23.10	2.09	0.21	0.16	33.40	3.79	114	2.63	626	161	144	131	776	223
	4263	PTRC44	10475	12725	3.50	55.00	18.00	1.81	0.38	1.44	18.40	0.31	214	1.15	302	122	252	187	405	135
	4264	PTRC3	10500	12725	0.50	30.60	22.60	2.59	0.20	0.15	37.60	2.60	195	2.96	751	132	182	140	875	263
	4265	PTRC3	10500	12725	3.50	40.10	21.20	2.35	0.52	0.71	29.20	0.33	144	0.82	492	118	117	95	686	174
	4266	PTRC52	10525	12725	0.50	41.10	17.20	2.04	0.41	3.66	32.10	0.94	384	0.82	493	123	220	100	766	199
	4267	PTRC52	10525	12725	3.50	53.20	23.60	3.09	0.44	0.52	21.70	0.06	122	0.00	320	115	350	83	475	165
	4268	PTRC55	10550	12725	0.50	30.30	13.30	1.63	0.29	2.64	27.30	1.04	321	2.96	408	121	171	88	668	159
	4269	PTRC55	10550	12725	3.50	40.80	17.70	2.39	0.35	0.42	16.50	0.06	107	1.64	267	86	270	114	366	134
	4270	PTRC107	10575	12725	0.50	27.30	11.50	1.33	1.47	12.40	23.90	0.34	251	0.00	360	91	184	76	602	126
	4271	PTRC107	10575	12725	3.50	42.00	18.70	2.59	0.39	0.56	20.90	0.06	136	0.00	340	77	144	60	429	147

1. Peach Tree entire chemical data set (cont.).

TYPE (select)	CO3	NUMBER	EAST	NORTH	DEPTH	SiO2 % (icp)	Al2O3 % (icp)	TiO2 % (icp)	MgO % (icp)	CaO % (icp)	Fe2O3 % (icp)	Au ppm (aas)	Ba ppm (icp)	Be ppm (icp)	Cr ppm (icp)	Cu ppm (icp)	Mn ppm (icp)	Ni ppm (icp)	V ppm (icp)	Zr ppm (icp)
Profile	High	4163C	10400	12744	0.5	16.50	5.66	0.35	2.30	33.30	9.50	1.50	147	1	197	6	123	44	243	44
4161	High	4164C	10400	12744	0.9	21.90	10.40	0.51	2.10	24.60	16.00	1.20	151	0	307	23	111	48	410	52
Profile	High	4178C	10400	12730	0.4	16.20	12.00	0.58	0.58	20.00	24.80	0.41	81	2	411	57	204	44	584	74
4177	High	4179C	10400	12730	0.7	27.60	8.14	0.50	1.14	22.00	13.10	0.66	136	2	266	21	250	45	318	104
	High	4180C	10400	12730	1.2	9.51	3.56	0.18	1.66	40.50	3.98	0.57	143	3	103	0	61	23	100	46
	Low	4180F	10400	12730	1.2	22.80	22.50	0.96	0.21	0.55	38.90	0.55	566	1	702	129	143	75	1017	118
	High	4181C	10400	12730	1.4	19.00	7.83	0.35	1.21	29.50	9.92	0.88	645	4	208	9	95	34	238	56

2. Lady Gladys entire chemical data set.

TYPE	NUMBER	EAST	NORTH	DEPTH	SiO2 % (icp)	AL2O3 % (icp)	TiO2 % (xrf)	MgO % (icp)	CaO % (icp)	Fe2O3 % (icp)	S % (xrf)	P % (xrf)	Na2O % (xrf)	Ag ppm (xrf)	As ppm (xrf)	Au ppm (esv)
Profile	4283	10014	9406	0.08	26.1	12.8	3.69	1.72	6.60	30.4	0.112	0.036	0.05	1	6	1.90
4283	4284	10014	9406	0.33	16.9	11.9	3.25	2.57	3.99	44.6	0.062	0.010	0.08	0	11	1.68
	4285	10014	9406	0.75	16.0	12.6	8.14	1.54	2.02	46.2	0.062	0.011	0.10	0	7	2.04
	4286	10014	9406	1.25	16.1	19.3	3.15	2.98	3.67	34.9	0.098	0.008	0.27	1	10	1.82
	4287	10014	9406	1.50	18.7	18.4	3.44	0.79	0.41	40.1	0.314	0.005	0.65	0	8	2.00
	4288	10014	9406	2.25	18.3	17.6	3.20	0.46	0.16	43.8	0.261	0.003	0.72	0	8	0.38
Profile	4289	10023	9400	0.15	25.4	14.9	1.51	4.24	12.20	17.7	0.125	0.028	0.05	0	5	2.76
4289	4290	10023	9400	0.65	17.9	15.1	1.08	7.55	13.90	11.5	0.168	0.005	0.10	0	20	2.00
	4291	10023	9400	1.25	13.7	21.4	1.34	7.03	10.50	12.7	0.242	0.005	0.34	0	7	1.14
	4292	10023	9400	1.75	11.8	27.6	1.62	4.57	6.12	18.2	0.316	0.008	0.43	4	7	1.48
	4293	10023	9400	2.25	18.0	34.3	1.44	0.84	0.39	18.1	0.479	0.006	0.83	0	1	0.30
Profile	4296	10033	9400	0.10	33.3	13.9	1.24	4.33	6.58	20.1	0.136	0.035	0.08	0	8	1.04
4296	4297	10033	9400	0.33	25.2	12.4	0.95	6.25	13.70	17.4	0.279	0.028	0.13	0	9	1.72
	4298	10033	9400	0.73	22.1	14.4	0.62	7.76	12.80	14.3	1.788	0.008	0.57	1	6	1.24
	4299	10033	9400	1.25	17.7	15.6	0.71	8.98	12.70	13.9	0.907	0.006	0.45	2	3	0.54
	4300	10033	9400	1.75	17.8	23.8	0.96	4.71	6.33	20.1	1.586	0.008	0.88	0	4	1.46
Profile	4301	10035	9408	0.10	34.3	14.3	0.98	2.88	8.81	20.1	0.234	0.029	0.10	0	9	1.64
4301	4302	10035	9408	0.50	27.1	17.7	0.98	5.01	11.90	10.5	0.262	0.016	0.12	0	13	2.52
	4303	10035	9408	0.90	17.6	8.94	0.60	11.30	19.70	4.5	0.178	0.002	0.12	1	9	1.22
	4304	10035	9408	1.35	4.3	2.78	0.13	16.00	26.00	1.0	0.101	0.000	0.16	2	4	0.22
	4305	10035	9408	1.35	24.4	30.3	1.32	1.86	1.31	16.7	0.993	0.009	0.50	0	12	1.52

TYPE	NUMBER	Ba ppm (xrf)	Be ppm (icp)	Bi ppm (xrf)	Cd ppm (xrf)	Ce ppm (xrf)	Co ppm (xrf)	Cr ppm (xrf)	Cs ppm (xrf)	Cu ppm (xrf)	Ga ppm (xrf)	Ge ppm (xrf)	In ppm (xrf)	La ppm (xrf)	Mn ppm (xrf)	Mo ppm (xrf)
Profile	4283	155	0.0	0	4	38	23	555	0	92	55	3	0	16	496	5
4283	4284	168	0.0	1	2	23	8	851	0	74	86	0	0	8	178	4
	4285	183	0.0	4	3	47	3	903	0	95	107	0	0	14	470	9
	4286	83	0.0	0	0	14	27	753	0	82	59	0	0	3	231	4
	4287	20	0.0	0	0	16	7	681	0	82	78	1	0	8	205	1
	4288	15	0.0	0	0	16	12	636	0	74	73	2	6	8	135	0
Profile	4289	126	0.0	0	0	25	3	357	0	85	34	0	0	2	294	3
4289	4290	107	0.0	0	0	15	6	285	0	68	22	0	0	8	201	0
	4291	96	0.0	1	0	12	1	322	0	73	28	0	0	5	214	1
	4292	54	0.0	2	0	13	17	445	0	89	31	0	4	6	240	3
	4293	24	0.0	0	3	10	15	336	0	91	26	1	0	6	223	2
Profile	4296	171	0.0	0	4	31	7	350	0	81	27	1	0	15	456	0
4296	4297	120	0.0	0	1	18	13	250	0	106	19	0	0	12	272	1
	4298	118	0.0	1	0	3	7	175	0	135	9	1	3	7	93	0
	4299	96	0.0	0	1	5	9	166	0	125	13	0	0	6	109	1
	4300	115	0.0	0	0	11	6	204	0	136	18	2	0	5	144	2
Profile	4301	162	0.0	1	0	27	13	292	0	123	20	1	0	13	363	4
4301	4302	99	0.0	0	0	12	0	211	0	109	15	0	4	3	195	3
	4303	80	0.1	1	0	5	1	98	0	53	8	0	1	1	116	2
	4304	87	0.0	1	0	0	0	27	0	16	2	0	0	4	39	0
	4305	52	0.0	1	3	8	12	310	0	149	22	1	4	4	170	1

TYPE	NUMBER	Nb ppm (xrf)	Nd ppm (xrf)	Ni ppm (xrf)	Pb ppm (xrf)	Rb ppm (xrf)	Sb ppm (xrf)	Sc ppm (xrf)	Se ppm (xrf)	Sn ppm (xrf)	Sr ppm (xrf)	V ppm (xrf)	W ppm (xrf)	Y ppm (xrf)	Zn ppm (xrf)	Zr ppm (xrf)
Profile	4283	10	9	39	4	22	3	28	3	0	137	1612	3	10	29	271
4283	4284	11	3	34	4	5	2	23	7	0	116	2404	0	4	3	226
	4285	21	3	42	4	2	1	24	8	9	76	2967	3	6	13	424
	4286	10	7	28	1	2	2	31	5	0	95	1774	4	5	11	208
	4287	12	3	51	0	1	0	25	8	1	45	1829	0	6	23	219
	4288	10	1	62	0	2	0	21	6	6	56	1615	0	3	10	192
Profile	4289	6	10	43	3	21	2	30	1	0	279	844	0	11	18	156
4289	4290	4	6	29	0	9	3	28	3	0	472	814	1	8	6	114
	4291	6	7	30	0	6	0	31	3	0	337	1033	0	9	5	126
	4292	4	7	39	0	4	0	30	3	0	197	1123	0	9	7	145
	4293	5	4	65	0	6	0	27	4	0	67	729	5	5	7	122
Profile	4296	6	13	59	5	33	0	36	0	1	223	631	1	12	37	159
4296	4297	5	9	49	3	18	0	35	3	0	368	523	1	9	19	131
	4298	3	6	35	0	5	1	42	4	0	590	466	6	5	4	63
	4299	0	5	28	0	2	0	39	1	0	581	465	4	7	3	62
	4300	5	11	32	0	4	0	45	3	2	426	703	4	6	6	77
Profile	4301	3	12	62	3	25	0	36	3	0	235	521	4	11	26	138
4301	4302	4	8	55	1	12	2	28	0	4	458	572	1	6	12	105
	4303	1	8	35	0	5	4	28	2	0	905	298	0	5	3	56
	4304	0	5	5	0	0	0	28	0	0	1442	113	2	4	0	10
	4305	4	4	63	0	3	0	32	4	0	232	1704	0	3	9	126

TYPE (select)	CO3	NUMBER	SiO2 % (icp)	Al2O3 % (icp)	TiO2 % (icp)	MgO % (icp)	CaO % (icp)	Fe2O3 % (icp)	Au ppm (aas)	Ba ppm (icp)	Be ppm (icp)	Cr ppm (icp)	Cu ppm (icp)	Mn ppm (icp)	Ni ppm (icp)	V ppm (icp)	Zr ppm (icp)
Profile	High	4280C	19.50	8.47	0.85	4.69	23.40	9.21	2.10	119	2	200	51	232	31	475	94
4283	High	4281C	9.35	3.37	0.54	14.80	23.70	4.18	0.67	49	3	98	0	108	23	245	52
	High	4282C	6.02	3.41	0.33	15.00	25.10	3.30	0.49	57	4	89	0	68	24	190	51
Profile	High	4283C	9.88	5.64	0.94	11.40	23.40	7.52	0.91	77	1	163	35	191	28	399	85
4283	Low	4283F	42.30	11.10	1.45	1.43	7.51	12.00	0.71	180	0	246	62	418	45	443	186

3a. Comparison of 0-1m composite chemical data distribution between 12700N and 12725N (plotted).

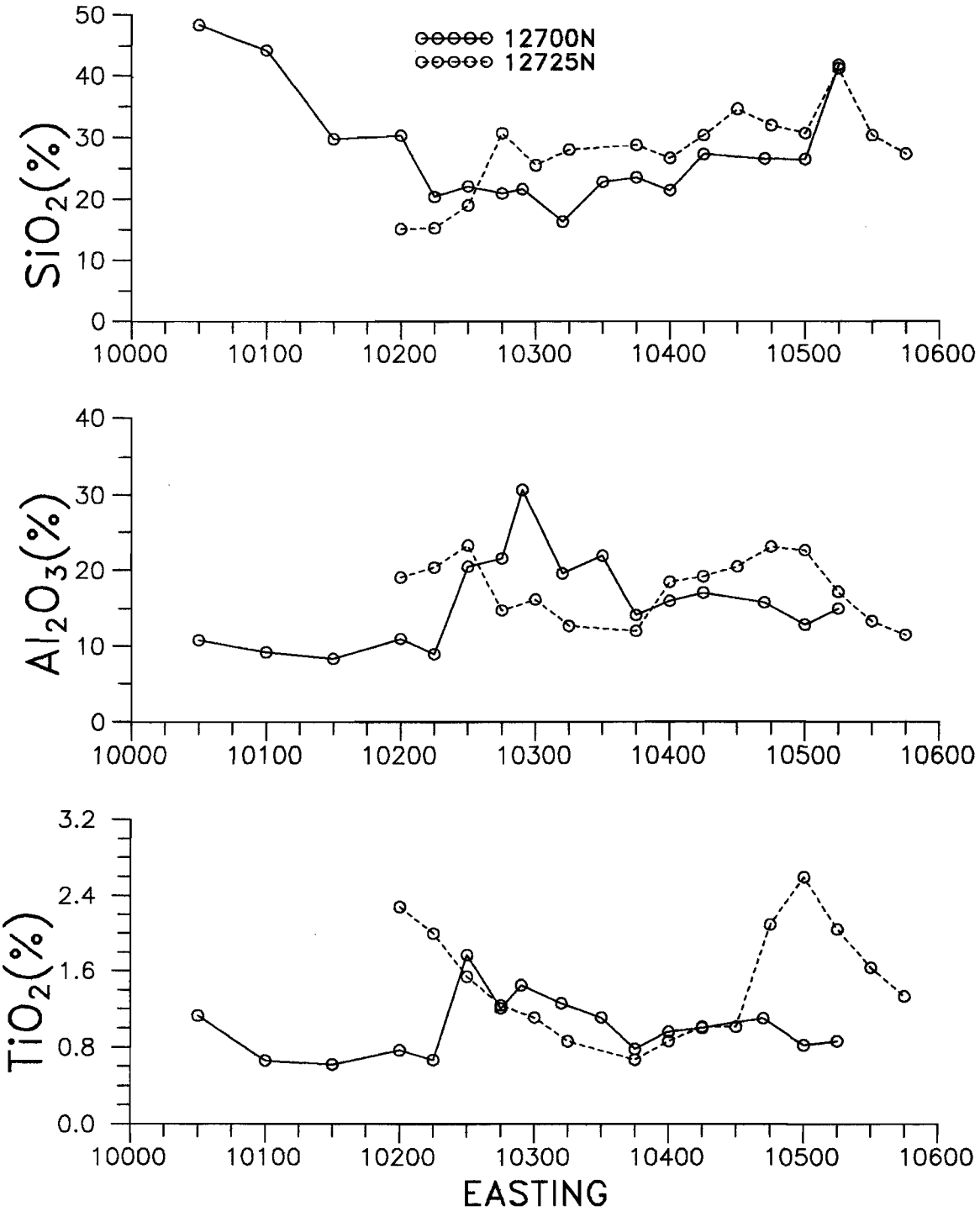

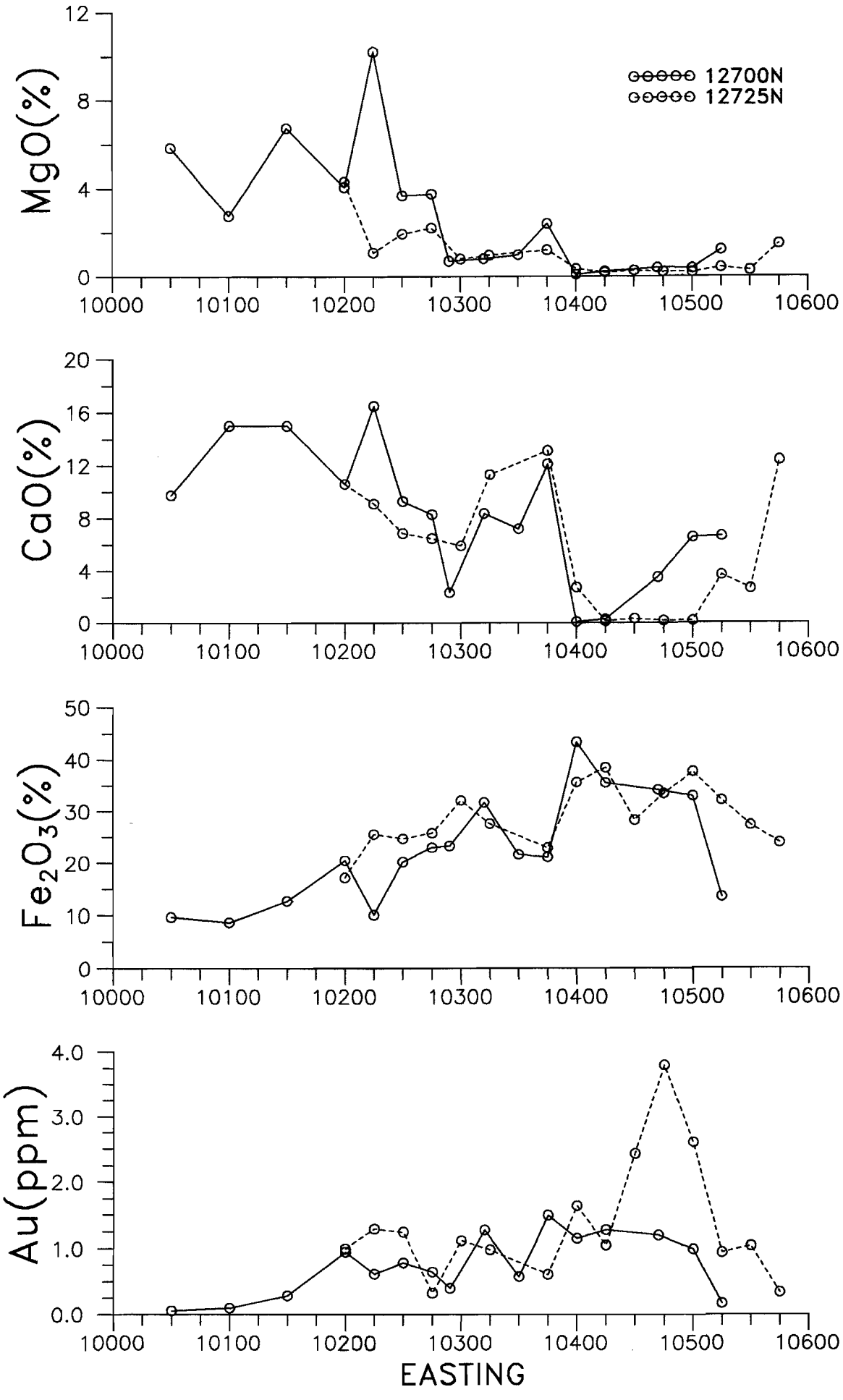
MgO(%)
CaO(%)
Fe_2O_3(%)
Au(ppm)
12700N
12725N
EASTING
10000
10100
10200
10300
10400
10500
10600

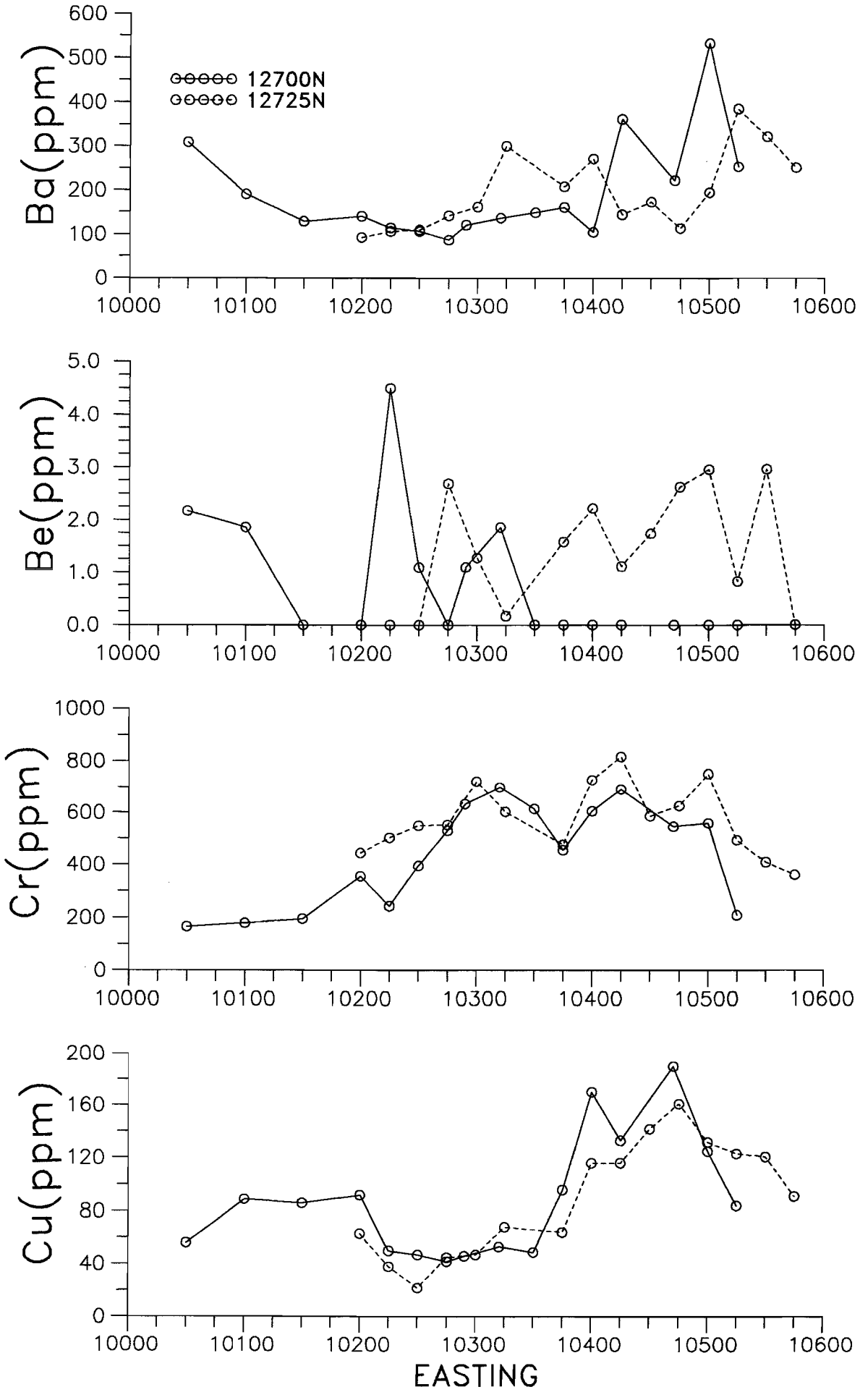
12700N
12725N
Ba(ppm)
Be(ppm)
Cr(ppm)
Cu(ppm)
EASTING
10000
10100
10200
10300
10400
10500
10600

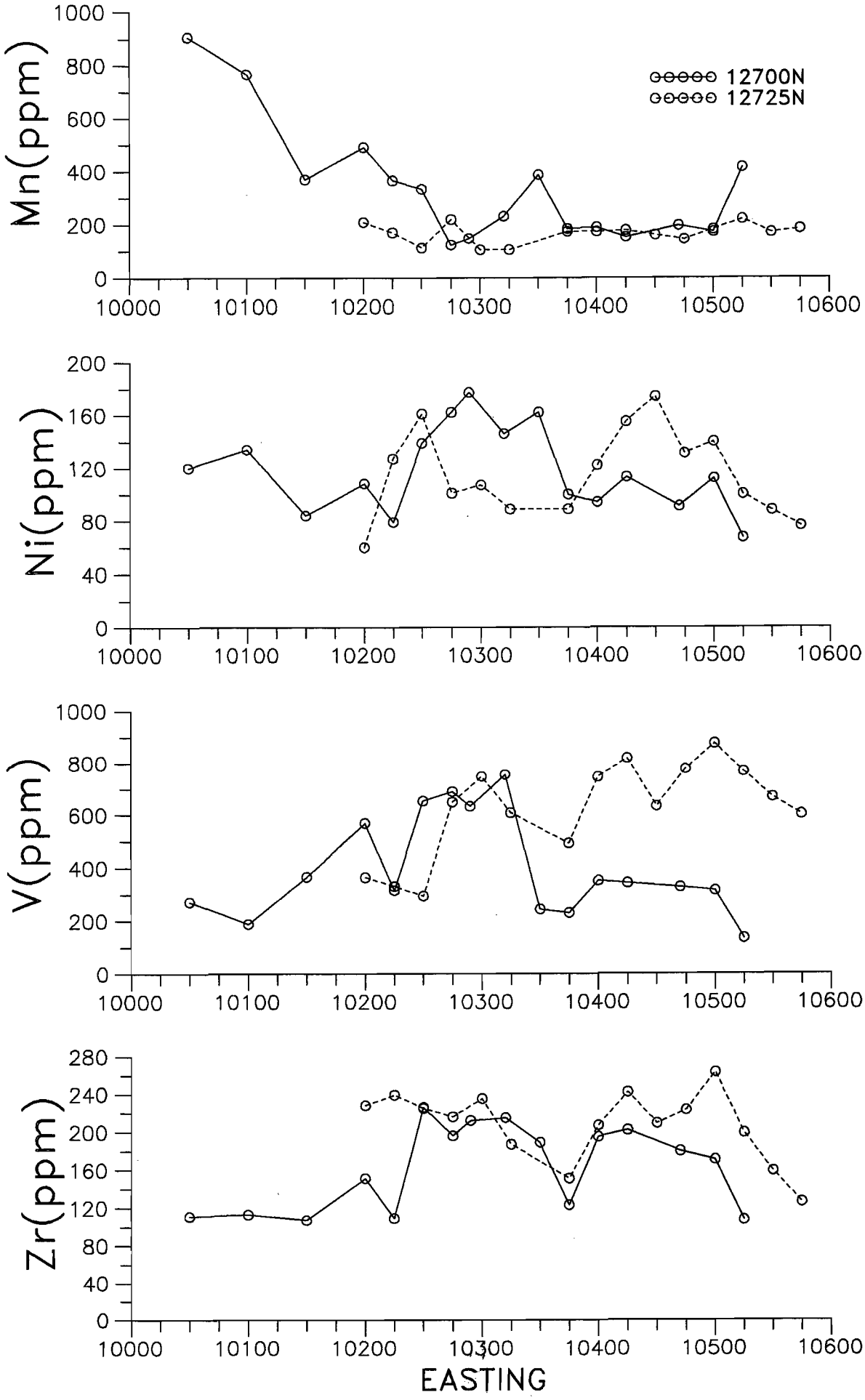
Mn(ppm)
1000
800
600
400
200
0
12700N
12725N
Ni(ppm)
200
160
120
80
40
0
V(ppm)
1000
800
600
400
200
0
Zr(ppm)
280
240
200
160
120
80
40
0
10000
10100
10200
10300
10400
10500
10600
EASTING

3b. Comparison of 3-4m composite chemical data distribution between 12700N and 12725N (plotted).

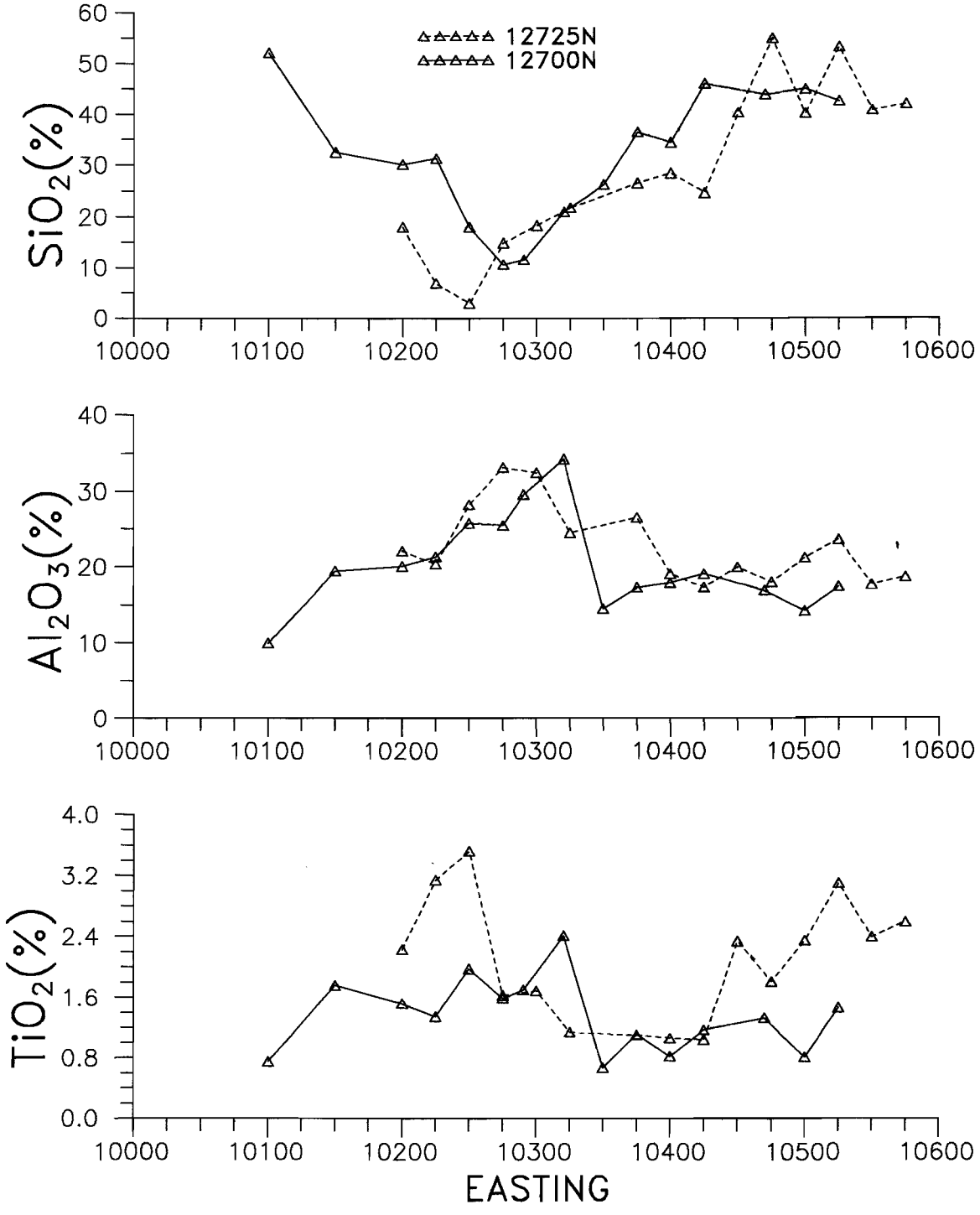

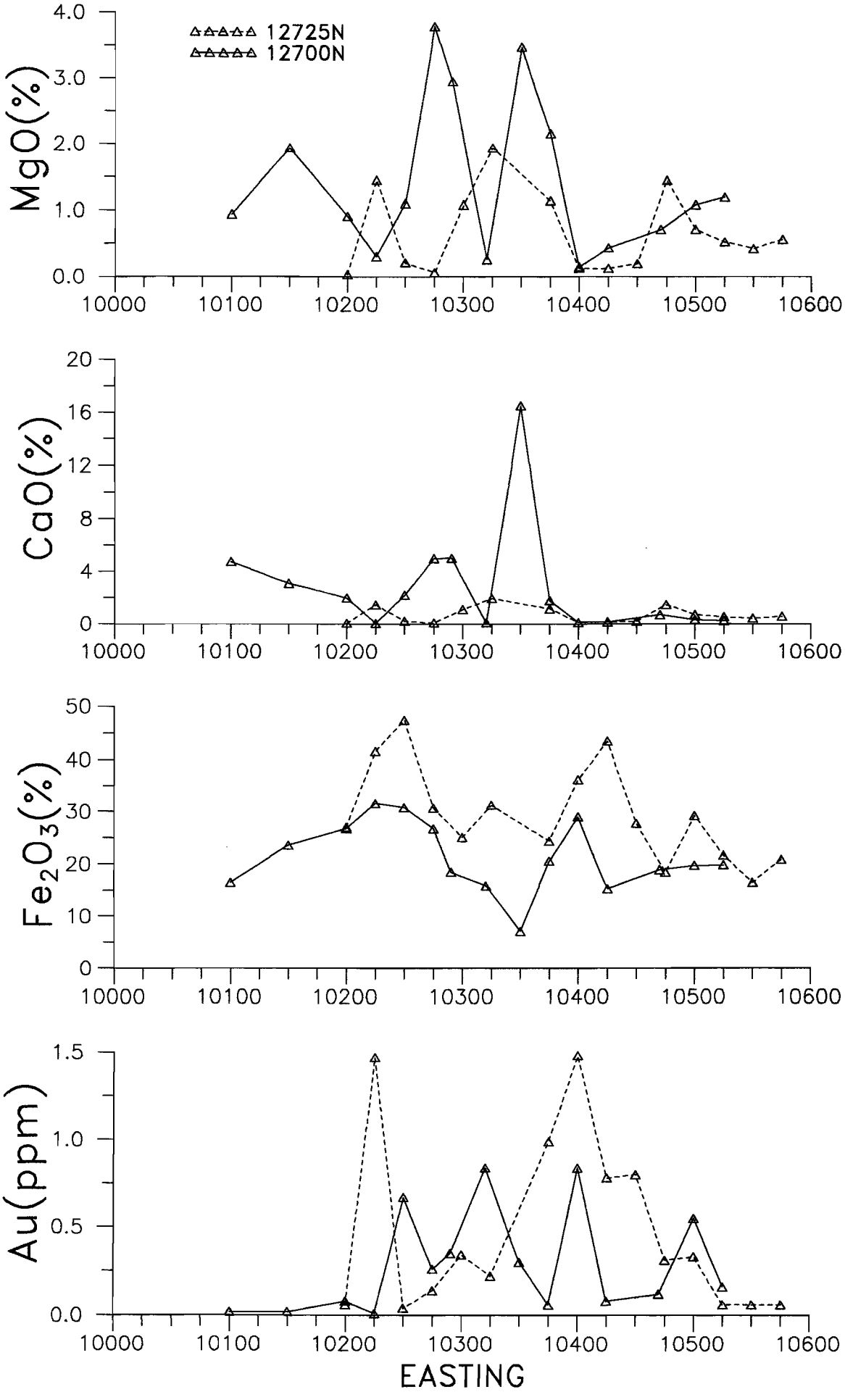
12725N
12700N
MgO(%)
CaO(%)
Fe2O3(%)
Au(ppm)
EASTING
10000
10100
10200
10300
10400
10500
10600

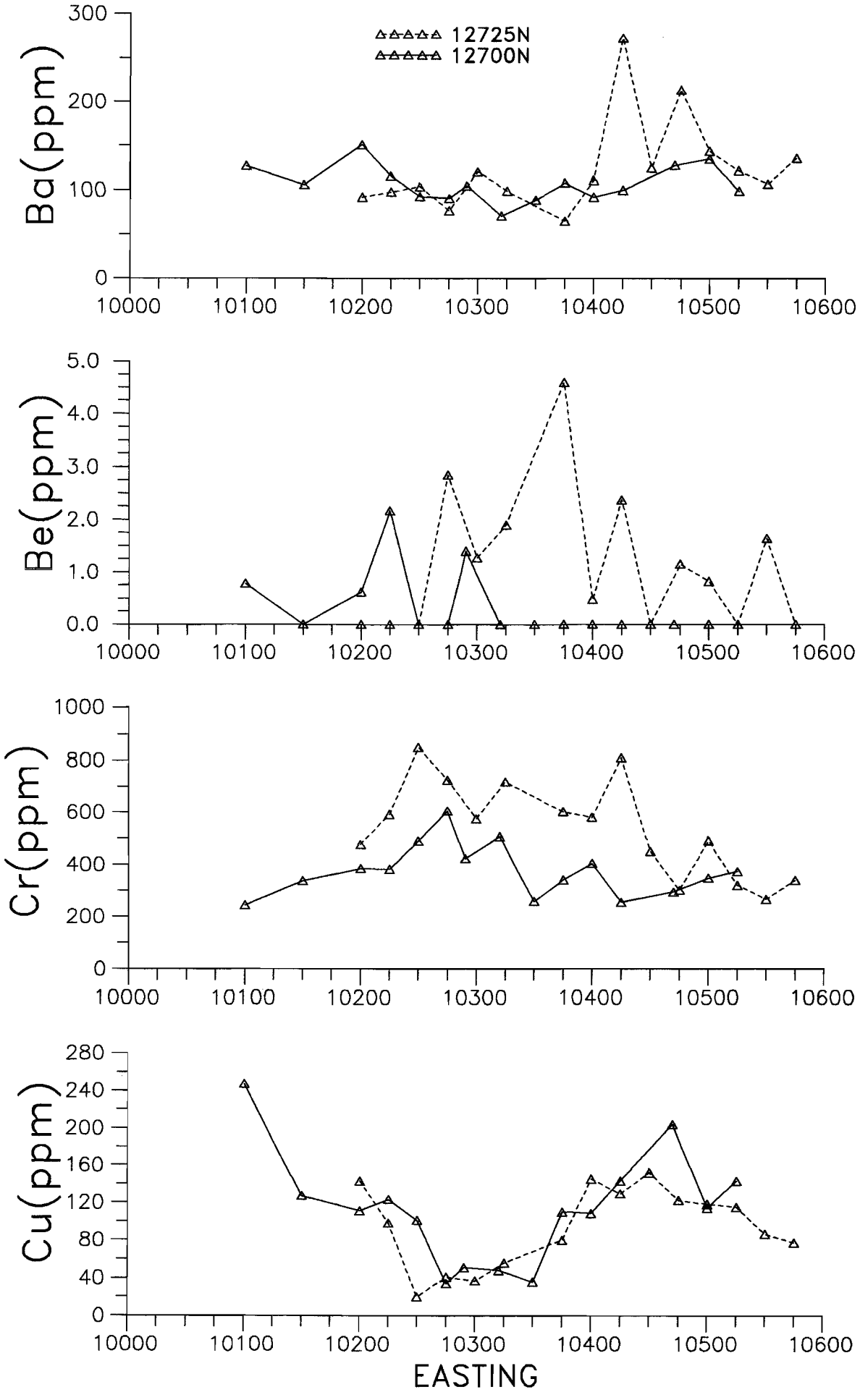
12725N
12700N
Ba(ppm)
Be(ppm)
Cr(ppm)
Cu(ppm)
EASTING
10000
10100
10200
10300
10400
10500
10600

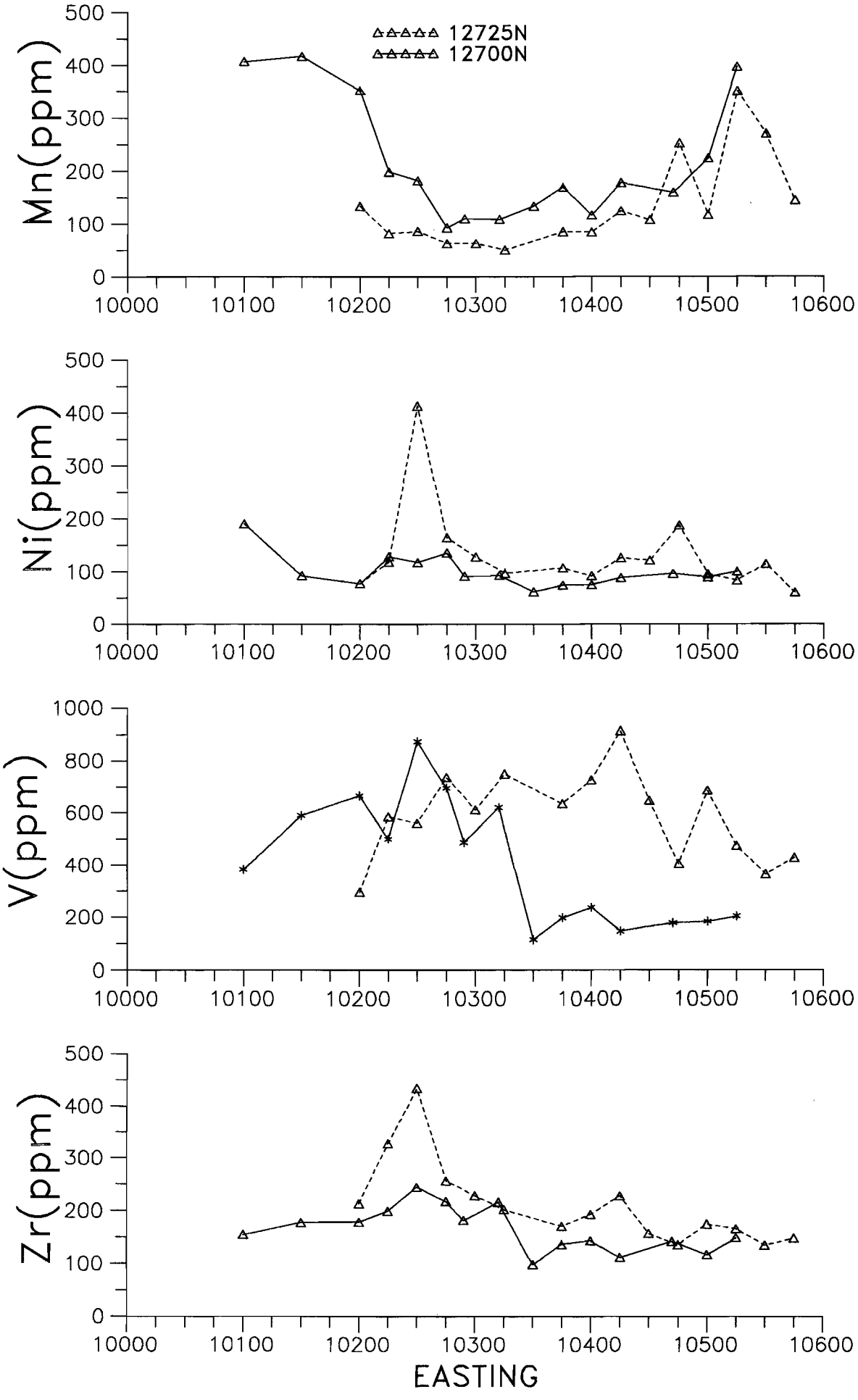
12725N
12700N
Mn(ppm)
Ni(ppm)
V(ppm)
Zr(ppm)
0
100
200
300
400
500
600
800
1000
10000
10100
10200
10300
10400
10500
10600
EASTING